REPORT NO.
UCB/EERC-78/17
SEPTEMBER 1978

EARTHQUAKE ENGINEERING RESEARCH CENTER

STRENGTH OF TIMBER ROOF CONNECTIONS SUBJECTED TO CYCLIC LOADS

by

POLAT GÜLKAN
RONALD L. MAYES
RAY W. CLOUGH

Report to the Department of Housing and Urban Development

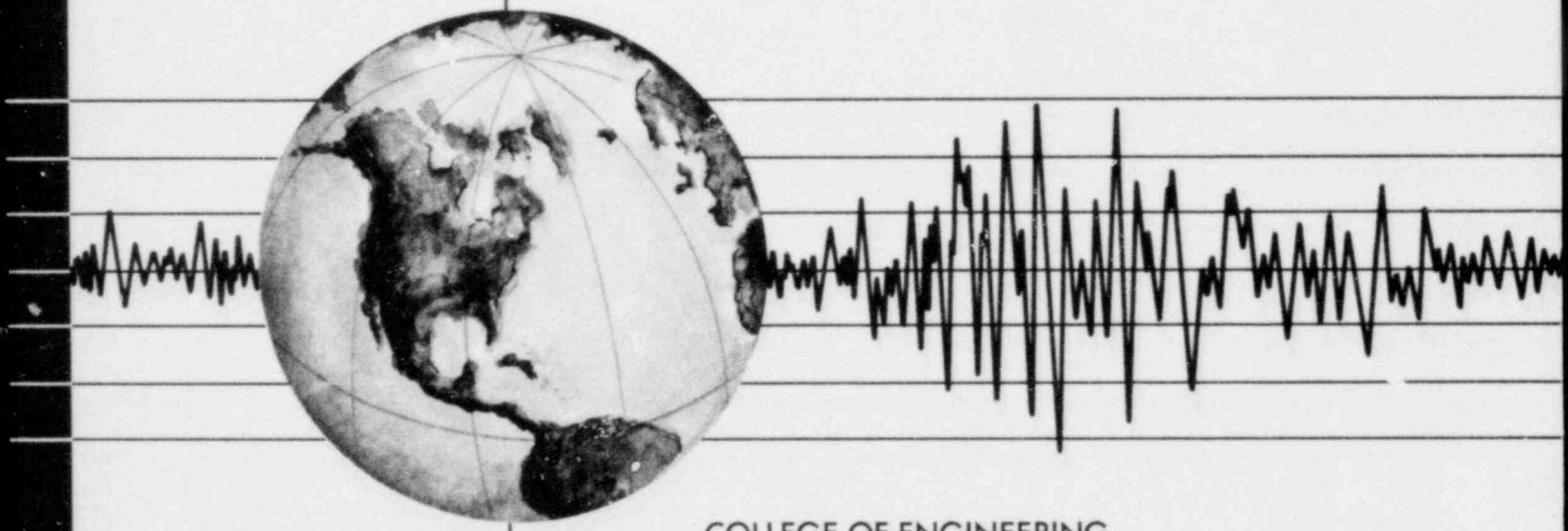

COLLEGE OF ENGINEERING

UNIVERSITY OF CALIFORNIA · Berkeley, California

STRENGTH OF TIMBER ROOF CONNECTIONS SUBJECTED TO CYCLIC LOADS

by

Polat Gülkan
Ronald L. Mayes
Ray W. Clough

Report to

Department of Housing and Urban Development

Report No. UCB/EERC-78/17
Earthquake Engineering Research Center
College of Engineering
University of California
Berkeley, California

September, 1978

ABSTRACT

Behavior of typical timber roof connections used in single-story masonry residential construction subjected to cyclic loads is the subject of this report. In order to assess the adequacy of connections in transferring roof inertia loads developed during earthquake ground motions, five basic types of roof-to-masonry wall connection mock-ups comprising a total of nineteen models were subjected to displacement controlled load tests using both in-plane (along the wall) and out-of-plane (transverse to wall) forces. The five types of connections contained load bearing and non-load bearing connection details of both gabled truss and flat roof construction. Behavior of the connections is described in terms of the deformations of the various components comprising the assembly. By examining the mode of failure and the code allowable loads on bolted and nailed connections, the margin of safety inherent in current code requirements is determined. From the test results, it appears that the connection of the truss rafters to bearing and non-bearing walls, as implemented in the program, was adequate. However, for connections employing ledgers supplementary anchorage devices need to be used since bolts tend to fail by pulling out of the face shell of the masonry units and ledgers fail easily when subjected to cross grain tension.

ACKNOWLEDGMENTS

The investigation described in this report is part of a research program entitled "Laboratory Studies of the Seismic Behavior of Single-Story Masonry Buildings in Seismic Zone 2 of the U.S.A.", sponsored by the U S. Department of Housing and Urban Development, under Contract No. H2387. Concrete block units were donated through arrangements made by the California Concrete Masonry Technical Committee; brick units were donated by Interstate Brick Co. of Salt Lake City, Utah, and were transported by H.C. Maddox Co. of Sacramento, California. Both are gratefully acknowledged. D.A. Sullivan Co. fabricated the masonry walls. Planning of the tests was carried out with suggestions from the Applied Technology Council Advisory Panel consisting of R.D. Benson, J. Gervasio, J. Kesler, O.C. Mann, L. Pritchard, and R.L. Sharpe. The government technical representatives on the project were the late W. J. Werner, and subsequently R. Morony. Further coordination with the Department of Housing and Urban Development was provided by L. Chang and A. Gerich. Student assistants T. Nearn and P. Buscovich did the laboratory work and M. Svojsik helped in reducing the data. D. Steere implemented the data acquisition setup, and the personnel of the Structural Research Laboratory, headed by I. Van Asten, contributed to nearly every phase of the experimental work. Initial phases of the study were carried out under the supervision of Y. Omote and R. Hendrickson.

The typing was done by T. Avery and the drafting by G. Feazell; the manuscript was reviewed by B. Bolt.

TABLE OF CONTENTS

LIST OF TABLES

LIST OF FIGURES

1. INTRODUCTION

1.1 Background

The investigation described in this report is part of a research program entitled "Laboratory Studies of the Seismic Behavior of Single-Story Residential Masonry Buildings in Seismic Zone 2 of the U.S.A.", which has been in progress at the Earthquake Engineering Research Center, University of California, Berkeley, (EERC), since April 1976. The fact that recent changes were made by the Department of Housing and Urban Development (HUD) in the Minimum Property Standards for One and Two Family Units[1]* reflecting the Seismic Zone 2 status recently designated for Arizona and parts of Utah, provided the impetus for HUD to request that the research be undertaken. The promulgation of "Local Acceptable Standard No. 2", by the HUD office in Phoenix, Arizona, was questioned by the local housing industry on the grounds that compliance with its requirements would lead to increased costs and unnecessarily high factors of safety for earthquake loads. The research program undertaken at EERC was designed to address the following areas of uncertainty:

(1) To observe the seismic behavior of masonry structures constructed from full-scale components when subjected to simulated earthquake motions.

(2) To determine the reinforcement requirements for the in- and out-of-plane resistance of typical masonry housing construction for the level of seismic excitation expected in UBC Zone 2 areas of the U.S.

(3) To determine the adequacy of typical roof connection details of masonry housing construction in resisting forces developed during seismic excitation.

---

* Numerals in parentheses refer to items cited in the References.

An integral part of the overall study has been the identification and evaluation of the mechanisms through which inertia forces generated at the roof level are transmitted to the masonry components and ultimately to the foundation. Strength, energy absorption properties and failure characteristics of various types of connections used in masonry construction in Arizona and Utah were investigated. For this purpose, five distinct groups of connections were identified and a total of 19 mock-up models comprising these groups was fabricated and tested. Three of these groups were typical of gable roof construction, while the other two were typical of flat roof construction.

This report is intended to serve as a companion volume to two further reports [2,3] which will address the first two items above.

1.2 Literature Review

Examination of damage in low-rise buildings during the San Fernando earthquake prompted the recommendation that the connection between the roof diaphragm and the supporting walls should be improved [4,5]. It was also recommended that criteria be developed to provide realistic design forces and detail requirements for connection of these elements. The use of steel joist anchors to anchor walls to the roof framing members was suggested as one effective method for improving roof-to-wall connections. Also, improved continuity of wall construction at the corners of roof diaphragms, tying purlins as well as joists and other members together, in addition to the plywood sheathing were cited as possible remedial measures. Essentially, the same topics were suggested for further study by Amrhein [6] and Meehan [7]. A major study on the seismic design and construction of single-family dwellings by Goers and Assoc. [8] presents recommendations for the anchorage of roof structures to load resisting walls.

Code requirements for allowable loads for various types of connections include significant factors of safety to allow for the great variability in the quality of workmanship encountered under field conditions. In addition, these allowable loads are based only on monotonic load test data since to the best of the authors' knowledge, research specifically aimed at the seismic behavior of timber connections has not been reported in the literature. It is generally recognized that methods for the design and analysis of timber construction are less developed than for most other building materials in spite of the fact that approximately three-fourths of all residential housing in the U.S. is currently constructed with wood[9]. Because of the wide natural variation in the physical properties of wood, allowable stresses for design have generally been determined with wider margins of safety than for other materials of construction. While this conservative approach has resulted in few structural failures, it may at times be uneconomical.

Timber roof elements are joined together by nails or spikes to form the completed roof assembly. Allowable loads for nails are given in design handbooks[10] or the Uniform Building Code[11], and are based on test data (furnished by National Forest Products Laboratory) which have been reduced by a factor of safety of approximately 5 for deflection control. Wilkinson[12,13] presented an analysis for the lateral resistance of nailed timber joints with similar or dissimilar members. His results indicated that a mathematical formulation could be developed to predict the load-slip relation for such joints. Moreover, a constant deflection value of 0.011 in. was suggested as the upper limit of the proposed relationship between the applied load and the resulting slip. For the most part, these studies were limited to monotonically applied forces; i.e., the effects of load reversals were not considered.

Sufficiently reliable methods are available for the analysis of flat roof diaphragms subjected to lateral forces (e.g., see references (14), (15)). Possibly because of the historical development of roof diaphragms these methods relate to straight, diagonally or double diagonally sheathed lumber diaphragms or to plywood diaphragms which are more commonly used today. The diaphragm proper is assumed to be firmly anchored to the end walls, and no consideration is given to possible deformation of anchor bolts or to the effects of reversed overloads. Although it is recognized that secondary forces are created in diaphragms which do not lie in a single plane, such as when a curved or pitched truss is used, no reliable method appears to have evolved for the structural analysis of such structures[14]. The size and spacing of anchor bolts are determined on the basis of code requirements which are presumably based on large factors of safety. A chronological listing of studies on wood and plywood diaphragms is contained in reference (16).

1.3 Object and Scope

The investigation reported herein was aimed at determining the strength and cyclic behavior of typical roof connections used in masonry residential construction in the less seismically active areas of the U.S. Five basic groups of connections were selected for testing. These included load bearing and non-load bearing connection mock-ups of both gable and flat roof construction. Cyclic in-plane and out-of-plane forces were applied to the models representing gable roof connection details. For flat roof models only transverse forces (applied normal to the plane of the wall supporting the roof) were considered; the time variation was a haversine wave.

In addition to the basic types of connections represented by the

models, several other parameters were considered in the experimental program. These included the type of unit used in constructing the masonry walls to which timber roof components were attached, addition of roof dead load, the diameter of bolts, and eccentric or symmetric application of the simulated earthquake forces to the entire connection assembly. This report describes results from 19 experiments involving these parameters. Each connection model included a reinforced masonry wall segment 8 ft in length and a part of a timber roof attached to the wall by means of anchor bolts. The test sequence involved applying sets of controlled displacements where each set consisted of three cycles of loading at a given actuator displacement. The imposed displacement limits were gradually increased after every set. Testing was stopped when the connection assembly reached its ultimate resistance and failure was initiated in either the masonry or the wood components.

The remainder of this report is organized as follows. In Chapter 2, selection, design considerations and material properties of the five basic types of connections are described. Chapter 3 contains a detailed description of the test procedure and instrumentation for the experiments. The experimental results are given in Chapter 4, and an overall evaluation of these findings is made in Chapter 5. A summary of the program and the results is presented in the concluding Chapter 6.

2. THE TEST STRUCTURES

2.1 Selection of the Test Specimens

An important consideration in the determination of the types of specimens to be included in the test program was that the data obtained should be relevant to a parallel study in which the seismic behavior of single-story masonry houses was being investigated experimentally on the EERC Shaking Table[17]. The transfer of inertia forces between the timber components of a roof assembly and the masonry components of walls during earthquake-induced base motions is a complicated phenomenon. In order to simulate adequately typical connection details different configurations were considered. A truss roof structure similar to that used in the shaking table program is shown in Fig. 2.1 together with an exploded view of the masonry wall components. The trusses, spaced 2 ft apart, comprising the roof assembly are joined together with plywood sheathing on the inclined rafters and are supported on top of the masonry components by a continuous top plate. Connection between the bottom truss rafters and the top plate is provided by means of toe-nails and metal framing anchors. The top plate is anchored to the top of the masonry walls by bolts and plate washers. The roof diaphragm is completed by nailing drywall sheathing to the bottom chords.

The experimental program involved the testing of five different types of roof connection details which were subjected to either in-plane (along the wall) or out-of-plane (transverse to the wall) loads. These were both load bearing and non-load bearing models of gabled truss and flat roof construction. The first three types were simulations of the roof structure shown in Fig. 2.1.

In the sequel to this report each specimen will be referenced by a code. The first group of characters in the code designates the type of the

roof connection, and ranges from C1 to C5. The letter S, preceding the first group of characters, implies that transverse forces were applied symmetrically with respect to the two bolts embedded in the masonry wall; otherwise some eccentricity existed between the line of action of the actuator force and the bolts. Additionally, if the letter B follows the first group of characters, it denotes that the masonry components were hollow clay bricks. However, all but two of the masonry walls were made from hollow concrete block units. The second group of characters designates the height of the wall portion in inches and the third is the diameter (in inches) of the anchor bolts which were built into the specimen and connected to the timber components during that particular experiment. The fourth group of characters applies to three specimens of the type designated as C3 which were either tested in-plane (IP) or had a special in-plane loading configuration (SP). For type C4, the fourth group of characters, if it exists, denotes the total weight of lead blocks superposed on the ledger in order to simulate a roof dead load of 180 lb/ft. A detailed description of the connection models is provided in the remainder of this section.

For example, the specimen for which the reference code name was SC4B-36-5/8-1450 had the following characteristics:

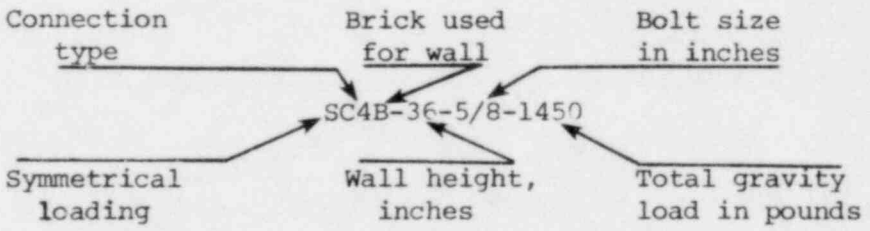

2.1.1 Specimens of Type C1 and C2 - Load Bearing Gable Roof Connections Subjected to In-Plane and Out-of-Plane Loads

Specimens designated as type C1 represented a portion of a load bearing wall subjected to in-plane loads by truss rafters located 2 ft apart. As shown in Fig. 2.2, this type of connection mock-up included the essential elements of the load bearing connections of Fig. 2.1. However, the specimen did not include the inclined top truss chords. As a compromise dictated by testing requirements the plywood sheathing was nailed directly to the "bottom chord" elements. This group of connections was tested by applying a force parallel to the longitudinal axis of the wall in the plane of the plywood. Each 2x4 in. rafter was toe-nailed by 16d-box nails into the 2x6 in. top plate. In addition, a proprietary metal framing anchor with a rated capacity of 290 lb against uplift and longitudinal shear was nailed to two alternate joists. Initially, it was decided to place two sets of anchor bolts with different diameters on each wall specimen, thus effectively to double the number of test models with respect to this parameter. However, during any given test only one set of bolts on each wall was tightened with the use of a 1/4 in. thick, 2½x2½ in. plate washer and the other set was bypassed by elongating the holes in the top plate at the proper location. The rationale behind this approach was the observation that bolts generally were not the critical elements of the assemblies tested. Besides nails and metal framing anchors, restraint against rotation of the rafters was provided by two 8 ft long, 2x6 in. fascia boards nailed to the two ends of the 45 in. long rafters. The resulting frame was then enclosed with 1/2 in. plywood at the top and 1/2 in. thick gypsum drywall on the "inside" bottom of the rafters. The space between the individual chords was blocked with 1x4 in. frieze boards toe-nailed into the rafters at each end with 8d-nails.

All masonry wall panels were built upon 7½x16 in. strip footings and all were 8 ft long. The footings contained 20 in. long, #4 bars which acted as lapped dowels at the locations corresponding to the #4 reinforcement at both ends of the walls. No attempt was made to simulate the dead load of the roof in connections of type C1.

With reference to Fig. 2.1 and the orientation of the roof structure shown there, the C1 type connections simulated the action of the truss rafters on the load-bearing walls when the base motion occurred exclusively in the direction of the 1-1 axis. If ground motion were to occur primarily along the axis designated as 2-2, then the same connection would be required to provide out-of-plane constraints for the load-bearing walls oriented normal to that direction. Connections of this type, denoted C2, were identical to C1 in every structural detail, except that the fascia board was deleted on one side to allow the actuator force to be applied to the rafters. The structural details of specimens in this group are shown in Fig. 2.3.

2.1.2 Specimens of Type C3 - Non-Bearing Gable Roof Connections Subjected to In-Plane and Out-of-Plane Loads

The connection designated as C3 was intended to simulate the roof action of the shaking table structure with the gabled ends of the trusses located above the non-load bearing walls normal to directions 1-1 and 2-2 in Fig. 2.1. A typical section normal to the trusses is shown partially in Fig. 2.4. The bottom rafter of the truss along the top of the masonry wall is nailed sideways into 1 ft long, 2x4 in. blocks spaced every 4 ft. Also, the gypsum drywall units are nailed into 2x6 in. blocks which cantilever from the top plate. Vibration of the roof structure in what is termed the out-of-plane direction would introduce forces into the transverse masonry wall primarily through the strut action of the 2x4 in. truss ties

nailed to the top of the three outermost bottom rafters on either side of the house. The amplitude of the displacements would, of course, be limited by the action of the shear walls parallel to the direction of base motion. The details of the connection model built to simulate the roof action described in Fig. 2.4 are given in Fig. 2.5. Transverse load effects were introduced through the two truss ties; therefore the plywood sheathing nailed to the top of these units served no structural function. Another objective in selecting this type of connection was to observe how effective the gypsum drywall unit nailed underneath the bottom chord elements was in distributing the applied force to the masonry wall.

Originally, only transverse loading was planned for connections in the C3 group. However, again with reference to Fig. 2.1, it is obvious that the in-plane capacity of the connection would have to be studied in order to be able to make an assessment of the transfer of roof loads to the resisting walls with a base motion directed along axis 2-2. In this case inertia forces generated at the roof diaphragm level would have to be transferred to the shear walls through the bottom chords of the two trusses at each gabled end, or normal to the plane defined by Fig. 2.4. The bottom chord directly above the top plate would tend to slip relative to the top plate and the masonry wall, but being nailed to the blocking would introduce forces into these elements. In the additional tests conducted to determine connection strength in this mode, cyclic displacements were imposed on the simulated truss chord; the rest of the components shown in Fig. 2.5 were omitted from the test assembly.

2.1.3 Specimens of Type C4 and C5 - Load Bearing and Non-Load Bearing Flat Roof Connections Subjected to Out-of-Plane Loads

The type C4 and C5 roof connections are typical of details commonly used in flat-roof buildings. Although there may be minor differences in

individual applications, two prevalent forms are shown in Fig. 2.6. In connections of type C4 (Fig. 2.7), the 2x8 in. joists were secured to the 3x8 in. ledger by means of proprietary metal joist hangers having a rated vertical capacity of 800 lb each. Again, only one of the two sets of bolts provided in the walls was used in any given test, and the other was made inoperative by drilling oversized holes in the ledger.

As stated earlier, the connection experiments were conducted with a view towards providing relevant data for the shaking table tests; the details were adapted from typical construction practices in Arizona and Utah after consultations with local professional engineers. Hence, the details may contain features which are "typical" but not necessarily desirable. For instance, no positive connection is provided between the diaphragm and the masonry wall by means of metal connectors in group C4. For horizontal strength, total reliance is therefore placed on the pullout strength of the bolts. Presumably because of insufficient data, the Uniform Building Code lists no allowable bolt pullout values for masonry. So, in designs involving bolts which will possibly be loaded in tension, allowable values are reportedly taken from concrete and used after "suitable" reductions.

Structurally, the C5 connection designed to represent the roof in Fig. 2.6(b) was the simplest. This is a non-load bearing connection required to transfer out-of-plane wall forces into the roof diaphragm. The corresponding mock-up consisted of a ledger bolted to the face of the masonry wall by two anchor bolts and 1/2 in. thick plywood sheet nailed to the top of the ledger. Joist elements which would normally exist parallel to the wall were not included in the model, because the strength of the specimen is derived from the nailed connection between the ledger and the plywood and the anchor bolts. Structural details of specimens of

type C5 are shown in Fig. 2.8. During testing only two similar bolts 4 ft apart were tightened with nuts and the other two were left inactive. It will be noted that, as in type C4 connections, the ledger board is forced to behave as a simple beam supported at the bolt locations with overhangs at the two sides, in contrast to the construction detail where the ledger is continuous over bolts spaced 4 ft apart. Also, the 2¾x2¾x1/4 in. plate washers used in the first two models were changed to 2½x6x3/8 in. washers for the tests of the last three models.

Specimens in the C4 and C5 groups were subjected to controlled displacements with a haversine time variation whereas the first three types were subjected to complete sine wave variations of displacement amplitudes. A roof dead load of 180 lb/ft was simulated in two tests of type C4 connections. This was achieved by placing lead blocks totaling 1450 lb on top of the 3x8 in. ledger. For all other tests involving load bearing connection models, no gravity roof loads were considered.

Anchor bolts of all sizes in the C1, C2, and C3 tests were embedded 8 in. into the masonry units and had 2 in. long hooks at the ends. For this purpose the top three courses of masonry units were filled with grout at cavities corresponding to the bolt locations. To place the horizontal bolts in the C4 and C5 connections, the top two courses only were grouted at the appropriate locations and a 3 in. embedment followed by a 2 in. hook was provided.

All masonry components of the test specimens were constructed by the same experienced contractor using techniques representative of good quality workmanship. The walls were fabricated and stored outside the laboratory area until the time of testing when they were transported by a forklift to the test bay. The timber components were built on the walls after the footings had been properly anchored.

2.2 Material Properties

The experimental program was carried out in two phases. During the first phase, two specimens from each of the five different types of connections were tested; the masonry unit used in these tests was the hollow concrete block of type 1. An evaluation of the results at the end of the first phase suggested that additional tests should be undertaken in order to arrive at a more complete matrix of parameters. During the second phase, usable wall specimens saved from Phase 1 as well as additional walls made either from a different shipment of concrete blocks (referred to as concrete block of type 2) or clay bricks were used. Therefore, distinction will be made between different shipments of concrete blocks and the mortar and grout used in conjunction with each of them.

Masonry components of the test specimens consisted of standard hollow concrete masonry units with nominal dimensions of 6x4x16 in. and standard hollow clay bricks measuring 6x4x12 in. In Fig. 2.9 plan views for these standard units are shown, and Table 2.1 lists their dimensions and physical properties.

Type S mortar designation of the Uniform Building Code with volume proportions of 1 cement:1/2 lime:4½ sand was specified for use in the fabrication of the specimens. Two samples of mortar were collected on every day of the period over which construction of the walls was continued, and the samples were tested when the first connection specimen was tested. During the first test phase, grout for filling the cells for bolt anchorage and reinforcing was the standard 1 cement:3 sand mixture. When additional testing was undertaken the contractor was instructed to make no distinction between mortar and grout, and the same Type S mortar mixture was used for grouting purposes. During both phases, however, mortar samples were collected in accordance with UBC requirements: the material was spread

on the masonry and allowed to rest for one minute before being placed into 2x4 in. cylinders. Grout was poured into the cavities of the masonry units and stored in the same condition as the walls. For compression tests of the grout, 2 in. cubes were cut from these samples. A summary of mortar and grout strengths is provided in Table 2.2.

In every connection, wall reinforcement consisted of one medium grade #4 bar placed vertically in each end cell. These bars were measured to have an average yield strength of 54,000 psi and an average rupture strength of 80,000 psi. Also, in all walls the top two bed joints were reinforced with 9-gage wire K-brace joint reinforcement. This reinforcement was observed to be effective in preventing shrinkage cracks.

The compressive strength of the masonry assemblies for Phase 1 was determined by compression tests of block prisms laid in stacked bond of various heights. The variables considered in the testing procedure were whether the cells of the single block wide prism were grouted and whether the top two courses of joint mortar were reinforced. The results are given in Table 2.3. For assessment of the shear strength of the masonry components, 32 in. square panels were fabricated at the time of construction of the concrete block walls of Phase 1. These panels were tested in diagonal compression in a specially designed jig[18]. Grout and horizontal reinforcement were again the variables in the specimens tested. Values of critical tensile strength, σ_{tcr} listed in Table 2.4 are based on the Blume[19] formulation

$$\sigma_{tcr} = 0.724\ \tau \tag{2.1}$$

in which

$$\tau = 0.707\ \frac{P}{A} \tag{2.2}$$

where τ is the average shear stress, P the maximum diagonal compression load and A the net cross sectional area of the square panel. For the additional

walls constructed during Phase 2, the prism tests were omitted.

A critical element in the connection assembly is the anchor bolt which is embedded in the grouted block cell. At the time of casting the masonry components for Phase 1, a number of control specimens were also fabricated for the determination of bolt pull-out and shear strength. Because of the inherent randomness of the basic material properties and the effect of parameters such as workmanship and compaction, a broad scatter in the test results was obtained. For the pullout tests, bolts with diameters of 3/8 in., 1/2 in., 5/8 in. or 3/4 in. were cast in either a single 8 in. high half block or in two 4 in. high half blocks on top of one another. Steel plate with an opening slightly larger than the grouted cell area was used as the restraint against the shell area of the blocks. The bolt was then pulled upward in a universal testing machine. A summary of the test results is provided in Table 2.5.

The bolt shear forces were applied by means of a 2x6 in. timber connector attached to the testing machine fixture at one end and to the bolt being tested at the other end. The testing device developed for this purpose is shown schematically in Fig. 2.10. This consisted essentially of a clamping mechanism, with an adjustable height, into which the test specimen could be inserted sideways. The timber connector had a series of bolt holes drilled into it. In each test, a hole was used that was 1/8 in. larger than the diameter of the bolt being tested. The test results are presented in Table 2.6. As with the bolt pull-out tests, a significant scatter is evident in the tabulated values.

The material for the timber components was select structural grade Douglas Fir for the top plate and ledger elements, and standard grade Douglas Fir for the remaining parts. The half-inch thick plywood was of type CD-X. Except where specifically noted to the contrary, all nails

were of the box type. No quality tests of the material were made on the timber components or the anchor bolts.

TABLE 2.1

DIMENSIONS AND PHYSICAL PROPERTIES OF MASONRY UNITS[1]

Masonry Unit Type	Width in.	Height in.	Length in.	Minimum Thickness, in.		Gross Area $in.^2$	Net Area %	Compressive Strength, psi		Oven Dry Weight lb	Masonry Unit Weight lb/ft^3
				Face Shell	Web			Gross Area	Net Area		
Conc. Block 1	5.61	3.62	15.60	1.37	1.50	87.5	64	980	1,530	10.9	92.9
Conc. Block 2	5.60	3.62	15.60	1.12	1.12	87.5	56	1,110	1,983	11.0	107.3
Brick	5.50	3.63	11.50	1.25	0.75	63.3	62	4,060	6,550	---	---

(1) Each value in the Table represents the average result from five specimens.

TABLE 2.2

COMPRESSIVE STRENGTH OF MORTAR AND GROUT

Phase	Mortar			Grout		
	Number of Specimens	Age Days	Strength psi	Number of Specimens	Age Days	Strength psi
1	6	29	2,650	3	43	6,300
2	5	39	2,530	5	39	2,530

TABLE 2.3

COMPRESSIVE STRENGTH OF MASONRY PRISMS: PHASE 1

Nominal Height of Prism in.	Prism No.	Grout	Joint Reinforcement	Failure Load, lb	Strength (1) psi
16	1	Yes	Yes	109,000	1,940
	2	No	No	76,000	1,350
	3	No	Yes	72,000	1,300
					Avg.=1,530
24	1	Yes	Yes	87,400	1,550
	2	No	No	51,700	920
	3	No	Yes	64,200	1,140
					Avg.=1,200
40	1	Yes	Yes	95,000	1,690
	2	No	No	56,200	1,000
	3	No	Yes	54,800	970
					Avg.=1,220

(1) Net area.

TABLE 2.4

CRITICAL TENSILE STRENGTH OF MASONRY: PHASE 1

Specimen No.	Grout in Two Edge Cells	Joint Reinforcement	Failure Load lb	Critical Tensile Strength (Eq. 2.1) psi
1	No	No	13,000	58
2	No	Yes	32,000	142
3	Yes	Yes	18,500	82
4	Yes	No	33,600	149
				Avg.=108

TABLE 2.5

ANCHOR BOLT PULLOUT TEST RESULTS: PHASE 1

Block Type

1 Two 6x4x8 in.

2 One 8x8x8 in.

Bolt Diameter, in.	Block Type	Embedment in.	Mode of Failure	Failure Load, lb
3/8	1	8	2	3,020
3/8	2	8	1	2,220
1/2	1	3	2	600
1/2	1	3	2	1,080
1/2	2	3	1	1,210
5/8	1	8	2	2,380
3/4	1	3	2	2,140
3/4	1	3	2	1,590
3/4	2	3	3	2,500

Failure Mode	Description
1	Grout pulled out from within cell.
2	Bolt begins to slip out, the straightening of hook cracks grout and shell concrete.
3	Grout restrained by plate so that failure mode 2 is induced.

TABLE 2.6

ANCHOR BOLT SHEAR TEST RESULTS: PHASE 1

Block Type

1 Two 6x4x8 in.

2 One 8x8x8 in.

Bolt Diameter, in.	Block Type	Bolt Embedment, in.	Failure Load, lb	Failure Description
3/8	2	8	3,320 (a)	Bolt bent; grout cracked
3/8	1	8	1,920 (a)	Mortar joint between blocks split; grout cracked
1/2	1	8	1,940 (a)	Mortar joint between blocks split; grout cracked
1/2	2	8	2,870 (a)	Shell concrete cracked only
1/2	1	8	3,940 (b)	Bolt bent; grout cracked
5/8	1	8	2,040 (b)	Shell concrete cracked only
5/8	2	8	3,210 (a)	Grout and shell concrete cracked
3/4	1	3	1,030 (a)	Mortar joint between blocks split; grout and shell concrete cracked
3/4	2	3	4,170 (a)	Grout and shell concrete cracked
3/4	1	3	995 (b)	Mortar joint between blocks split; shell concrete cracking only

Note:

(a) Force applied normal to 8 in. side of block.

(b) Force applied normal to 6 in. side of block.

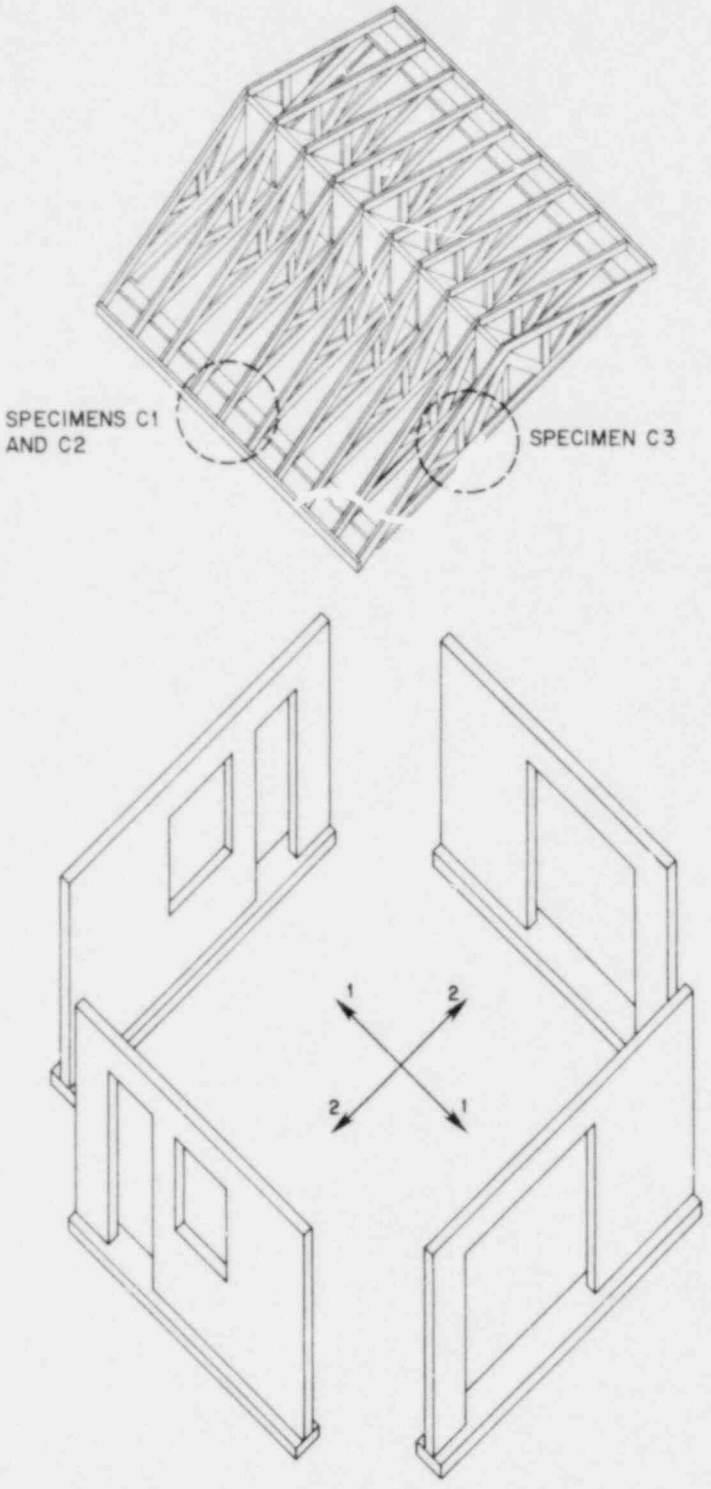

FIGURE 2.1 ROOF STRUCTURE FOR A MASONRY HOUSE

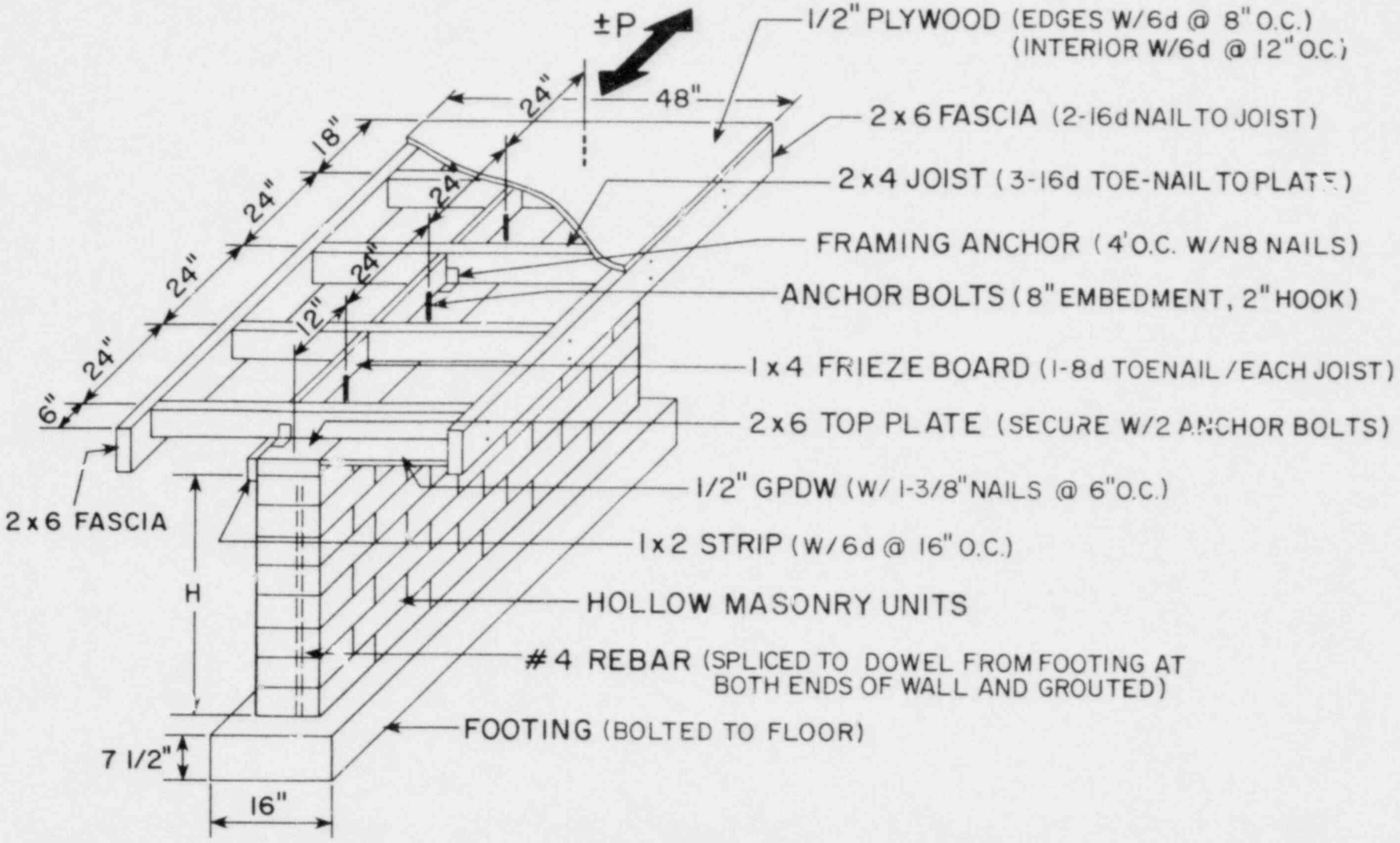

FIGURE 2.2 CONNECTIONS OF TYPE C1

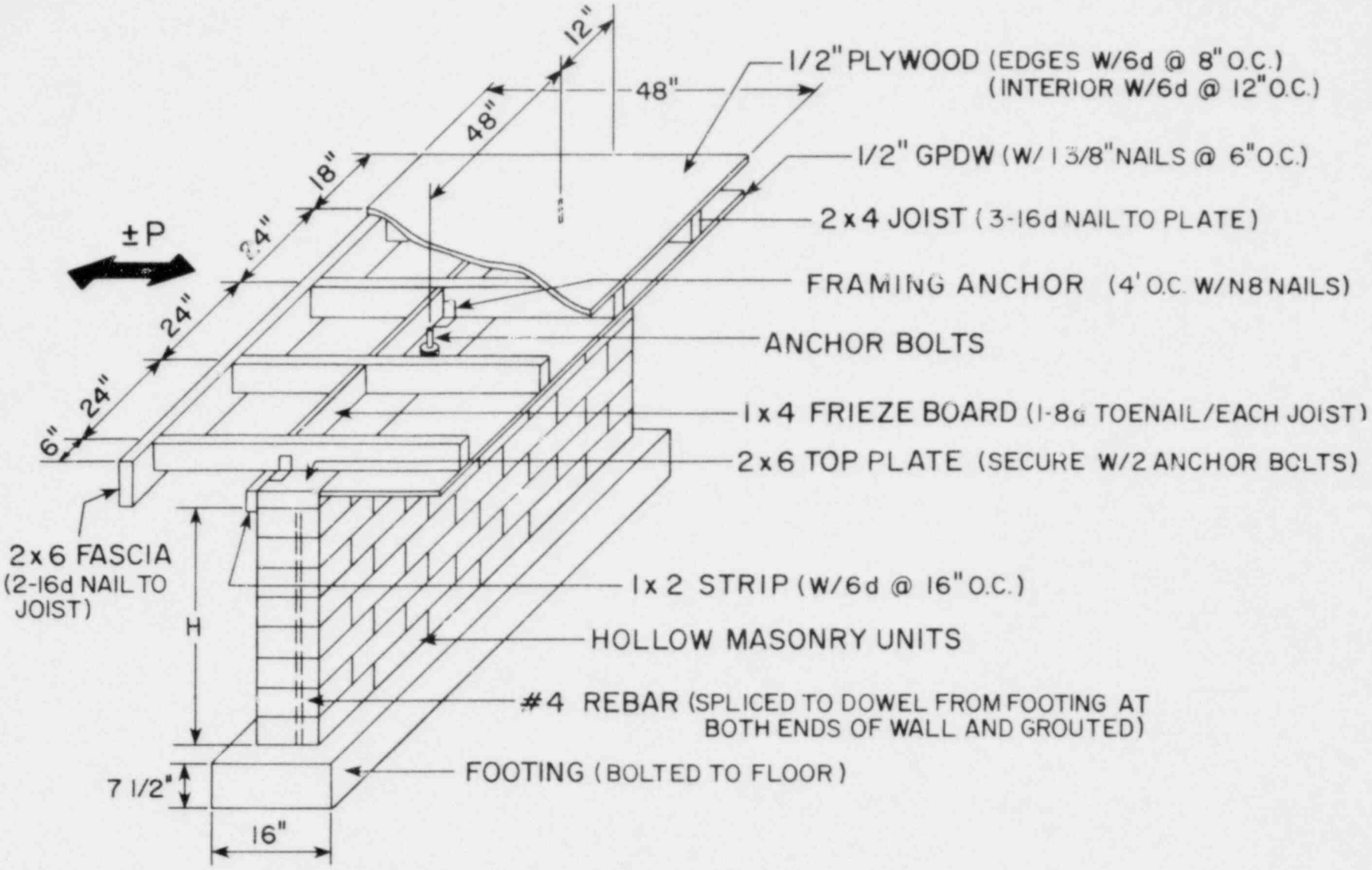

FIGURE 2.3 CONNECTIONS OF TYPE C2

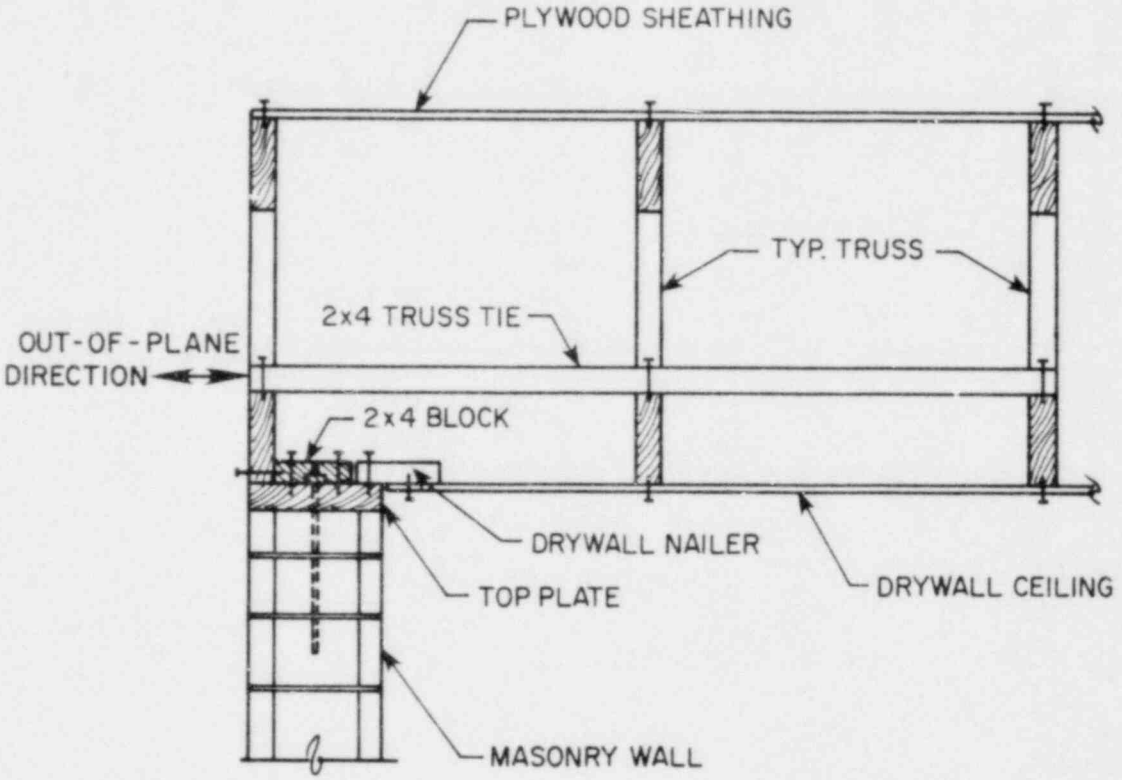

FIGURE 2.4 SECTION AT THE GABLE END OF A TRUSS ROOF

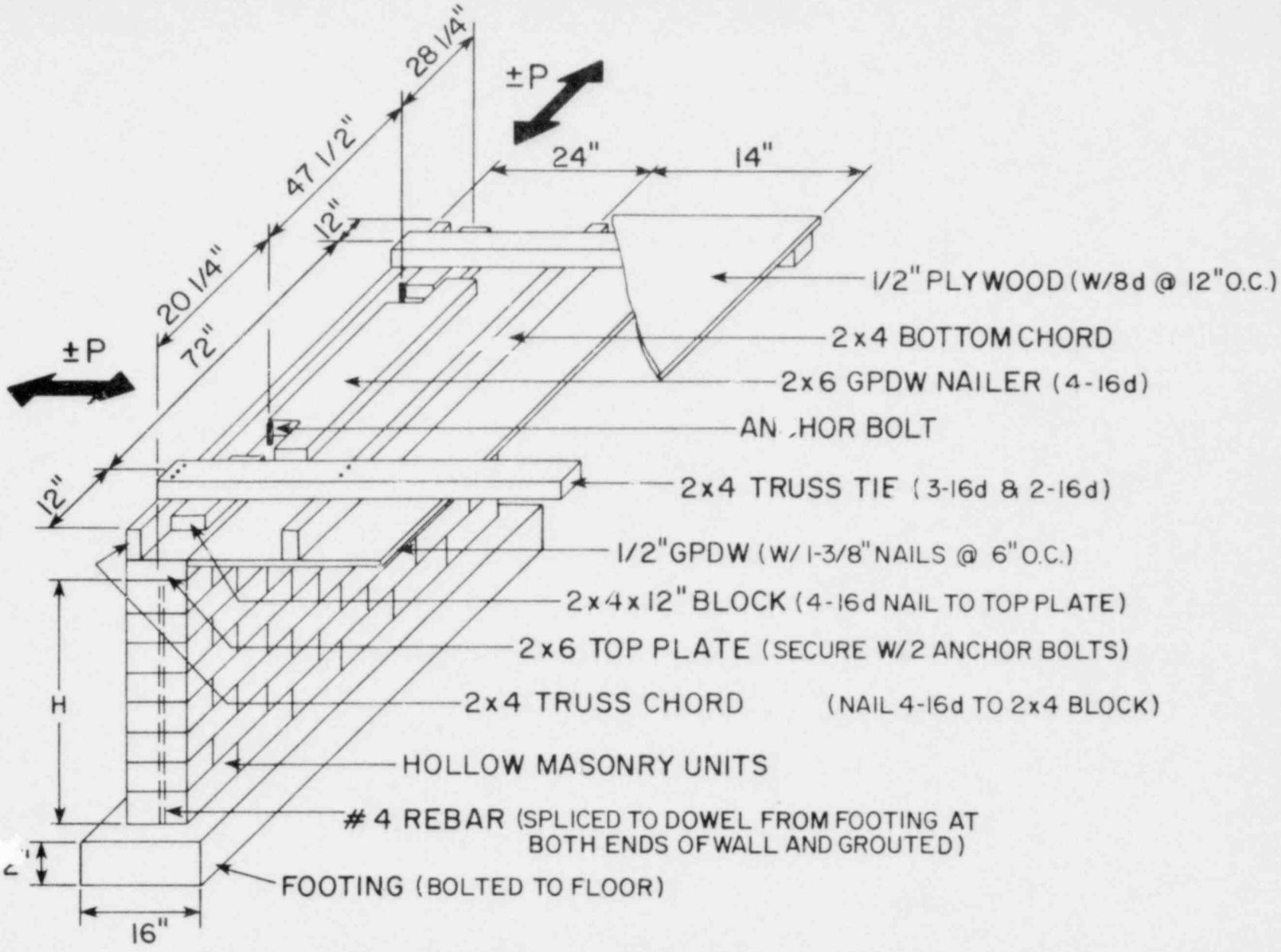

FIGURE 2.5 CONNECTIONS OF TYPE C3

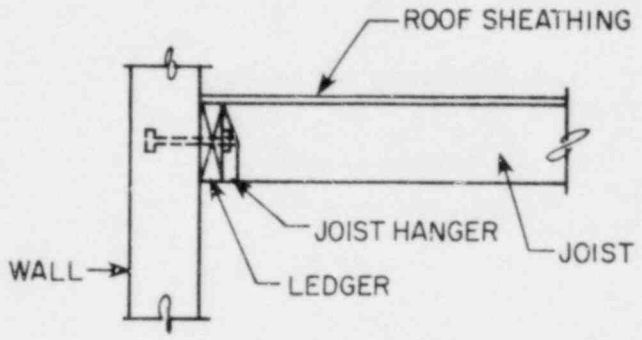

(a)

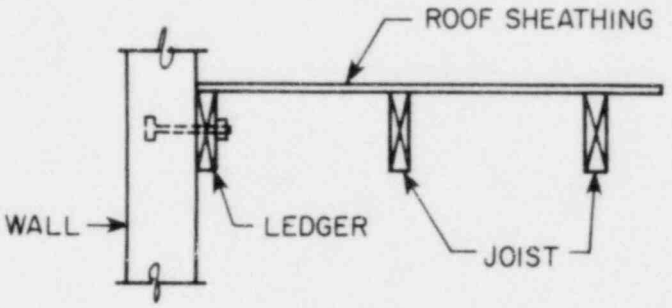

(b)

FIGURE 2.6 TYPICAL FLAT ROOF CONNECTIONS

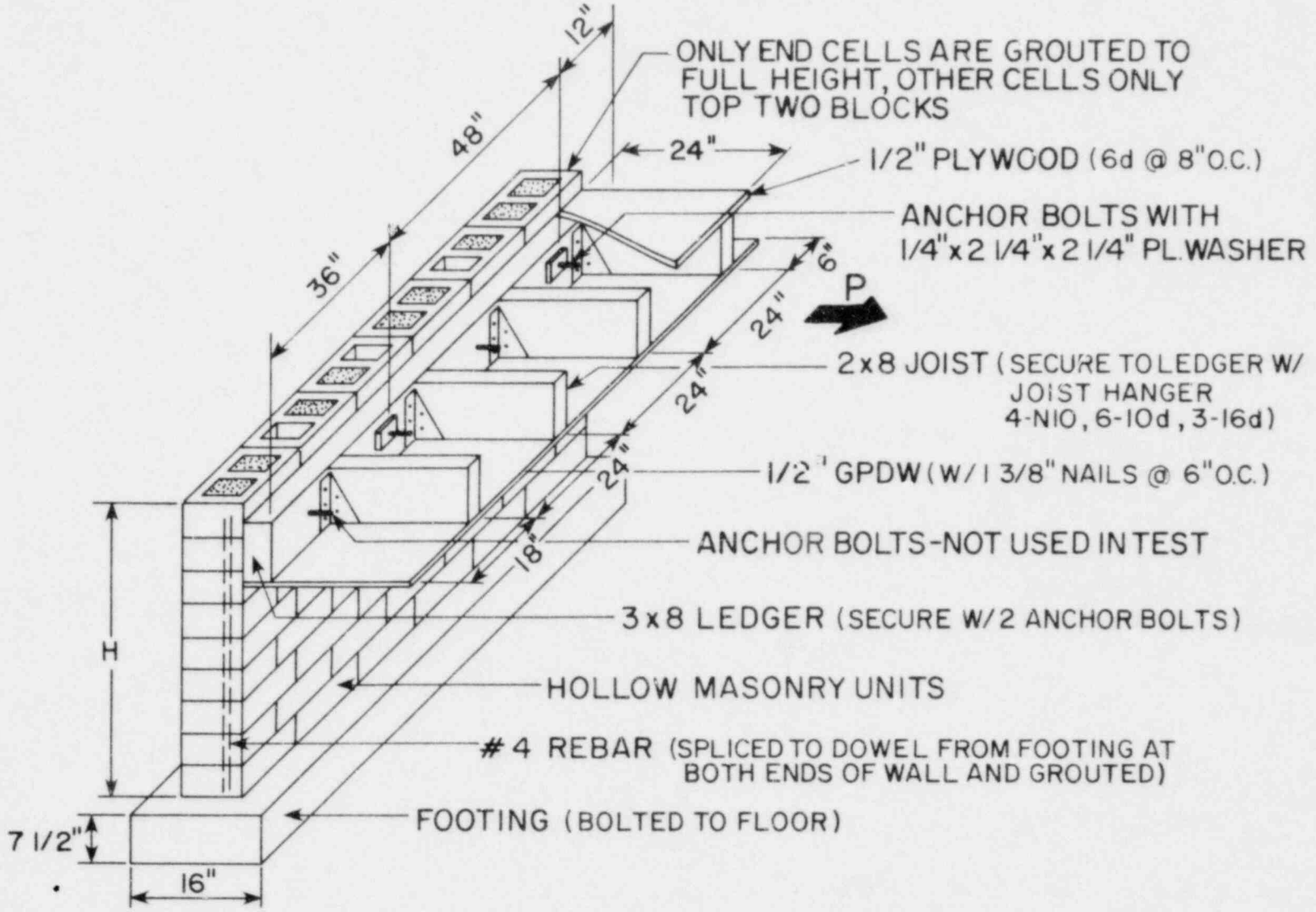

FIGURE 2.7 CONNECTIONS OF TYPE C4

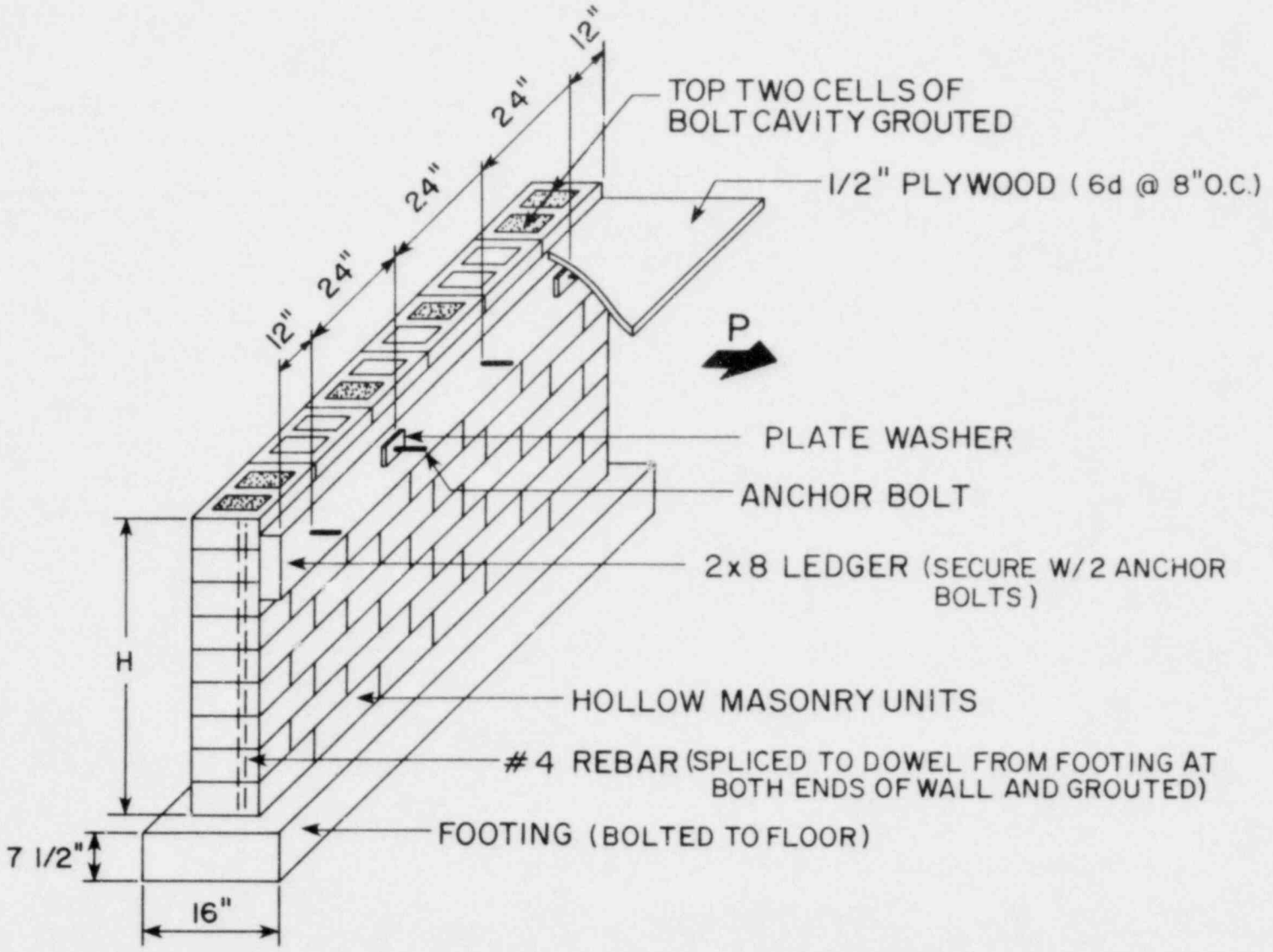

FIGURE 2.8 CONNECTIONS OF TYPE C5

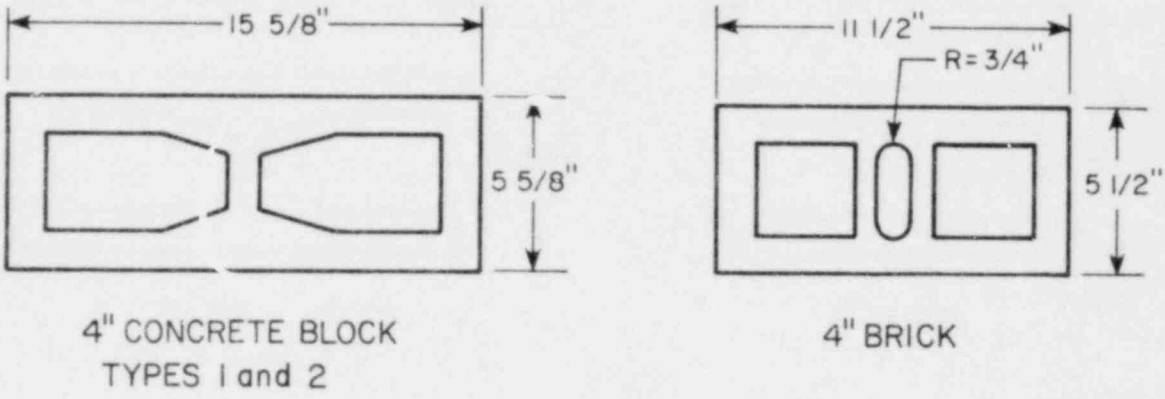

FIGURE 2.9 MASONRY UNITS

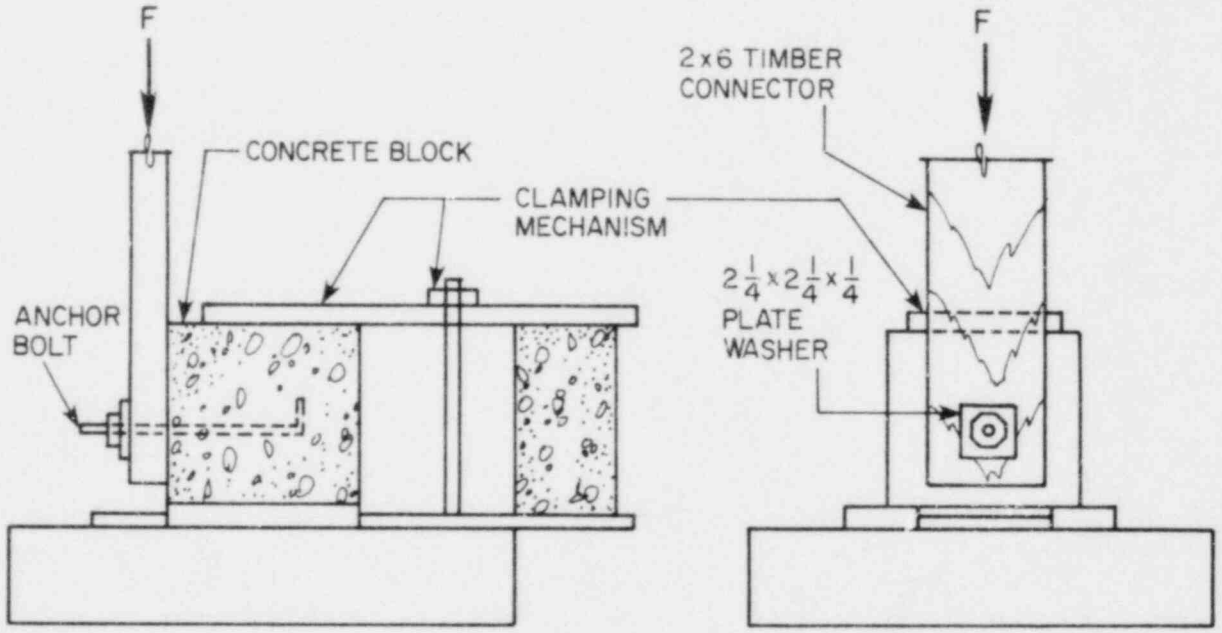

FIGURE 2.10 BOLT SHEAR STRENGTH TEST ARRANGEMENT

3. TEST PROCEDURE AND INSTRUMENTATION

3.1 Simulation of Earthquake Effects

The forces which a base motion would induce in the roof connection details were simulated by applying a series of cyclic loads at increasing amplitude to the connection assemblies. Generally, three cycles of loading (full sine wave for C1-C3, and half sine wave for C4 and C5) at a given displacement amplitude constituted a test "run". After each run, the measuring devices were checked to ensure that they were still within their recording range, and cracks and separations were noted. The electro-hydraulic actuator used during Phase 1 of the test program had a capacity of 20 kips and a stroke of 12 in. For Phase 2 a 100 kip actuator was employed. The attachment pieces for transmitting the actuator force to the test specimen depended on the geometry of the type of connection.

For specimens of type C1, the in-plane force from the actuator was applied to the plywood sheathing by a 7 ft extension, which was attached to the load cell at the end of the actuator on one side and to a 60x15 in. steel plate bolted to the plywood sheathing on the other. The actuator extension was pinned to the steel plate so that slight vertical movements which accompanied the induced horizontal displacements did not introduce vertical forces. This attachment is illustrated in Fig. 3.1.

For connection models designated as group C2, it was necessary that all four joists (see Fig. 2.3) be subjected to equal forces. To achieve this, the loading attachment illustrated in Fig. 3.2 was constructed. It consisted of two 7-in. deep channels with a central structural tube welded at the middle. The actuator extension was inserted into the tube and pinned at the end so that slight rotations about a vertical axis would not cause bending of the actuator cell. The weight of the attachment was

balanced by a stand supported on an inflatable air bag.

Because of the similarity of the transverse loading requirements for connection models of the C3 group, the same attachment used for C2 was employed again with only a slight modification. The truss-like attachment was bolted to the 2x4 in. "truss ties" placed 6 ft apart (Fig. 2.5) and the cyclic displacements of the actuator were introduced into the roof assembly through these elements. The testing arrangement is illustrated in Fig. 3.3. When the connection was tested in the in-plane direction, the specimen was rotated 90 degrees and the actuator was directly linked to the 2x4 in. simulated bottom chord and the rest of the components for the model were eliminated.

Specimens designated as C4 were subjected to half-sine loading cycles in the same manner as connection models of type C2. The similarity of the four 2x8 in. joists (Fig. 2.7) to the truss bottom chord elements made it possible to use the "strongback" shown in Fig. 3.2 in this series of tests also. The stand and air bag arrangement again supported the weight of the steel attachments. Likewise, plywood sheathing for specimens of type C5 was clamped at a spacing of 2 ft by means of metal connectors which in turn were bolted to the same strongback used in testing all of the transversely loaded roof mock-ups. In Fig. 3.4 a test for a specimen of the C5 group is shown in progress.

The effect of the vibration of the roof was simulated by initially applying three displacement controlled cycles of loading at an amplitude of 0.1 in. Testing was continued by increasing the induced displacement limits in increments of 0.1 or 0.2 in., and was terminated when the strength of the connection assembly was judged to have been reached. Because there will be numerous references to the roof connection models later in the text and because there were physical differences between

models of a given type, the significant features of all 19 specimens are tabulated in Table 3.1.

3.2 Instrumentation and Data Acquisition

The structural behavior of the connections was monitored and recorded by means of an array of transducers. Measurements for specimens of the C1 type included rotation and slip of two typical bottom chord elements (one with and the other without the metal framing anchor) with respect to the top plate, rotation and slip of a chord with respect to the plywood, total in-plane wall displacement, and top plate slip relative to the wall, in addition to actuator force and actuator travel. The simultaneous measurement of rotation and slip was made by means of the displacement measuring attachment shown in Fig. 3.5. With the direct current displacement measuring transducers (DCDTs) reading the displacement of a "bottom chord" element at two different heights, the rotational and translational components of the total motion could be extracted from simple geometrical relations.

The measured quantities for the second group of specimens (C2) included transverse wall displacements, relative joist-plate movements, plate-wall slips as well as actuator force and total displacement readings. Type C3 connections were tested in the transverse direction during Phase 1 when measured quantities included lateral wall displacements, rotation of the "bottom chord" above the top plate (see Fig. 2.5), displacements of the truss ties relative to the two blocks, and top plate slip relative to the wall, in addition to actuator force and displacement. When additional experiments were undertaken, intact walls from the earlier sequence of tests were used again Measurements of the in-plane tests included relative slip of the bottom chord to the top plate and to the

nailing blocks, slip of the top plate relative to the wall as well as the usual actuator load and displacement.

As pointed out earlier only the "pull" type of loading was performed on specimens of the C4 and C5 types. The quantities measured in the first group were the separation between the ledger board and each of the four joists (Fig. 2.7), wall-ledger separation at points adjacent to the bolts and plywood-ledger relative slips measured above the bolts, as well as transverse wall displacements. As with all other specimens, the actuator force and displacement were also included in the measurements. In the final group of specimens of type C5 (Fig. 2.8), in addition to the usual actuator force and travel readings, the monitored quantities were the following: separation of the upper edge of the ledger from the wall measured above the bolts, separation of the plywood from the ledger board, and transverse wall displacements. When additional experiments were conducted during Phase 2, direct pullout readings were also made of the anchor bolts for both types of specimens.

The total capacity and resolution of all measuring devices were selected such that accurate readings could be made within the expected range of behavior. After each test run, all transducers were checked to ensure that they were still properly anchored and aligned, and that the displacements they were measuring were still within range. If this was not the case for any particular transducer, it was either disconnected or readjusted. In Chapter 4, where test results are presented in quantitative terms, additional references will be made to the exact locations of the instruments.

The signals obtained from the direct current displacement transducers (DCDTs) were conditioned and amplified before they were read by means of a high speed scanner (Kinemetrics model DDS-1103). A constant scan rate of

5 Hz was adopted for every channel that was read, i.e., each transducer output was read 5 times a second and recorded in digital form on a magnetic tape. Data stored on the "raw" tapes were later transferred to a permanent data file tape compatible with the CDC 6400 system.

TABLE 3.1

FEATURES OF CONNECTION MODELS

No.	Reference Code	Wall Material	Construction Phase	Test Phase	Lateral Wall Support	Max. Imposed Disp., in.
1	C1-28-5/8	Conc. Block	1	1	---	0.5
2	C1-28-1/2	Conc. Block	1	1	---	0.5
3	SC2-28-5/8	Conc. Block	1	2	Yes	0.6
4	SC2-28-5/8 (2)	Conc. Block	1	2	Yes	0.6
5	C3-32-1/2	Conc. Block	1	1	No	0.9
6	C3-52-3/8	Conc. Block	1	1	Yes	0.9
7	C3-28-3/8-IP	Conc. Block	1	2	---	0.6
8	C3-28-5/8-IP	Conc. Block	1	2	---	0.6
9	C3-28-5/8-3/8-SP	Conc. Block	1	2	---	0.6
10	C4-36-5/8	Conc. Block	1	1	Yes	0.9
11	C4-56-1/2	Conc. Block	1	1	Yes	1.1
12	SC4-36-5/8-1450	Conc. Block	1	2	Yes	0.5
13	SC4-36-5/8	Conc. Block	2	2	Yes	0.6
14	SC4B-36-5/8-1450	Brick	2	2	Yes	0.6
15	C5-56-1/2	Conc. Block	1	1	Yes	0.9
16	C5-36-5/8	Conc. Block	1	1	Yes	1.0
17	SC5-36-5/8	Conc. Block	2	2	Yes	0.6
18	SC5-36-1/2	Conc. Block	2	2	Yes	0.7
19	SC5B-32-5/8	Brick	2	2	Yes	0.8

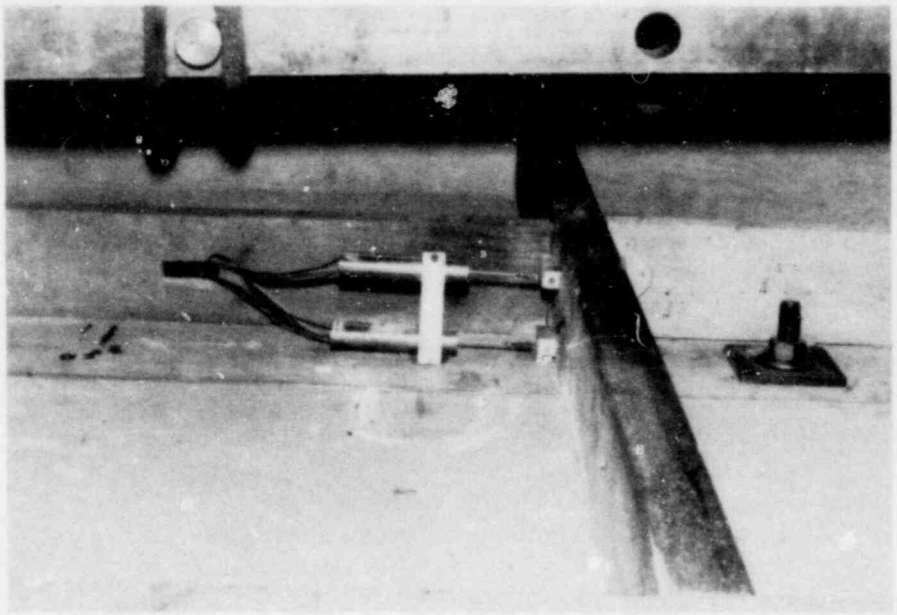

FIGURE 3.5 SIMULTANEOUS MEASUREMENT OF ROTATION AND SLIP

4. TEST RESULTS

4.1 Introduction

Measured strength and deformation characteristics of the test specimens are described in this chapter. As pointed out in Chapter 2 the dual requirements of effectively doubling the number of connections tested by placing two sets of anchor bolts in every 8 ft long wall as well as maintaining a spacing of 4 ft between similar bolts was relaxed when it was noted that bolts were generally not the critical elements. However, this earlier decision led to the actuator force being eccentric with respect to the centerline of the two bolts in some of the experiments. In Fig. 4.1, the exact location of the actuator force with respect to the bolts is indicated for those connections in which this eccentricity existed. Of course, for all models of the C1 group as well as the three of the C3 type which were loaded in-plane, location of bolts was immaterial. Also, for the case of the transversely loaded models of type C3 and C4 the relative positioning of the actuator force, as shown in Fig. 4.1, does not automatically determine the ratio by which it was divided between the two anchor bolts; the location of the "chords" for these specimens caused the actuator force to be shared among the bolts in a different manner from that which simple statics would indicate.

The transverse strength of transverse connections frequently exceeded that of the walls. To ensure that imposed actuator displacements resulted in deforming the connections rather than in causing the walls to displace transversely, a lateral support system was implemented. In Fig. 4.2 the two horizontal steel beams bracing the walls laterally are shown. The system reduced wall displacements considerably, but did not eliminate them totally.

A standard "package" of diagrams accompanies the discussion on the behavior of each type of connection. The diagrams comprising a given set are similar for similar connections. The deformation characteristics are described with respect to the overall force to which the specimens were subjected; therefore, the ordinate in these diagrams is always the "actuator force".

4.2 Connections of Type C1

The two C1 models were subjected to five test runs, each run consisting of three cycles of loading. The initial command amplitude on the actuator was ± 0.1 in.; this value was incremented to ± 0.5 in. in steps of ± 0.1 in. The strength of the C1 connections was controlled by the resistance against rotation and slippage provided by the four "bottom chords" nailed to the top plate (Fig. 2.2). In order to provide similar strength in both directions of loading, the direction in which two of the three 16d-nails were toe-nailed was alternated between adjacent joist elements. The proprietary metal framing anchors nailed into every other joist were known to be ineffective against "shear", however, to produce a faithful duplication of roof connections typically built in masonry residences, these were nailed as shown in Fig. 2.2.

A description of the deformation of the specimens is provided in Figs. 4.3 and 4.4. The general appearance of many of these diagrams is affected by the signal-to-noise ratio of the recorded DCDT voltage outputs. Although these were measured, there was no noticeable displacement at the top of the walls or relative slip between the top plate and the walls, and the corresponding diagrams are excluded from the set which is presented. The anchor bolts were provided with 2½x2½x1/4 in. plate washers which were followed by regular washers. The absence of top plate movement

indicates that the bolts themselves did not deform significantly. Inspection of the grout around the bolts after the tests indicated no cracking.

Both specimens exhibited increasing strength with additional cycling at greater amplitudes. Although both were constructed according to the same specifications, C1-28-1/2 developed a maximum resistance of 3.55 kips at the end of the first negative half cycle with an amplitude of 0.5 in., whereas the corresponding value for C1-28-5/8 was 2.44 kips. The cyclic behavior of the specimens was characterized by the separation of the joists from the top plate in a similar fashion to when two nailed pieces of wood are worked loose from one another by twisting one in alternate directions. Figures 4.3(a) and 4.4.(a) depict the general behavior of the specimens in terms of the actuator force and displacement. At the end of the last loading cycle, the gap between the top plate and the bottom chord elements was between 1/8 and 1/4 in.; the framing anchors appeared to be effective in reducing this separation. The absence of vertical forces to simulate roof dead load also contributed to the uplifting of the chords from the top plate. At the end of the fourth cycle for C1-28-5/8, because of the excessive rotations of the joists, the cores of the DCDTs attached to these members could no longer maintain the orientation required for correct measurements, and they were disconnected. Hence, although there were five runs, only the first four are represented in Figs. 4.3(b)-(f). The rotation of the chords was determined by measuring the lateral displacement at two points along the height and dividing the difference by the distance between them. The slip then follows from the total lateral displacement at any one of these points and the contribution of rotation to that displacement. The rotation of a chord with the metal framing anchor (referred to as a strap in the figures) with respect to the plywood sheathing, shown in Fig. 4.3(b), is not correct

because of a malfunctioning measuring device. However, comparison of Fig. 4.4(b) with Fig. 4.4(e) indicates that the amount of rotation relative to the more flexible plywood was about three times greater than that relative to the rigid top plate.

Figures 4.3(c), (e) and 4.4(c), (e) indicate that the rotational component of the lateral displacement of the chords is partially reversible. The curves describing the rotation of the chords are qualitatively similar to the overall force-displacement response obtained from the actuator. However, the slip components shown in Figs. 4.3(d), (f) and 4.4(d), (f) represent permanent deformations which apparently can only be recovered by applying force in the opposite direction. The striking dissimilarity between the characteristics of these figures is observed particularly well in Fig. 4.4 in which the final excursion limits are greater. Rotation of the joists was resisted also by the 1x4 in. frieze boards which blocked the space between them. However, the 8d-nails on either side of the frieze boards frequently split the wood and did not provide complete fixity. Also, for rotations of the magnitudes involved, the tightness with which the boards were fitted into the 2 ft wide gap between the chord members appeared to be a potential source of asymmetrical behavior under load reversals. The asymmetry of the rotations of the joist without the framing anchor, shown in Fig. 4.4(c), was probably caused by this effect. Measurements of the slip and rotation of the joists were made on the middle two (see Fig. 2.2), so that the directional bias caused by the frieze boards would be minimized. Any asymmetry of the response of the chords with the framing anchors, shown in Figs. 4.3(e), (f) and 4.4(e), (f), should be attributed to the effect of the frieze boards as well as the anchors themselves. The anchors were nailed to one side of the chords so that during load reversals they were alternately called

upon either to stretch (providing a great resistance against rotation) or to bend (when their contribution was negligible).

A summary of the strength and deformability of the connections determined from the actuator readings is provided in Figs. 4.3(g), (h), and 4.4(g), (h). The first diagram in both sets is a plot of the average actuator force versus the average actuator displacement, denoted as the "envelope of hysteresis loops". The average force is determined by taking the average of three consecutive "positive" and "negative" loading cycles at a given excursion limit. The initial stiffness is defined as the ratio of the average resistance during the first three cycles to the corresponding displacement amplitude. Figures 4.3(h) and 4.4(h) describe the reduction in the similarly defined stiffness values of the following cycles expressed as a fraction of the initial stiffness. The initial stiffnesses for C1-28-5/8 and C1-28-1/2 were 9.24 and 12.12 kip/in., respectively. The average stiffness at the end of the fifth run decreased to about one half of the value at the beginning for both specimens. Also, there was no reduction in strength up to the larger cycles of imposed displacements, which are excessive for the type of connection simulated in the tests.

It is difficult to predict what effect roof dead load would produce on the observed response, or to state if the simulation of the truss depth above the chords would have led to significantly different behavior. The reasonable assumption that each of the four "bottom chords" was subjected to the same shear and twisting moment, and information on the geometry of the specimen given in Fig. 2.2 permit the determination of the shear force-slip or twisting moment-rotation curves. These would of course be identical to the curves given in Figs. 4.3 and 4.4, but would have different scales

4.3 Connections of Type C2

From a comparison of Figs. 2.2 and 2.3 it can be seen that these connections were intended to simulate the transfer of out-of-plane effects on load bearing walls. Essentially, the specimens in the C1 group were rotated 90 degrees, and the horizontal loads were applied into the four 2x4 in. joists which were nailed to the top plate. The two C2 specimens tested both had the same wall height (28 in.) and bolt diameter (5/8 in.); for identification purposes the second model is referred to as SC2-28-5/8(2). During testing both specimens were restrained laterally so than any applied loading resulted in deformation mostly within the connection; the greatest stroke of the actuator was 0.6 in. for both tests.

The structural design of the C2 specimens was intended to model details of a simple masonry house subjected to simulated earthquakes[17]. In reference (17) the observation was made that the restraint provided by the roof assembly controlled the response of laterally unrestrained transverse walls. However, for cases where these walls are laterally stiffened by normally intersecting walls, their strength under load reversals would have a significant influence upon overall structural behavior.

Structurally, these connections were the simplest to model. With reference to Fig. 2.1 for purposes of illustration, and assuming base motion to occur in the direction of the 2-2 axis, roof action in the wall would in fact be as depicted in Fig. 2.3. For these connection mock-ups, there was no need to include the sloping upper truss chord elements since the strength of the connection is not derived from them. The function of the plywood sheathing was to help distribute the actuator force, applied directly to the joists (see Fig. 3.2), more evenly among the anchor bolts.

Measured quantities are displayed in Figs. 4.5 and 4.6 for models SC2-28-5/8 and SC2-28-5/8(2), respectively. As shown in Fig. 2.3, two

of the "joists" were connected to the top plate by proprietary metal framing straps in addition to three 16d-nails which were provided for all joists. The slip of all joists relative to the top plate, as well as the slip of the top plate relative to the wall adjacent to the two bolts, were continuously recorded, in addition to actuator functions and transverse wall displacements.

It is apparent that although both connections were subjected to the same displacement limits, wall deformations in SC2-28-5/8(2) were greater (Figs. 4.5(b) and 4.6(b)). This caused the overall limits of the joist slip readings in Fig. 4.6 to be less in magnitude than the corresponding quantities in Fig. 4.5. There are, however, qualitative similarities between Figs. 4.5 and 4.6. First, "negative" actuator forces corresponding to pushing the wall away from the horizontal strut supports caused greater displacements at the top of the walls. (The quantities displayed in Figs. 4.5(b) and 4.6(b) were both measured centrally 2 in. below the top edge of the wall.) With the imposed negative displacement absorbed by the deformation of the wall, joist slip readings were all biased towards the "positive" half cycles. Secondly, it can be verified from the response of both models that the sum of wall displacement, joist slip and top plate slip readings is roughly equal to actuator displacement, although individual readings do not resemble the overall response represented by actuator force - travel plots. It is significant also, that the presence of framing anchors on individual joists did not reduce the slip of such joists although the imposed longitudinal displacements were in the direction in which they would be effective. It is plausible to argue that the two joists with the metal anchors resisted a greater part of the actuator force because the plywood sheathing and the "strongback" attachment shown in Fig. 3.2, were coupled to form a rigid

"diaphragm" forcing the joists through equal displacements regardless of strength. Frames (c) through (f) of both Figs. 4.5 and 4.6 verify this.

The nuts on the anchor bolts were tightened with a wrench, but no torque measurements were taken. Also, bolt holes in the top plates were drilled 1/4 in. larger than the bolts themselves. Naturally, the amount of top plate slip relative to the walls is a function of the tightness of the nuts and roughness of the top of the walls, as well as the amount of play around the bolts. Slip readings were taken adjacent to the two bolts and these are shown in frames (g) and (h) of Figs. 4.5 and 4.6. Both sets of diagrams are typical of the force-deformation characteristics for systems governed by Coulomb friction; i.e., slip is induced only when the imposed force is in excess of frictional resistance. For specimen SC2-28-5/8 the top plate apparently slipped in equal amounts near both bolts, whereas, for SC2-28-5/8(2) it was observed during testing that the plate seemed to rotate about the left bolt while translating in the vicinity of the right bolt. This is verified in Figs. 4.6(g) and (h). Later inspection revealed that the right bolt had widened the hole in the top plate through alternate crushing resulting from excessive bearing stresses. The bias in Fig. 4.6(h) suggests that the bolt may not have been located centrally within the hole in the beginning.

The last two frames in both figures indicate the strength envelope and stiffness reduction for the connections. Since the strength envelope is based on the average resistance of the connection measured during three consecutive cycles, it is a more reliable index of maximum strength and is not governed by peaks which may be attained during the first cycle of loading at a given amplitude, but which may not be attained again. A complete evaluation of the resistance and stiffness degradation for each connection will be made in Chapter 5.

As suggested by the top wall displacement readings, wall components were cracked above the lateral supports in both specimens. However, bolts were intact and did not deform within the cells where they were grouted.

4.4 Connections of Type C3

These connections were designed to yield information on the mechanism of inertia force transfer between in- or out-of-plane walls, spanned by the outermost trusses and the roof diaphragm. With reference to Fig. 2.1 which represents a single-story masonry house and assuming the base motion to occur either exclusively along the 1-1 axis or along the 2-2 axis, then the connections at the gabled ends of the roof assembly would be subjected to forces described by Fig. 2.5. A commonly encountered type of connection is achieved by nailing blocks at 6 ft intervals, to the top plate to which the bottom chord of the truss above the transverse wall is nailed horizontally (Fig. 2.4). The representation of this type of connection in the test program did not have the third dimension corresponding to the height of the trusses although the plywood sheathing nailed above the truss ties was intended to represent partially the action of the sloped roof sheathing (Fig. 2.5). In the shaking table experiments[2,3] the truss ties were not continuous across all roof trusses, but were terminated at the third truss chord at a distance of 4 ft from the face of the wall. The structural action of the truss ties is to reduce the lateral displacement of the bottom chords by providing a restraint which augments the action of the gypboard sheets nailed underneath the chords. The actual magnitudes of the transverse forces transmitted by the connection are a function of the in-plane stiffness of the gypboard units relative to the ties, as well as the degree of horizontal fixity provided by the nailed blocks at the top plate. With forces applied normal to the plane of the wall, the strength of the connection assembly is derived primarily from the rotational restraint

of the bottom truss chord nailed horizontally to two 1 ft long blocks of the top plate, but an additional restraint would be available at the truss supports where the chord is toe-nailed and anchored with a metal anchor to the top plate of the intersecting wall. Also, the diaphragm forces transmitted by the drywall could only be partially represented by the arrangement shown in Fig. 2.5 since the cyclic loads were applied only to the ends of the truss ties.

Five connections of type C3 were tested. Two of these were subjected to transverse forces, and three were tested in the in-plane mode. The fifth connection designated as C3-28-5/8-3/8-SP differed from the others in that rather than representing an intermediate 8 ft long part of the connection, the entire in-plane fixity along a 16 ft long truss bottom chord was represented. In this model, the truss bottom chord was nailed with four 16d-nails to three 1 ft long 2x4 in. blocks at a spacing of 3 ft. The blocks themselves were similarly nailed to the 2x6 in. top plate. Additionally, at either end of the wall the support fixity of the truss was modeled with three 16d-toe nails driven into the chord as well as metal framing anchors with a maximum allowable load of 290 lb. Both sets of bolts on the wall were tightened to the top plate during testing.

For the two models tested in the transverse direction, maximum imposed displacement limits were ± 0.9 in. with intermediate cycles at 0.1, 0.2, 0.3, 0.5, and 0.7 in. Measured response quantities are given in Fig. 4.7 for C3-32-1/2 and Fig. 4.8 for C3-52-3/8. From the first plot in each group of diagrams it is seen that the maximum forces attained were never more than 1.0 kip; therefore, the flexural yielding capacity of the walls in the transverse direction was not exceeded. However, specimen C3-32-1/2 underwent displacements at the top of the wall exceeding 0.25 in. during the final three cycles as shown in Fig. 4.7(b). To guard against

the flexural failure of the wall, the taller specimen C3-52-3/8 was braced laterally by means of horizontal struts so that the contribution of the wall deformations to the observed actuator displacements was minimized. A comparison of Figs. 4.7(a) and 4.8(a) shows that the effect of wall bracing on the measured connection strength was not significant.

During cyclic loading it was noted that the drywall sheets nailed underneath the simulated bottom truss chord 2 ft from the wall, and the nailing block at the edge of the top plate were effective in transmitting a part of the imposed force in the "compressive" half cycles; that is, when one edge of it was in direct contact with the side of the top plate. However, this contact produced a disintegrating effect on the gypsum board edge which began to fray with increased cycling. Also, the cyclic nature of the loads destroyed the fixity of the 1-3/8 in. long dry-tite nails in the sheetrock around which a gouging effect was evident. The capacity of the sheetrock to "pull" on the wall, as illustrated in the sequence in Fig. 4.9, was rapidly diminished. The implication of this observation is that drywall sheets contribute no significant diaphragm action during continued cyclic loading, because of their brittleness.

The slip of the top plate relative to the wall was not large enough to be measured in specimen C3-32-1/2. For specimen C3-52-3/8 the average of the readings taken at the bolt locations is shown in Fig. 4.8(b). This variable is a function of the tightness of the bolts and the friction at the interface between the top plate and masonry. Rotation of the bottom chord was derived from displacement transducers mounted on the two 1 ft long blocks. Figures 4.7(c) and 4.8(c) show the average of the two readings as a function of the actuator force. Inasmuch as the chord bears against the blocks during the "compressive" half cycles and is pushed away from them during the "tensile" half cycles, there is asymmetry

in the rotations. This is more pronounced for specimen C3-52-3/8. During the half cycles when the actuator travelled in the opposite direction to that shown in Fig. 4.9(b), the strength of the assembly was derived only from the pullout strength of the eight 16d-nails (Fig. 2.5) in the blocks and the rotational restraint on the bottom chord provided by the truss ties. It is interesting to note that for equal displacement limits imposed by the actuator on specimen C3-32-1/2, rotation of the bottom chord and the slip of the truss tie away from it occurred between increasing limits indicating progressive pullout of the nailed connections (Figs. 4.7(c) and (d)). During the last three cycles of loading for this specimen, the transducer measuring the relative slip of the truss tie was removed because the excessive rotation of the bottom chord made it impossible to obtain linear measurements. This tendency apparently, developed earlier for specimen C3-52-3/8 because there is strong evidence to indicate that during "negative" slips the core of the DCDT did not travel freely and was affected by friction as shown in Fig. 4.8(d).

The average transverse strength of both specimens remained below 800 lb, a force level at which bolt diameter is not of significance (see Table 2.6). The average initial stiffnesses of 3.15 and 2.15 kip/in. for the connections diminished as indicated in Figs. 4.7(f) and 4.8(f). The imposed rotation on the bottom chord was well beyond the order of magnitude which would be attained in an earthquake-induced environment[2], but as for specimens in group C1 this large deformation was necessary to determine the strength of the connections.

For the in-plane test of connections of type C3, the only items retained from the specimen of Fig. 2.5 were the truss chord above the top plate and the 1 ft long blocks to which the chord was nailed by four 16d-nails. One end of the 2x4 in. bottom truss chord was extended and linked

directly to the actuator, an arrangement shown in Fig. 4.10. Measurements were made of the relative motion between the chord and the top plate, as well as between the blocks (numbered in increasing order from the end of the wall away from the actuator) and the bottom chord. Relative slip of the top plate to the wall was also recorded, but was insignificant for connections C3-28-3/8-IP and C3-28-5/8-IP. Predictably, the greatest strength belonged to model C3-28-5/8-3/8-SP, and for this model some slip occurred between the wall and the top plate although all four bolts were tightened. Hysteretic force-deformation diagrams are presented in Figs. 4.11 - 4.13. The frames displayed in part (b) of each figure indicate that the bottom chord followed the actuator displacement exactly noting the absence of top plate slippage for the first two connections. The difference between parts (a) and (b) of Fig. 4.13 which reaches a maximum of 0.07 in. during run 6 is attributable to the slip of the top plate and the deformation of the chord itself. In spite of this minor difference the following features were common to all C3 connections loaded in-plane:

(a) Force-deformation characteristics are strongly reminiscent of the cyclic behavior of reinforced concrete beams with low shear span-depth ratios.

(b) The sum of relative bottom chord-block and block-top plate movements are constant and equal the imposed displacement. However, although both chord-to-block and block-to-top plate connections were made with four 16d-nails, the former contributed to the measured deformation to a much greater extent. This may be explained by noting that when the nails were driven vertically into the blocks and the top plate, the blocks were in effect post-tensioned. Therefore, resistance to forces was derived from

friction as well as nail deformation.

(c) No failures in the walls or bolts occurred for either type of loading.

Inspection of chord-to-block nailing after the completion of the tests indicated that under cyclic forces the nails had gouged wedge shaped spaces in the wood, and could develop progressively increasing forces only if imposed displacements tended to enlarge the wedges by causing the nails to bear further against them.

Strength envelope and stiffness reduction curves constitute the last two frames in Figs. 4.11 - 4.13. In Chapter 5, a comparison of code allowable loads and measured strengths of connections is offered.

4.5 Connections of Type C4

The computed transverse strength of the masonry walls for C4 specimens showed that it was necessary to provide lateral supports to the walls in order to avoid flexural failure at the footing junction. For all specimens tested, the centerline of two horizontally placed steel restraining I-beams was approximately 1 ft below the bolts. To reduce the bearing stresses in the walls and to avoid punching of the lateral supports into the walls square plates were welded at the ends of the I-beams. Further, the narrow gap between the plate and the wall was filled with a quick-curing gypsum cement so that, as soon as a horizontal force was applied to the connection, the beams would function as supports. In Fig. 4.2, the arrangement is shown during the testing of specimen C4-56-1/2.

The bolts were tightened with 2½x2½x1/4 in. plate washers. Also, the action of the actuator was transmitted to the four joists in the same plane as the bolts. Because of the difference between the distances of the bolts from the top of the wall due to construction tolerances, measured average distances from the top of the ledger board (see Fig. 2.7) to bolt center-

lines varied from 3 to 4-1/8 in.

As implied in Table 3.1 specimens designated as C4-36-5/8 and C4-56-1/2 were tested such that the actuator centerline was not located midway between the bolts. If it is assumed that the actuator force diffused uniformly through the plywood and the joists into the ledger board, then the "left" and the "right" bolts in Fig. 4.1 should resist 5/8 and 3/8 of the total applied load, respectively. In the following, a discussion will first be made for the eccentrically loaded connections for which no roof load was simulated. In the second part of the discussion, the three symmetrically loaded moduls will be described.

Specimen C4-36-5/8 was subjected to six test runs at half-sine amplitudes of 0.1, 0.2, 0.3, 0.5, 0.7 and 0.9 in. For specimen C4-56-1/2 the same sequence was followed by three additional cycles at 1.1 in. for a total of seven runs. Because of recording equipment malfunction, however, the fourth run (amplitude 0.5 in.) could not be recorded and is not reported in the corresponding set of diagrams. The measurement of the wall displacement was made at the geometric center of the wall 6 in. from the top. Separation of the four joists from the ledger board was measured in the same horizontal plane as the bolts. However, these measurements are not included in the set of figures describing the deformation because the small measurements were strongly affected by "noise" in the recording environment and reached a maximum of only 0.06 in. during the fifth run of specimen C4-56-1/2. The lack of consistency for the separation of different joists from the ledger in the same specimen indicated that they were subjected to different pull forces with the difference being dictated by the amount of "lack of fit" between the loading arm (Fig. 3.2) and the timber components. Additional measurements were also made for plywood slip relative to the two outside joists, but these also are omitted because of

the insignificant amounts of deformation involved.

For both specimens in this category, the observed deformation stemmed largely from displacements induced in the walls. Comparison of parts (a) and (b) of Figs. 4.14 and 4.15 supports this statement. The hysteretic nature of the response of the assembly required the application of a "negative" force to bring the actuator displacement back to zero, and the magnitude of this force became progressively larger. During the final two cycles at an amplitude of 0.9 in. for specimen C4-36-5/8, the DCDT measuring the wall displacement shifted, indicating a sudden permanent slip of 0.3 in. Although this coincided with the pulling out of the "left" bolt, its occurrence is still puzzling since wall displacement should be independent of bolt slip. A careful examination of Fig. 4.14(c) shows that during the first three runs, the 5/8 in. diameter bolt experienced no slip. When the actuator travel was increased to 0.5 in., the bond between the grout and the steel bolt was suddenly destroyed and it slipped approximately 0.05 in. During the next three cycles of loading at an actuator displacement amplitude of 0.7 in., this slip was doubled and retained its strongly plastic character. With a further increase in the imposed displacement, the bolt ruptured the face shell of the block into which it had been grouted. From that point on, the only resistance was provided by the remaining bolt on the right. Since the total actuator force was nonzero, it appears from Fig. 4.14(c) as if the failed bolt could still resist the applied loads. This is, of course, due to the manner in which the diagrams are constructed. The separation of the ledger directly above the bolts was measured with displacement transducers which had a linear range of 0.1 in. The failure of this bolt obviously destroyed the exactness of the measurements. From Fig. 4.14(d) it appears that the behavior of the bolt on the right (the directions are determined according to Fig. 4.1) during the first

three test runs was very similar. However, the impending pullout of the companion bolt and its gradually accumulating slip were converted into an apparent negative separation due to the uneven distortion of the ledger. (Note that the horizontal scales for Figs. 4.14(c) and (d) are not the same.) A study of Figs. 4.15(c) and (d) indicates that for specimens C4-56-1/2 also the distortion of the ledger adjacent to the left bolt was greater than that at the right. Although there was no cracking around the face shell containing the bolt, an extrapolation of the behavior of the corresponding bolt in specimen C4-36-5/8 indicates that it would also have been pulled out if the wall had not reached its flexural strength first. Again the distortion of the ledger board from which the readings were taken partly obscures the exact slip of the bolts.

The absence of measurable relative movement between the joists and the top plywood indicates that a very small portion of the applied load was transferred by the diaphragm action of the plywood sheathing. Likewise, the drywall plate nailed underneath the joists (Fig. 2.7) contributed very little to diaphragm behavior because of the much greater in-plane stiffness of the joists. Loosening of the dry-tite nails in the drywalls was not observed in either specimen.

Behavior of the first two specimens appeared to indicate that the limiting factor in the strength of the connection was the pullout strength of the bolts. This strength is dependent on the type of masonry material, grout properties, care with which grout was placed in the cell with the bolt and the proximity of the bolt to the web of the masonry unit, in addition to the magnitude of gravity load on the bolt. Because of the complicated interdependence of these factors, the limited number of pullout tests conducted on concrete block units yielded significant scatter (Table 2.5). In the second group of C4 type connections the actuator force was applied

midway between the bolts. A roof dead load of 180 lb/ft was included in two connection mock-ups, one of which was bolted to a brick wall. The third specimen was similar to C4-36-5/8 except that it was constructed with a different shipment of concrete block. Measurements of the deformation of connections SC4-36-5/8-1450, SC4-36-5/8, and SC4B-36-5/8-1450 are contained in Figs. 4.16, 4.17, and 4.18, respectively.

Connection model SC4-36-5/8-1450 was subjected to five runs of imposed displacements, each run consisting of three half cycles. As with all other transversely loaded models the actuator force caused deformations in the wall as well as in the connection itself. Wall displacement was measured in the same plane as the two bolts, so by examining Fig. 4.16(b) it becomes readily apparent that roughly half of the imposed displacements were transformed into wall deformations. As noted in Fig. 2.7, the four 2x6 in. joists were connected to the ledger by means of metal hangers. The specified allowable vertical load capacity for the hangers is 800 lb and the nailing schedule calls for six N10-nails into the ledger (these were replaced by six 10d-nails in actual construction) and four N10-nails into the joist itself. The height of the hanger was 4-3/4 in. so the upper 3 in. of the joists were exposed. A second modification in the nailing schedule was made by driving three 16d-toe nails in this upper portion for improved horizontal strength. As stated earlier, the attachment of the actuator arm to the specimen was made so that the bolts and the actuator force lay in the same plane. However, the joists through which the actuator force was transmitted to the bolts were connected to the ledger so that a vertical eccentricity existed between the bolt locations and the points at which joists were pinned to the ledger. Consequently, the ledger was subjected to a complex set of forces from which it underwent biaxial bending and warping. Whereas, in the first two

connections bolt pullout was measured indirectly by two DCDTs placed on the top edge of the ledger above the bolts and connected to the wall, a direct measurement was undertaken for the last three models. As Fig. 4.16(f) indicates, the ultimate strength of the connection assembly was reached when the "right" bolt was pulled out from the face of the wall. Figures 4.16(g)-(j) illustrate the separation of the joists (numbered 1-4 from the left of Fig. 2.7) from the ledger. It is significant to note that the middle two joists appear to deform more since they transmit the bulk of the actuator force to the ledger in between the bolts. Joists 1 and 4 were connected to the 2 ft long overhangs on either side of the ledger.

The maximum resistance of the connection was 5.51 kips (Fig. 4.16(k)). Again a "negative" force was required to complete a half cycle and bring the actuator displacement back to zero.

Diagrams shown in Fig. 4.17 describing the deformation of SC4-36-5/8 are included for the sake of completeness. Although this wall was constructed according to the same specifications by the same contractor, evidence of bolt embedment flaw became evident immediately. As noted in Chapter 2, rather than providing a mix of grout for walls constructed during Phase 2, the mason was instructed to substitute mortar instead. Although no apparent deficiency existed as far as the strength of the mortar was concerned, it was noted that the bond between the masonry unit and the two block high pour of mortar containing the 3 in. embedment of bolt was poor due to shrinkage and lack of adhesion. Consequently, as soon as a force was exerted on the bolt, its resistance to pullout was derived only from the face shell strength of the masonry unit. As Figs. 4.17(c) and (d) illustrate, both bolts were quite loose in their embedments where a cone of mortar around each bolt moved relatively freely. Because of the

extremely small bolt pullout strength, the timber components were not deformed and the resistance of the assembly reached only 1.24 kips.

Inadequate bolt pullout strength was also evident during the testing of SC4B-36-5/8-1450. Deformation of the wall itself again absorbed much of the imposed displacement as shown in Fig. 4.18(b). However, progressive bolt pullout, evident from Figs. 4.18(e) and (f), limited the strength of the assembly to a maximum of 3.35 kips. The improved strength (compared with Fig. 4.17) obviously stemmed from the greater pullout force required to fracture the face shell of the brick units. Deformations of the joist hangers displayed in frames (g) and (h) of Fig. 4.18 were minimal.

An overall evaluation of the five C4 type connections indicates that if no other type of anchorage is used for linking the roof diaphragm to the wall, bolt pullout strength would have to be assessed with an extremely generous margin of safety for design purposes. The simulation of vertical roof load on the bolts did not appear to produce adverse effects on strength; however, it is plausible to argue that in an actual earthquake the bolts would be subjected to a horizontal shear in addition to vertical shear and pullout forces, a condition which was not considered in this program. The transverse flexural strength of the ledger board was augmented by the use of plate washers. Also, the nominal 3-in. thickness appeared to provide the bending capacity required by the bolt, even for the simply supported ledgers in the test specimens. Joist-ledger connection was adequately accomplished with the hangers for horizontal loads.

4.6 Connections of Type C5

In these connections the simulated unidirectional earthquake forces were transmitted into the plane of the 1/2-in. thick plywood at four equally

spaced points by means of the load attachment arm shown in Fig. 3.2. Holes for the bolts were drilled at the center of the ledger; this gave the diaphragm force a moment arm of 3.6 in. with respect to the centerline of the bolts. Specimens in this group were tested after the wall panels were laterally supported by means of horizontal struts. Because of the lower strength of the connection assembly compared with specimens in group C4, walls generally did not deflect significantly.

The separation of the plywood from the ledger board was measured at three locations (denoted as stations 1, 2 and 3). The first and third stations were directly above the left and right bolts (Fig. 4.1), and the second was placed midway between these. In Fig. 4.19, the 0.5-in. transducers at stations 2 and 3 are shown for specimen C5-56-1/2. Another set of measurements was made by means of 1-in. capacity DCDTs to evaluate the distortion of the ledger as shown in Fig. 4.20. Measurements taken by these devices are referred to as "separation of ledger from wall" in the deformation diagrams.

Connections C5-56-1/2 and C5-36-5/8 were subjected to eccentric actuator forces as shown in Fig. 4.1. No direct readings of bolt slip were taken during the testing of these models although, for the remaining three connections, measuring devices were included for this purpose. Deformation of specimen C5-56-1/2 is described in the set of drawings in Fig. 4.21; that of C5-36-5/8 is described in Fig. 4.22.

Both eccentrically loaded connections failed because of the failure of the ledger board. The eccentric pulling force applied to the top of the ledger by the plywood caused the board to bend about its weak axis, as shown in Fig. 4.23, generating cross-grain tension. During the fifth run at an imposed displacement limit of 0.7 in., the ledger board in specimen C5-56-1/2 suddenly cracked along this axis (Fig. 4.24). The

actuator force attained just before this occurred was recorded as 1.46 kips. As seen from Fig. 4.24, due to the rotation of the top of the ledger, the plywood sheathing was not normal to it at the extremes of the cycles, causing the displacement measuring devices to record substantial rotational components. During the fifth test run of specimen C5-56-1/2, the instrument at station 1 became inoperative; therefore, Fig. 4.21(b) is discontinued after the last cycle corresponding to 0.7 in. displacement. Failure of the ledger in specimen C5-36-5/8 occurred near the right bolt relative to Fig. 4.1, but in this case the axis of bending was vertical. The board deflected outward from the right side of the wall over the 36 in. moment arm, and began to break in the vicinity of the bolt on the right as seen in Fig. 4.25. This affected the ledger-wall separation readings above the bolt shown in Fig. 4.22(f). The maximum recorded actuator force was 1.69 kips. Failure of the ledger board in specimen C5-36-5/8 affected the separation of the plywood from it. Figures 4.22(b), (c), and (d) show that in going from the intact side toward the right bolt the apparent amplitude of this separation also increased. In contrast to this observation, the corresponding measurements in specimen C5-56-1/2 indicated a more uniform deformation pattern up to the point of failure as indicated in Figs. 4.21(b), (c) and (d).

Anchor bolts in specimens C5-56-1/2 and C5-36-5/8 (Table 3.1) were not pulled out. Post-experiment inspection indicated that all bolts were still securely contained in the pocket of grout, and that there was no loosening. In addition to the failure of the ledger, (due to cross-grain tension in C5-56-1/2 and bending in C5-36-5/8) the 6d-nails at 8 in. spacing, with which the plywood was connected to the upper edge of the ledger, were gradually pulled out and were observed to dig into the bearing side of the softer plywood as cyclic loads continued. It appeared that if the premature

failure of the ledger boards had not occurred first, failure of the assembly would have been initiated at these nails.

The poor behavior of the connection was attributable to the incorrectly conceived, but apparently widely used detail through which in-plane diaphragm loads were transferred to the non-load bearing transverse wall. For the additional batch of models constructed during Phase 2 it was decided to use 2½x6x3/8 in. plate washers (placed with the long side vertical) on the symmetrically loaded ledger. With the ledger placed centrally on two bolts located 4 ft apart, this gave 2 ft long overhangs on both sides. Deformation diagrams describing the behavior of connections SC5-36-5/8, SC5-36-1/2 and SC5B-32-5/8 are displayed in Figs. 4.26-4.28.

Connections with the concrete block walls appeared to behave similarly. As seen in frames (b) of Figs. 4.26 and 4.27, wall displacement was not significant for either specimen. Measurements of plywood separation from ledger made directly above the left bolt (station 1), and the right bolt (station 3), and midway between the two (station 2), appeared to yield inconsistent readings because of the deformation of the ledger and the fact that compressive forces had to be applied to the plywood diaphragm in order to bring the actuator displacement to zero. The sequence of photographs in Fig. 4.29 describe the nature of plywood deformations at the two extreme displacements. In part (a) of Fig. 4.29, the actuator is at maximum retraction applying a pull force which deforms the ledger board to the point where the angle between the top edge of the ledger and the plywood is greater than 90 degrees. On returning to zero displacement as shown in Fig. 4.29(b), the plywood appears to lift up and become curved under the action of compressive actuator force. In both specimens failure was caused by the pullout of the left bolt (Figs. 4.26(f) and 4.27(e)). Connection SC5-36-5/8 lost its strength much more rapidly when the left

bolt broke the face shell and could no longer resist pullout forces. However, since the experiments were displacement controlled total failure was not precipitated and the actuator force was resisted largely by the bolt on the right for which no outward pull was recorded. Ledger separations from the wall in Figs. 4.26(g) and (h) reflect both bolt pullout and ledger deformations; it may be ascertained that frames (f) and (h) in Fig. 4.26 can be superposed to obtain frame (g). The same effect is noticeable for C5-36-1/2 from a comparison of Figs. 4.27(e), (g) and of Figs. 4.27 (f), (h). Symmetrically loaded concrete block wall connections SC5-36-5/8 and SC5-36-1/2 attained maximum averaged resistances of 1.50 and 1.70 kips, respectively.

Specimen SC5B-32-5/8 with the brick wall failed due to flexural failure of the wall above the lateral supports. Visual comparison of Figs. 4.28(a) and (b) suggests that actuator displacements were closely followed by the wall which absorbed the bulk of the imposed displacements. Separation of the plywood from the ledger (Figs. 4.28(c) and (d)), as well as the ledger deformation (Figs. 4.28(e) and (f)) itself, remained below a maximum displacement of 0.1 in. each. Although the actuator force reached 1.52 kips, neither bolt showed any signs of pullout indicating the higher strength of brick face shell.

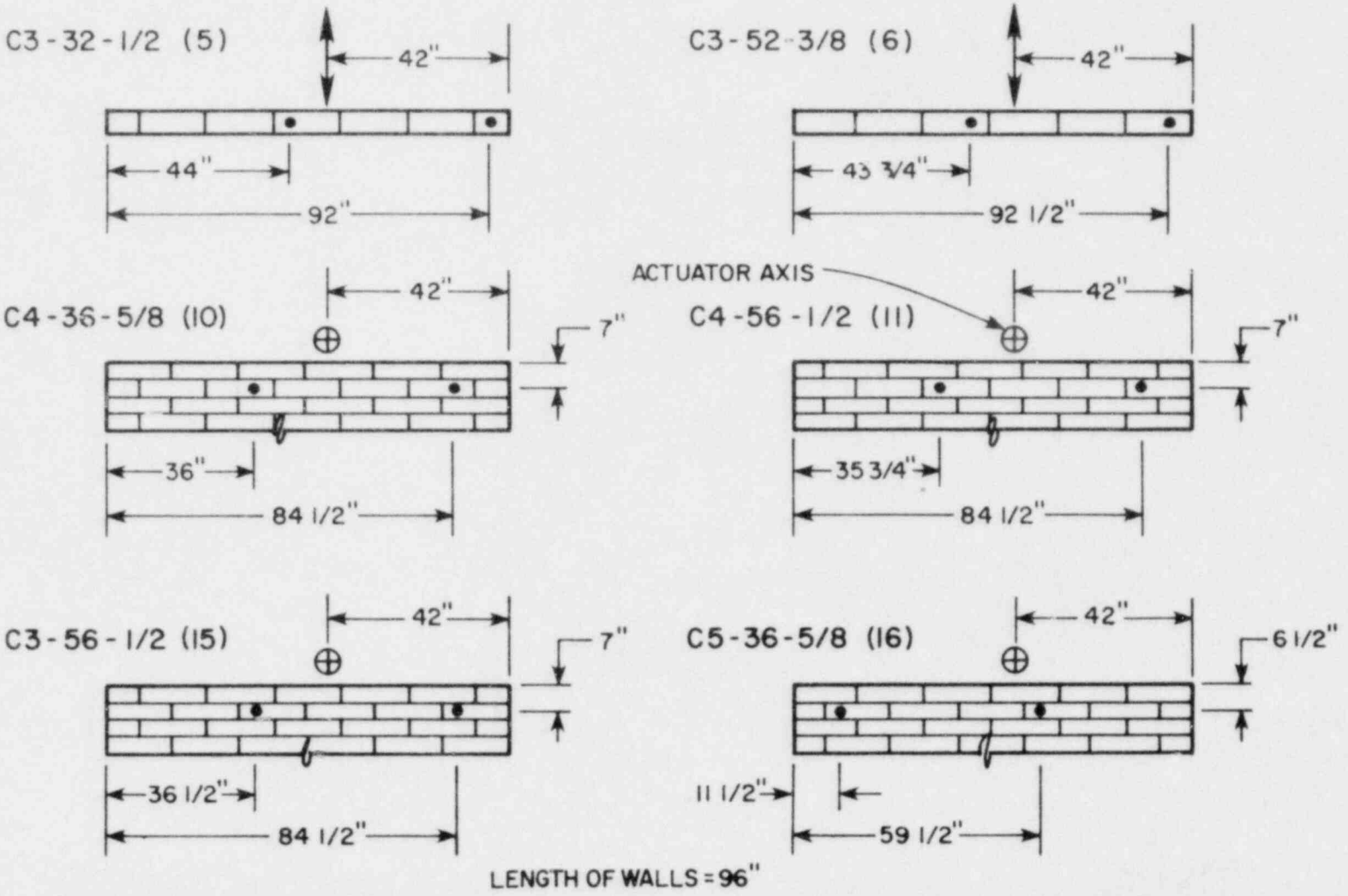

FIGURE 4.1 LOCATION OF ACTUATOR RELATIVE TO BOLTS IN ECCENTRIC TRANSVERSE TESTS

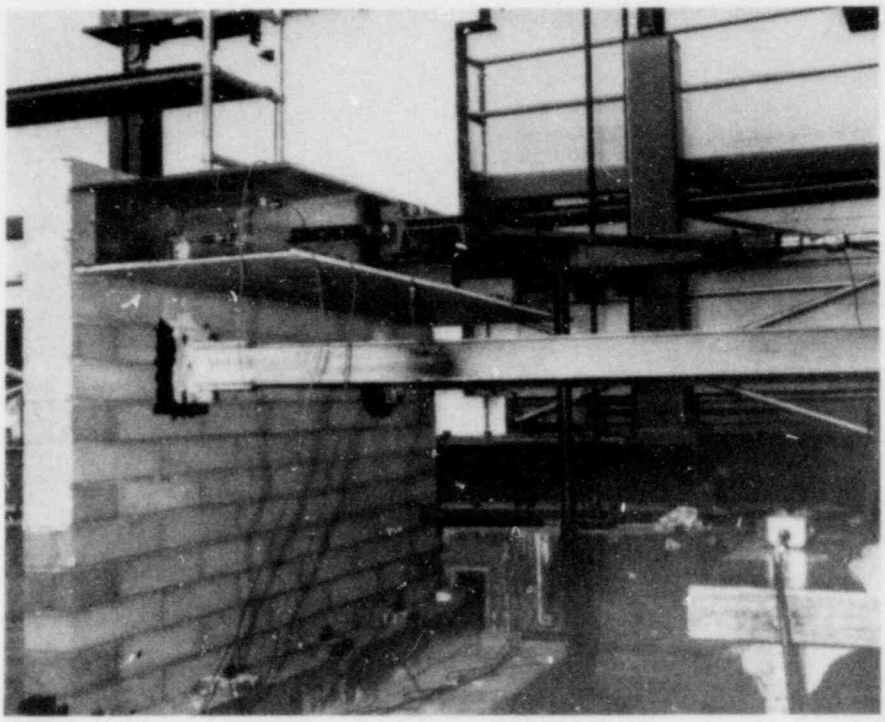

FIGURE 4.2 LATERAL WALL SUPPORT

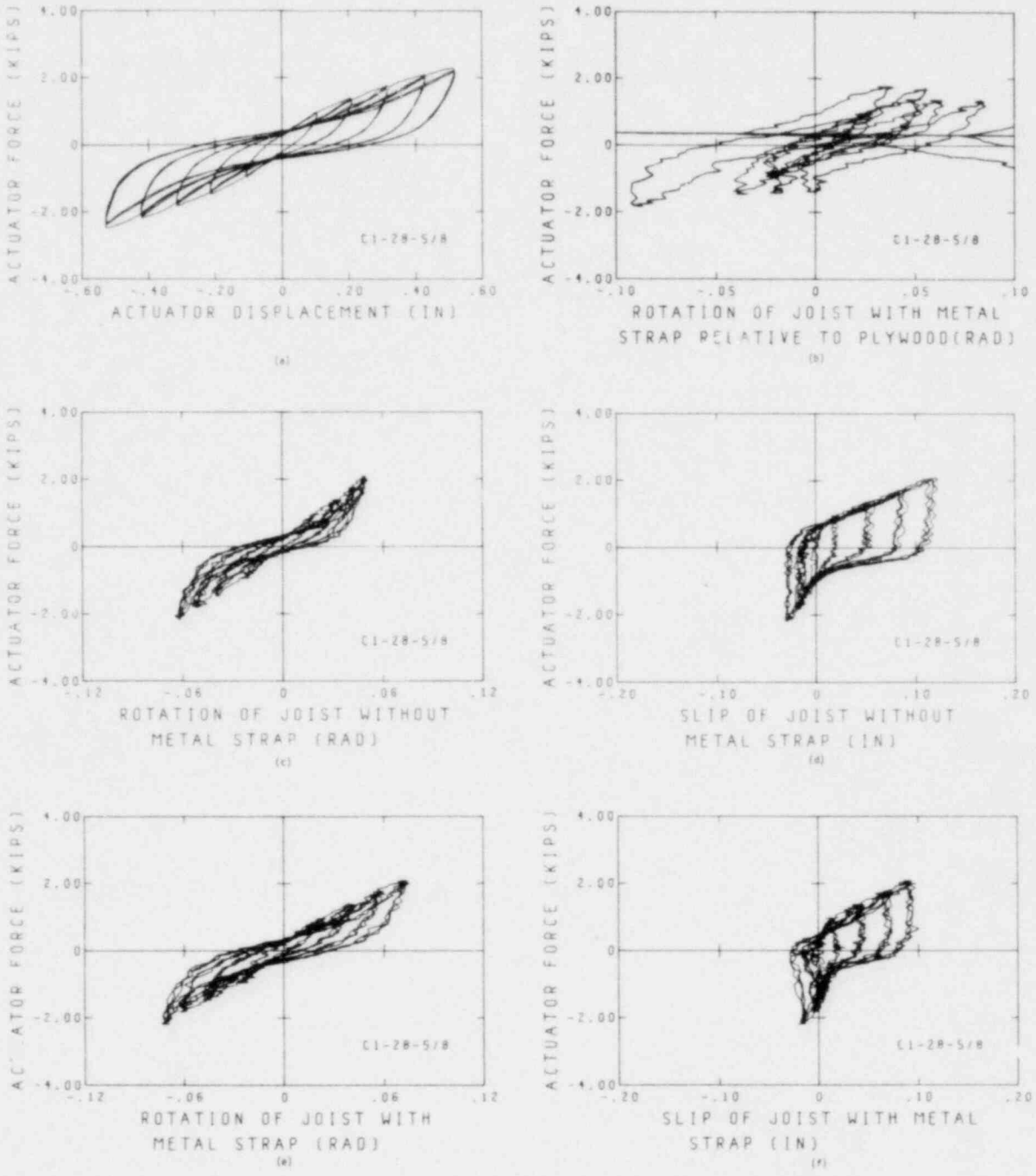

FIGURE 4.3 MEASURED DEFORMATION OF SPECIMEN C1-28-5/8

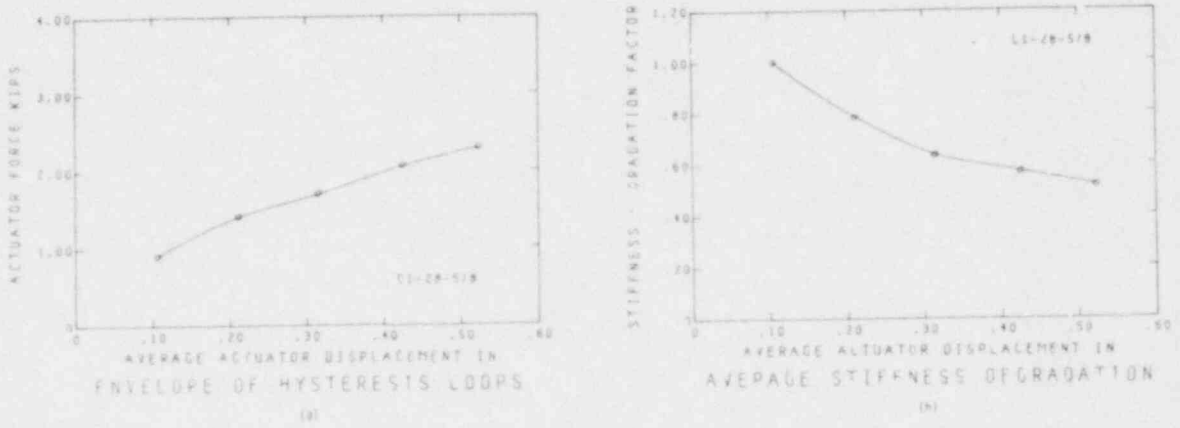

FIGURE 4.3(CONT.) MEASURED DEFORMATION OF SPECIMEN C1-28-5/8

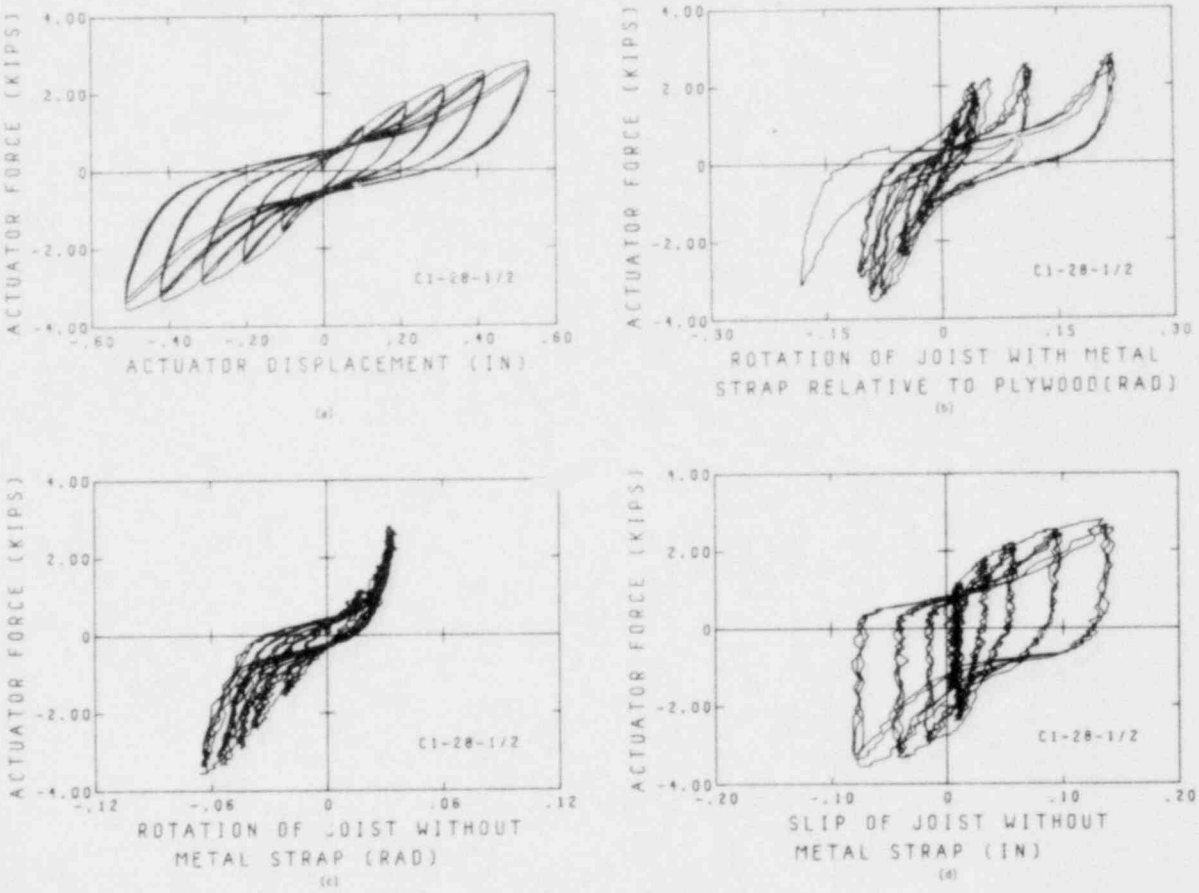

FIGURE 4.4 MEASURED DEFORMATION OF SPECIMEN C1-28-1/2

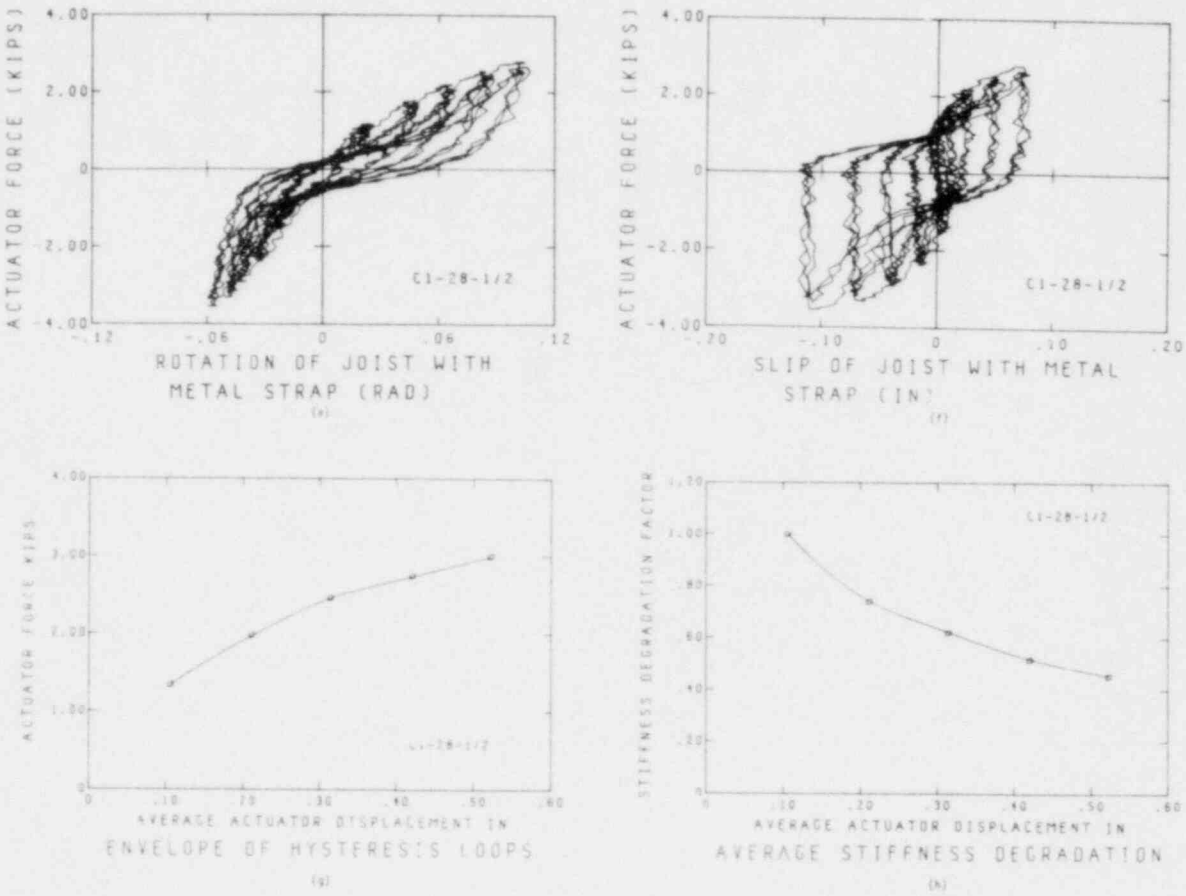

FIGURE 4.4(CONT.) MEASURED DEFORMATION OF SPECIMEN C1-28-1/2

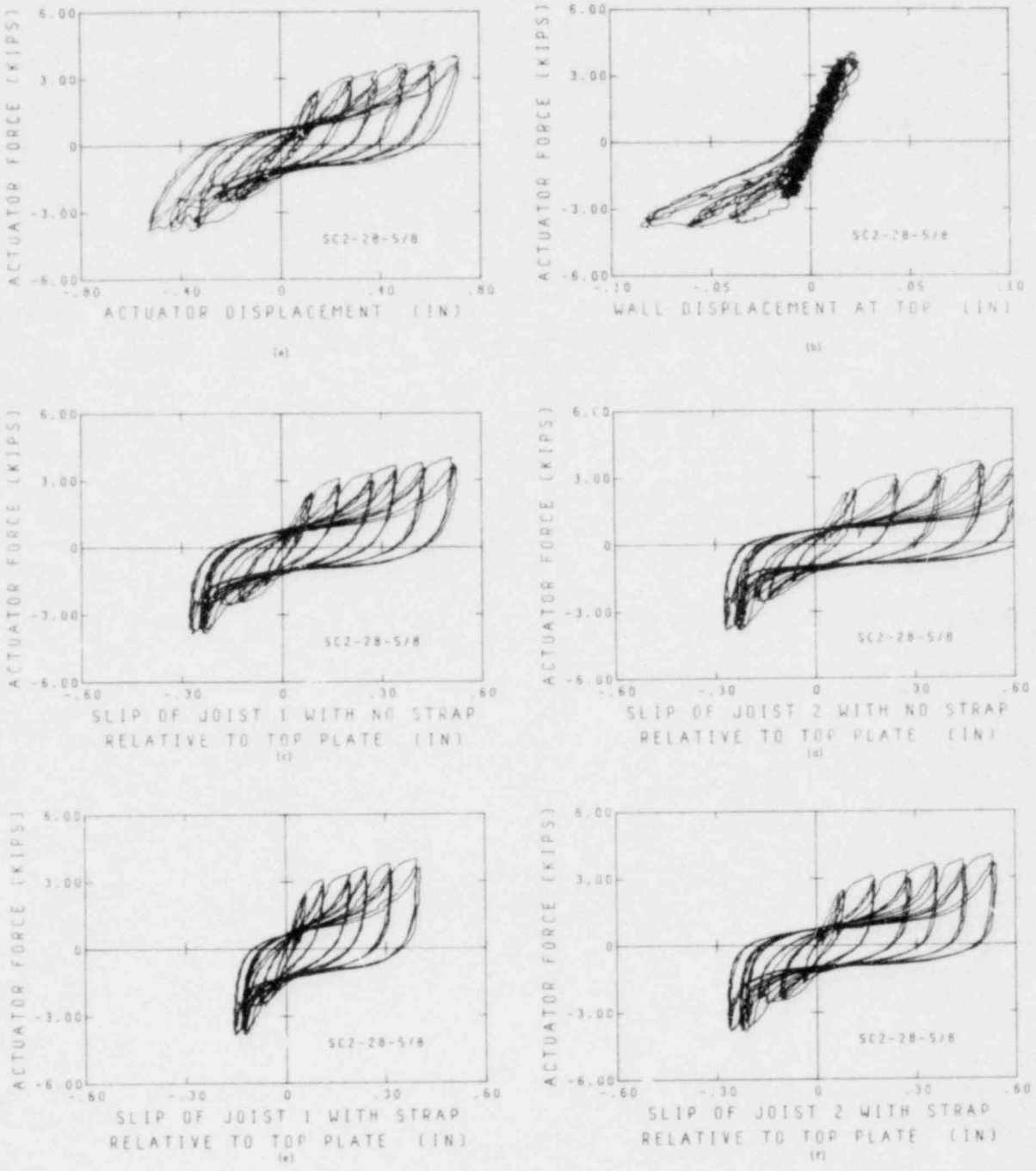

FIGURE 4.5 MEASURED DEFORMATION OF SPECIMEN SC2-28-5/8

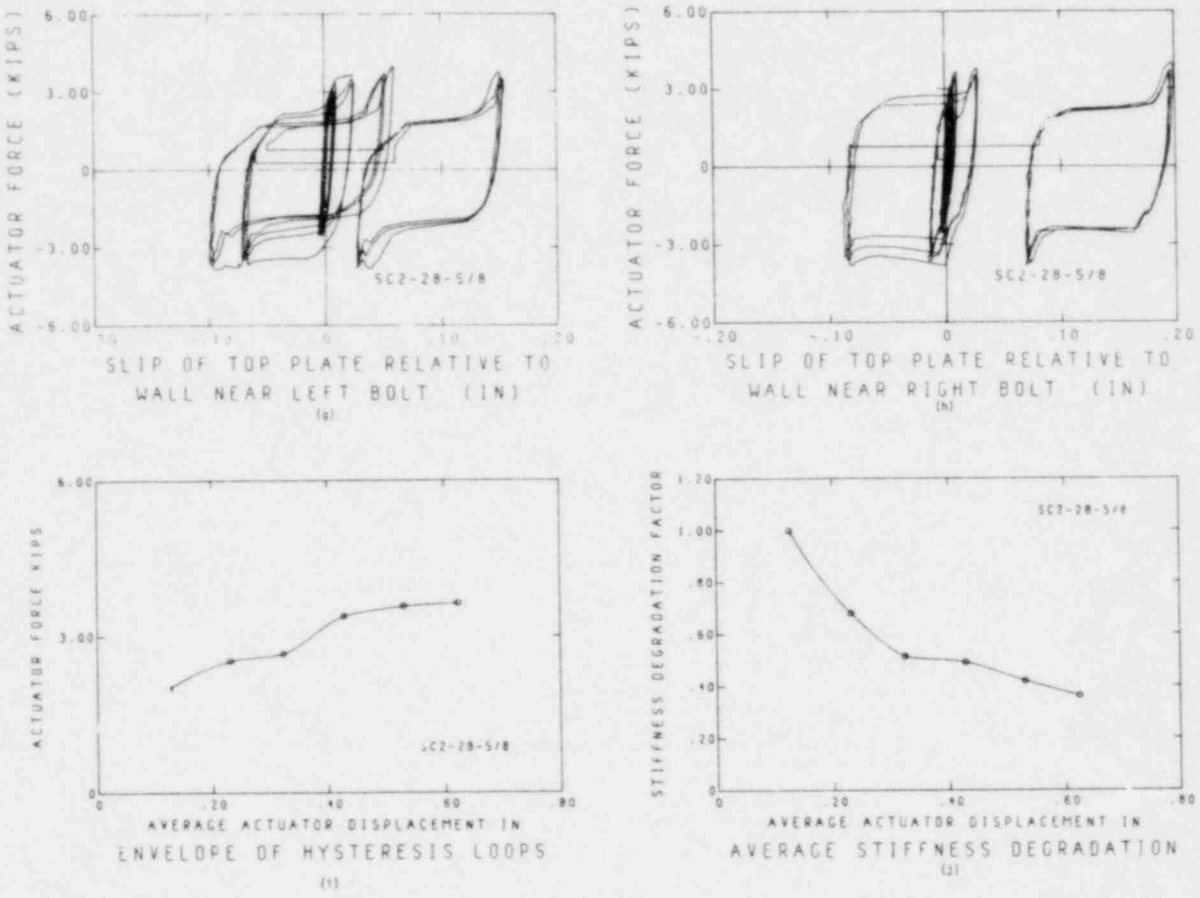

FIGURE 4.5(CONT.) MEASURED DEFORMATION OF SPECIMEN SC2-28-5/8

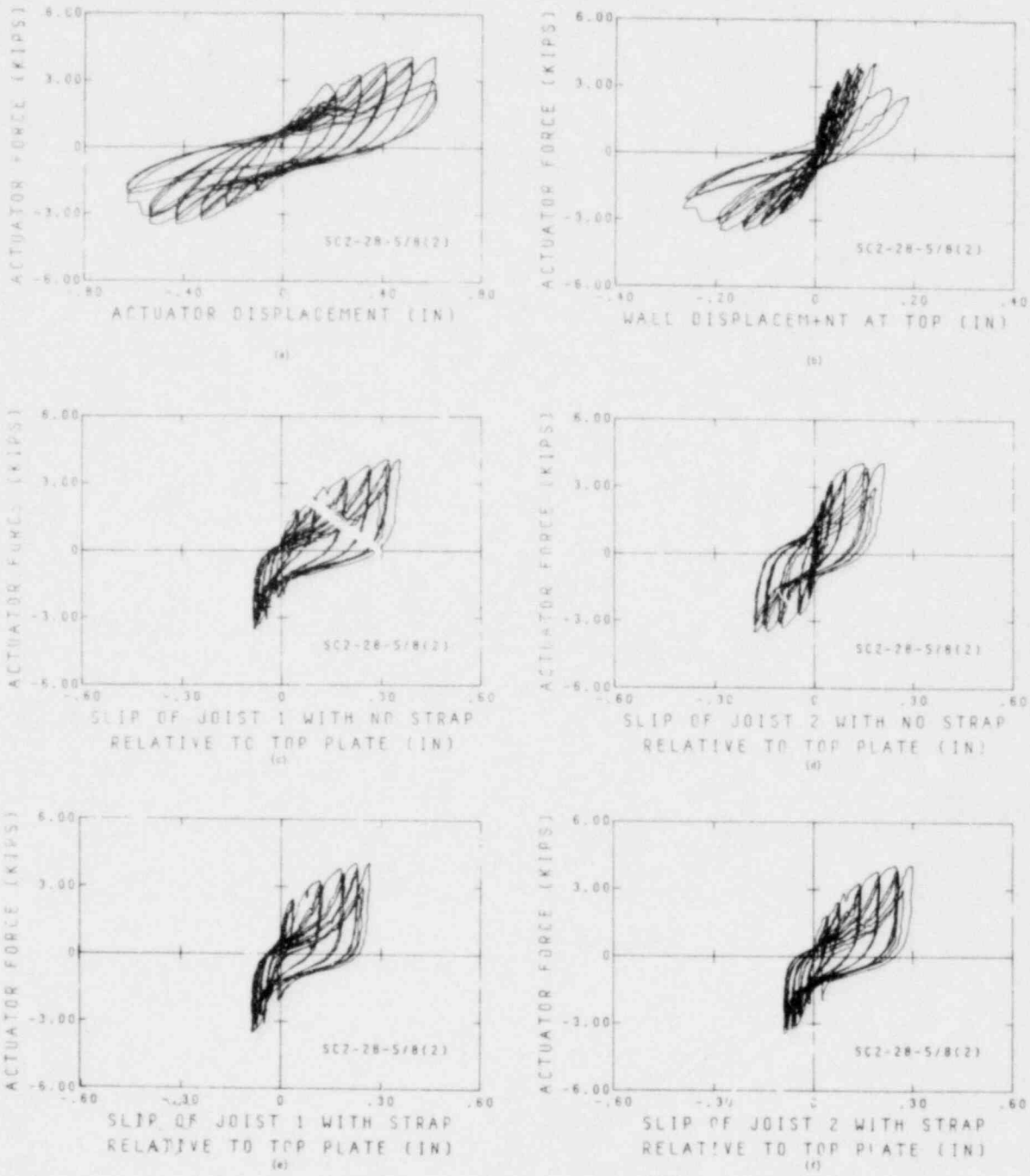

FIGURE 4.6 MEASURED DEFORMATION OF SPECIMEN SC2-28-5/8(2)

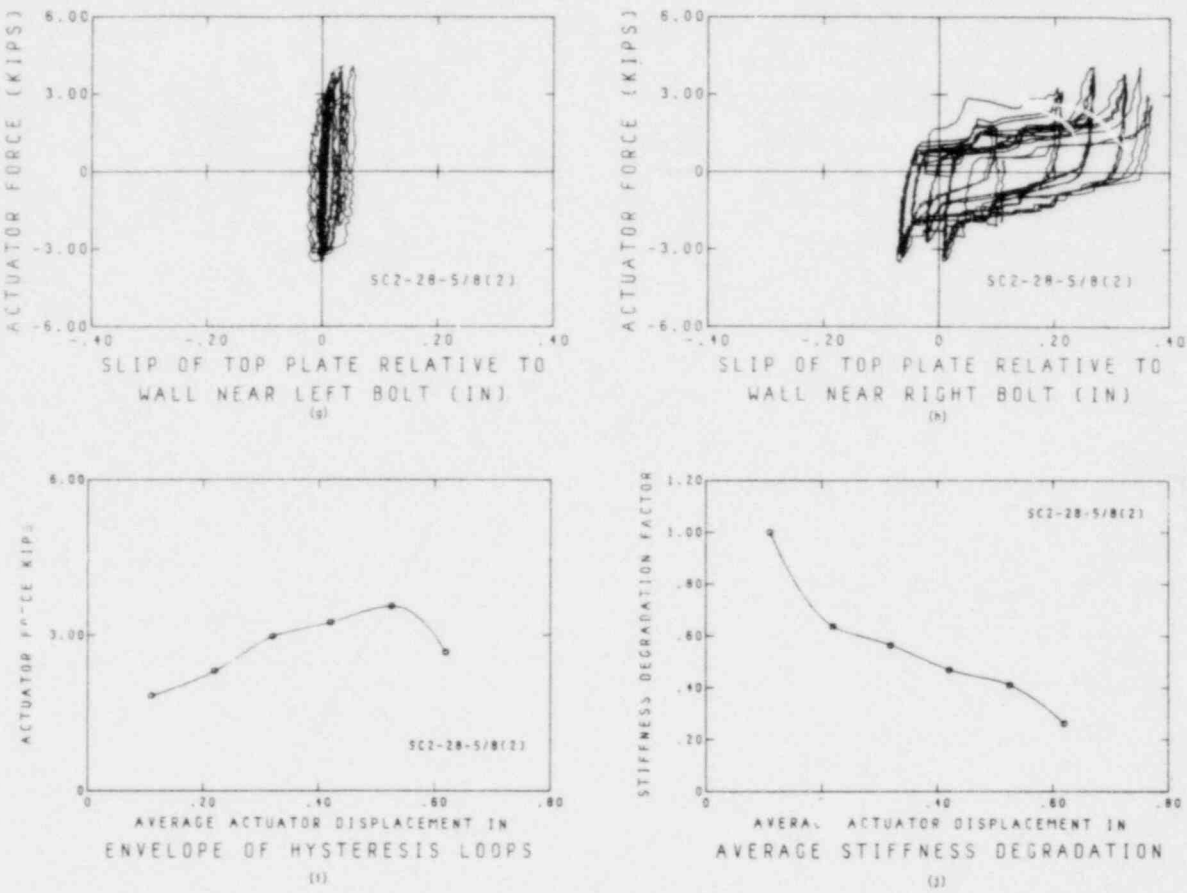

FIGURE 4.6(CONT.) MEASURED DEFORMATION OF SPECIMEN SC2-28-5/8(2)

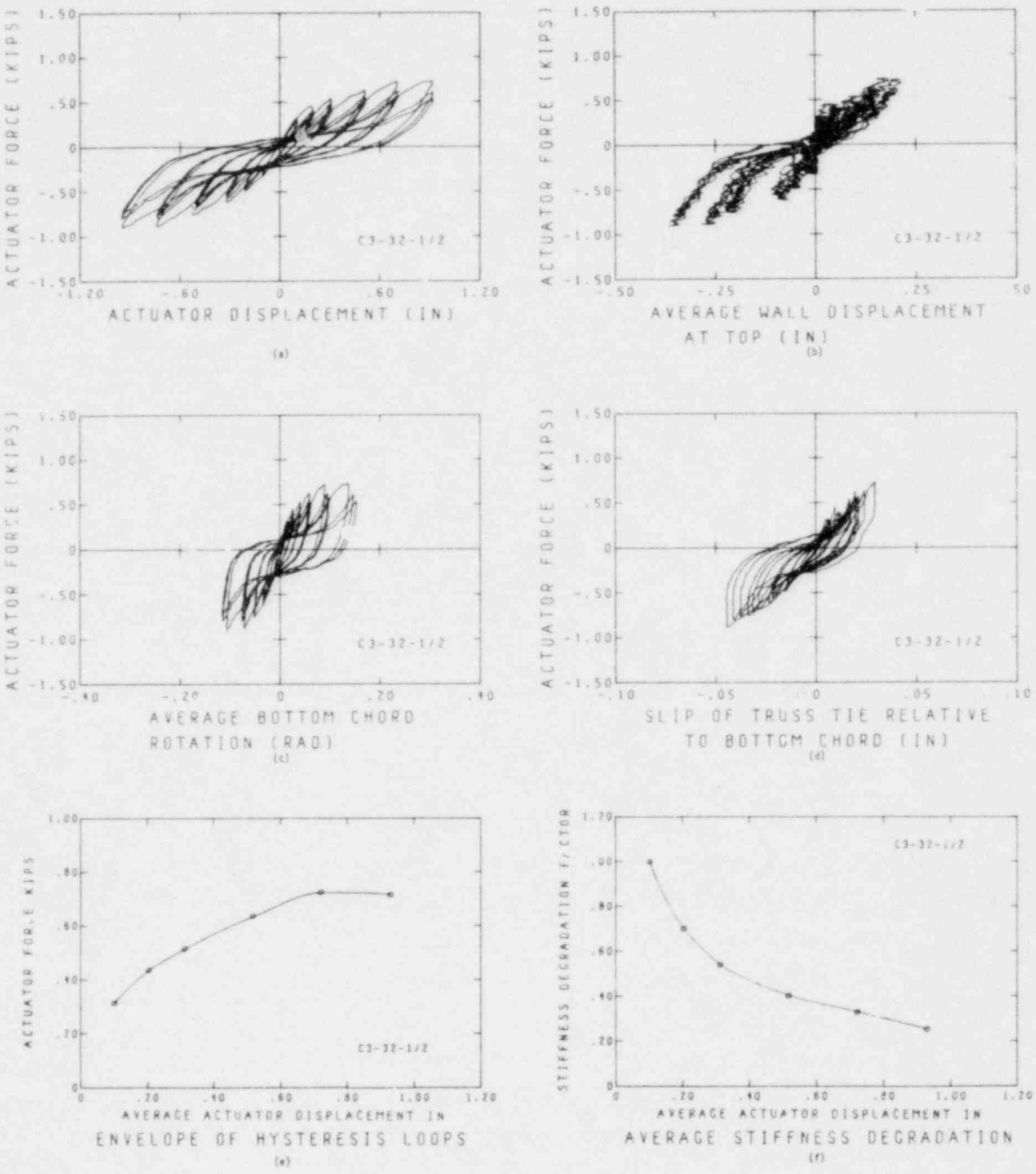

FIGURE 4.7 MEASURED DEFORMATION OF SPECIMEN C3-32-1/2

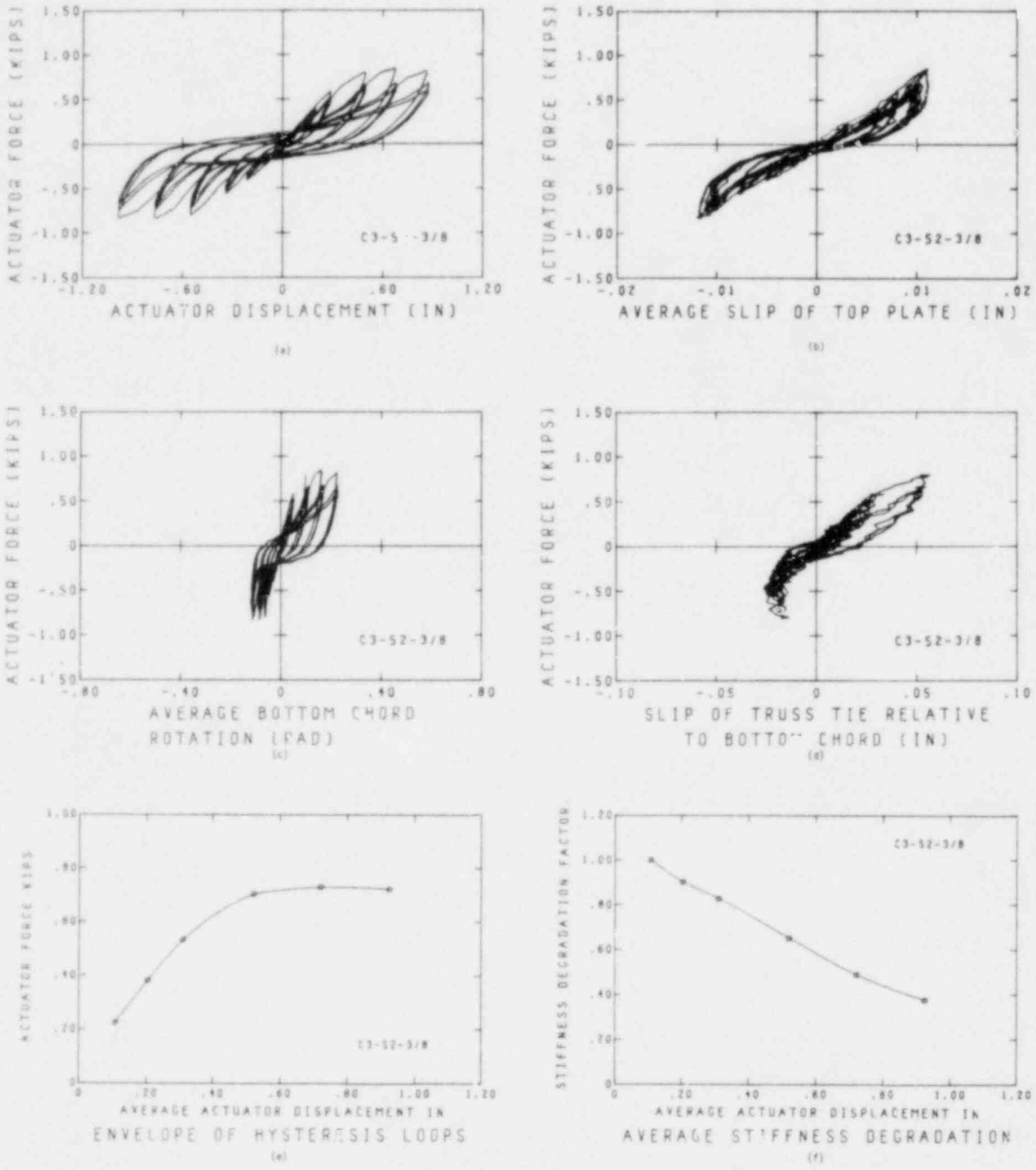

FIGURE 4.8 MEASURED DEFORMATION OF SPECIMEN C3-52-3/8

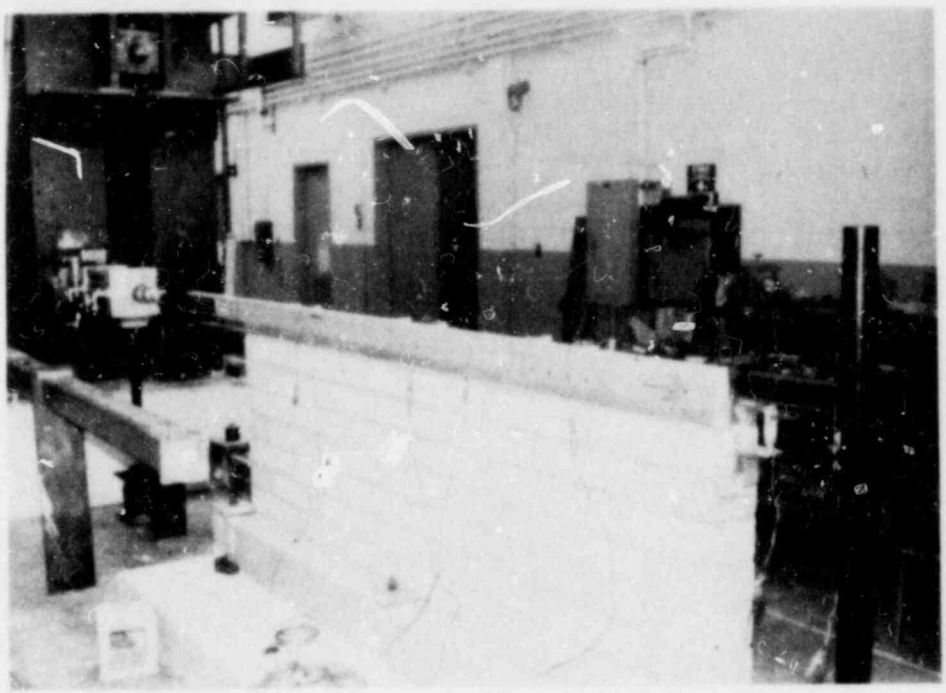

FIGURE 4.9 TEST OF SPECIMEN C3-32-1/2

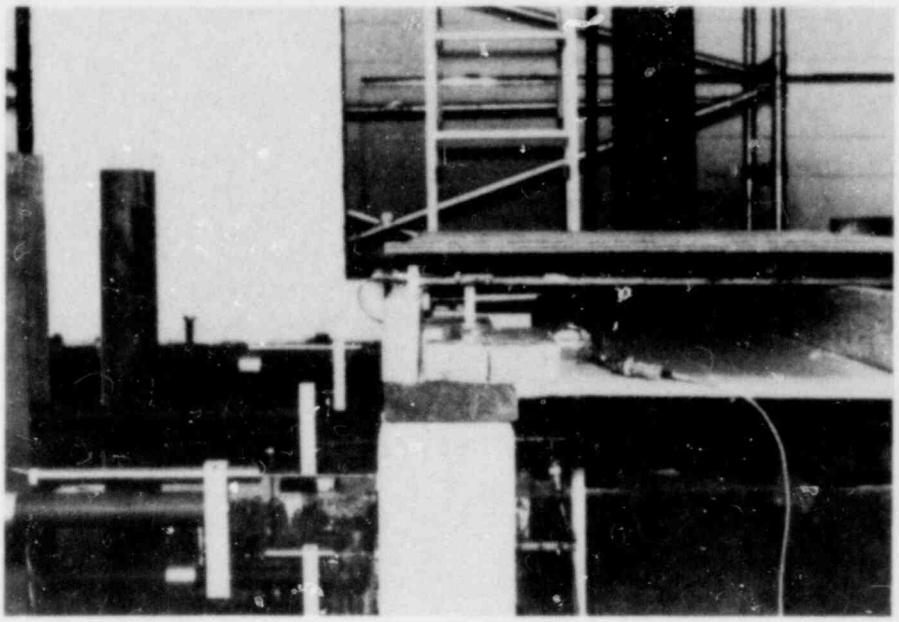

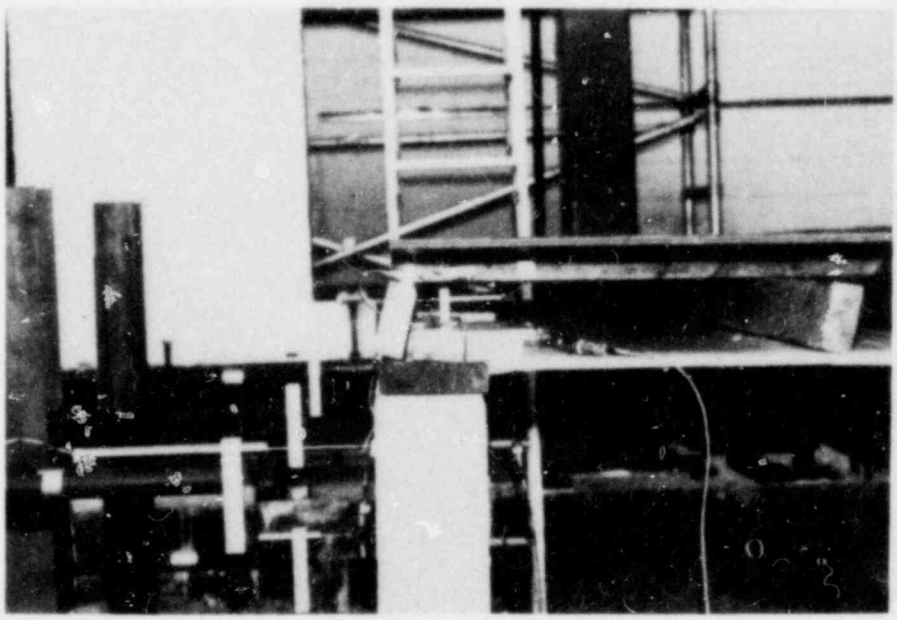

FIGURE 4.10 IN-PLANE TEST ARRANGEMENT FOR C3 TYPE CONNECTIONS

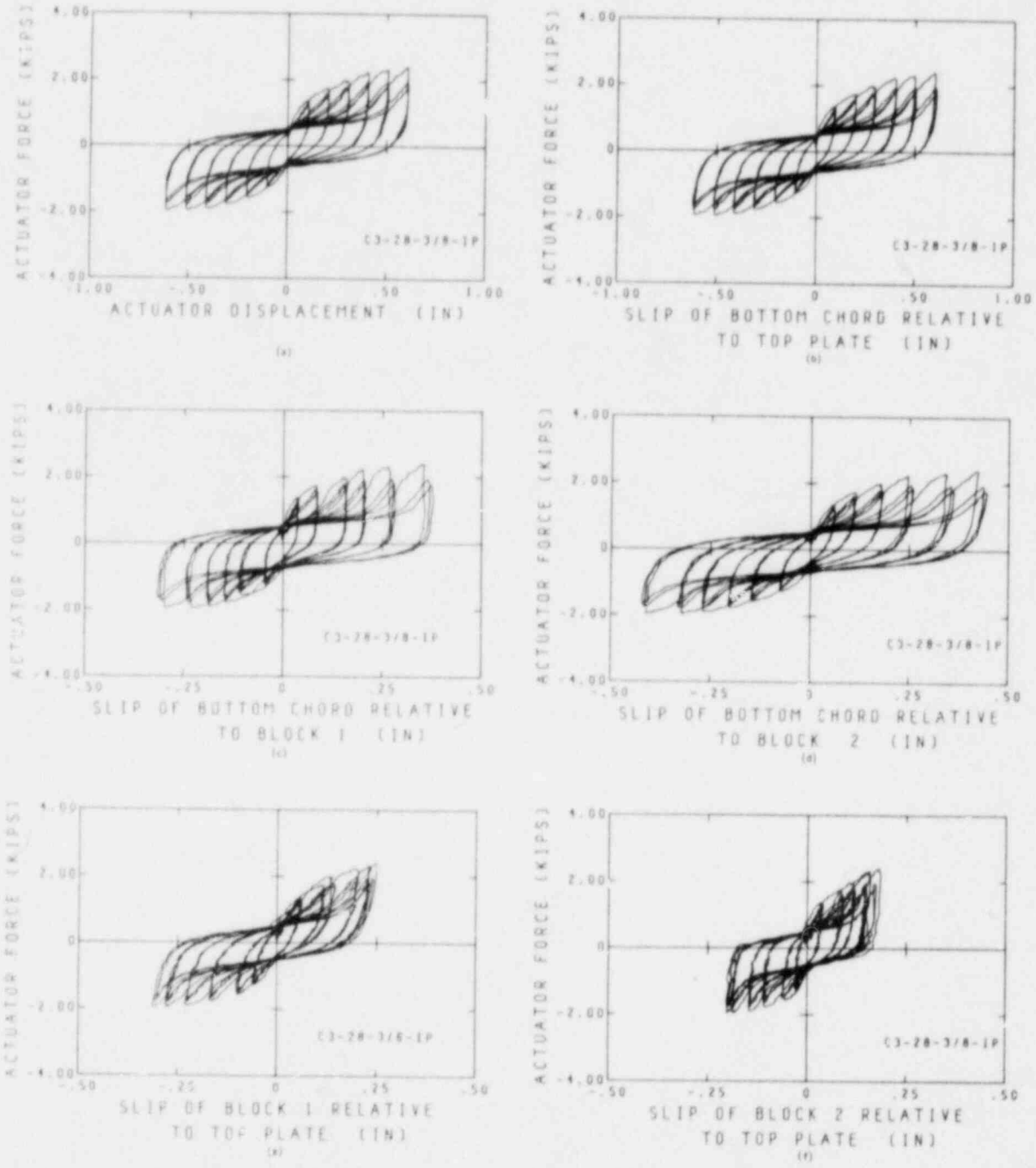

FIGURE 4.11 MEASURED DEFORMATION OF SPECIMEN C3-28-3/8-IP

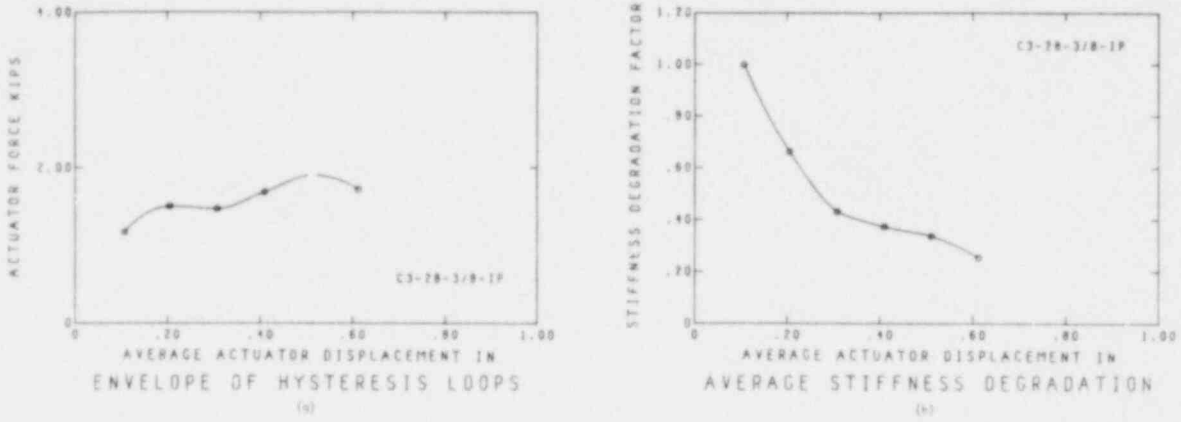

FIGURE 4.11(CONT.) MEASURED DEFORMATION OF SPECIMEN C3-28-3/8-IP

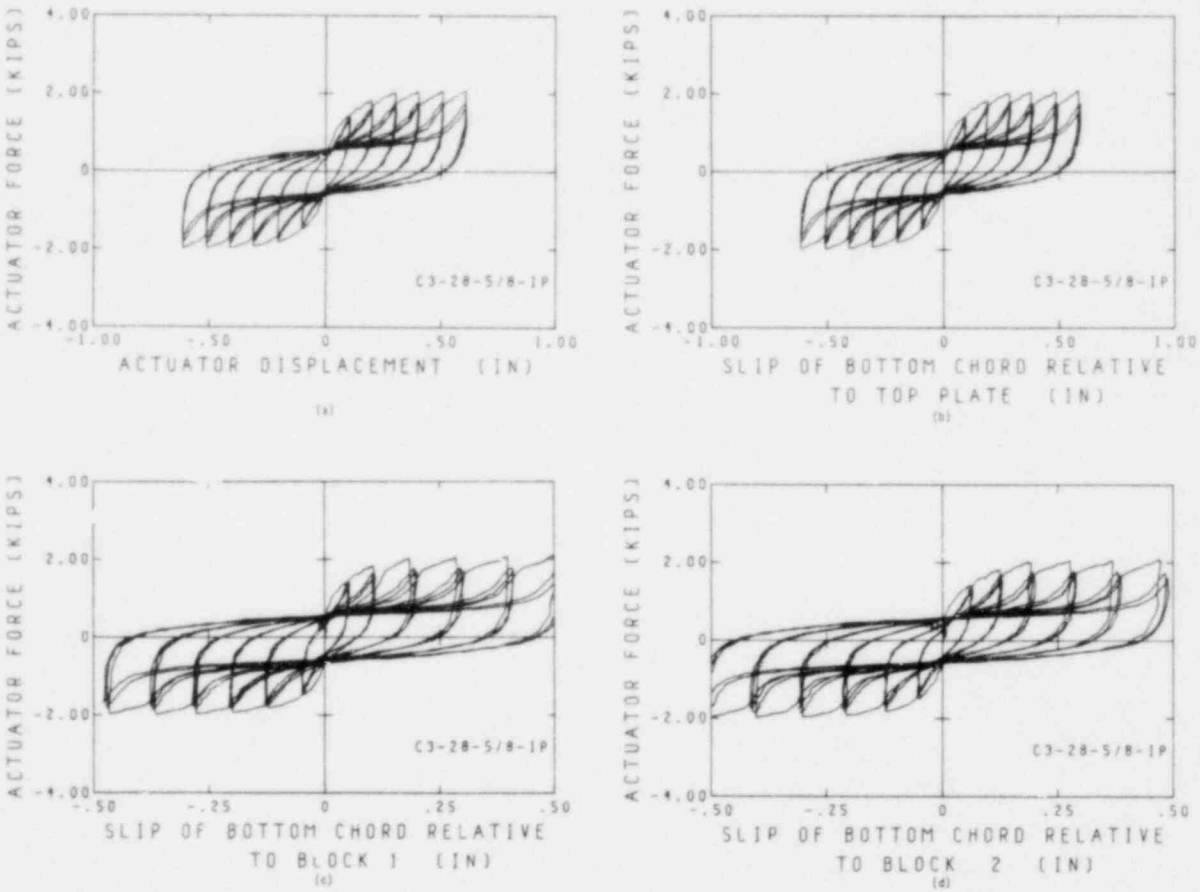

FIGURE 4.12 MEASURED DEFORMATION OF SPECIMEN C3-28-5/8-IP

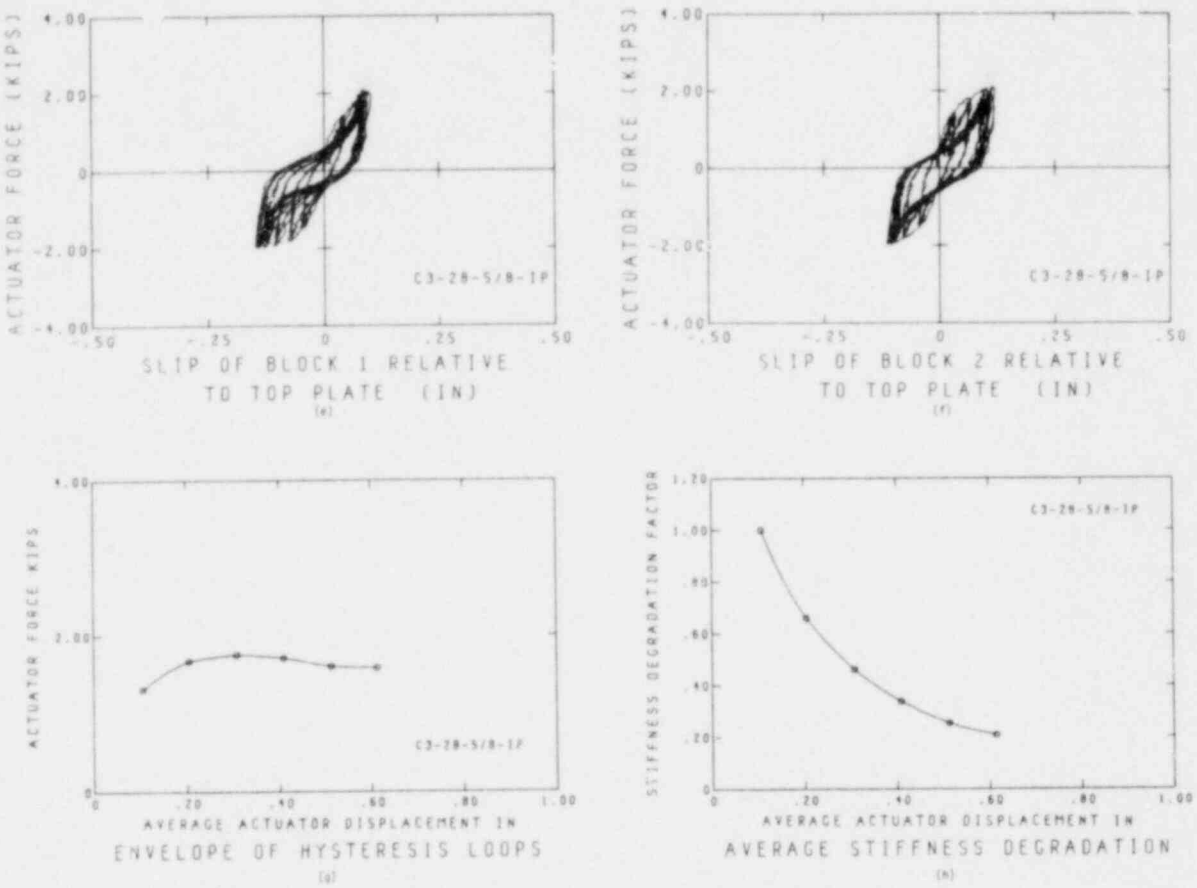

FIGURE 4.12(CONT.) MEASURED DEFORMATION OF SPECIMEN C3-28-5/8-IP

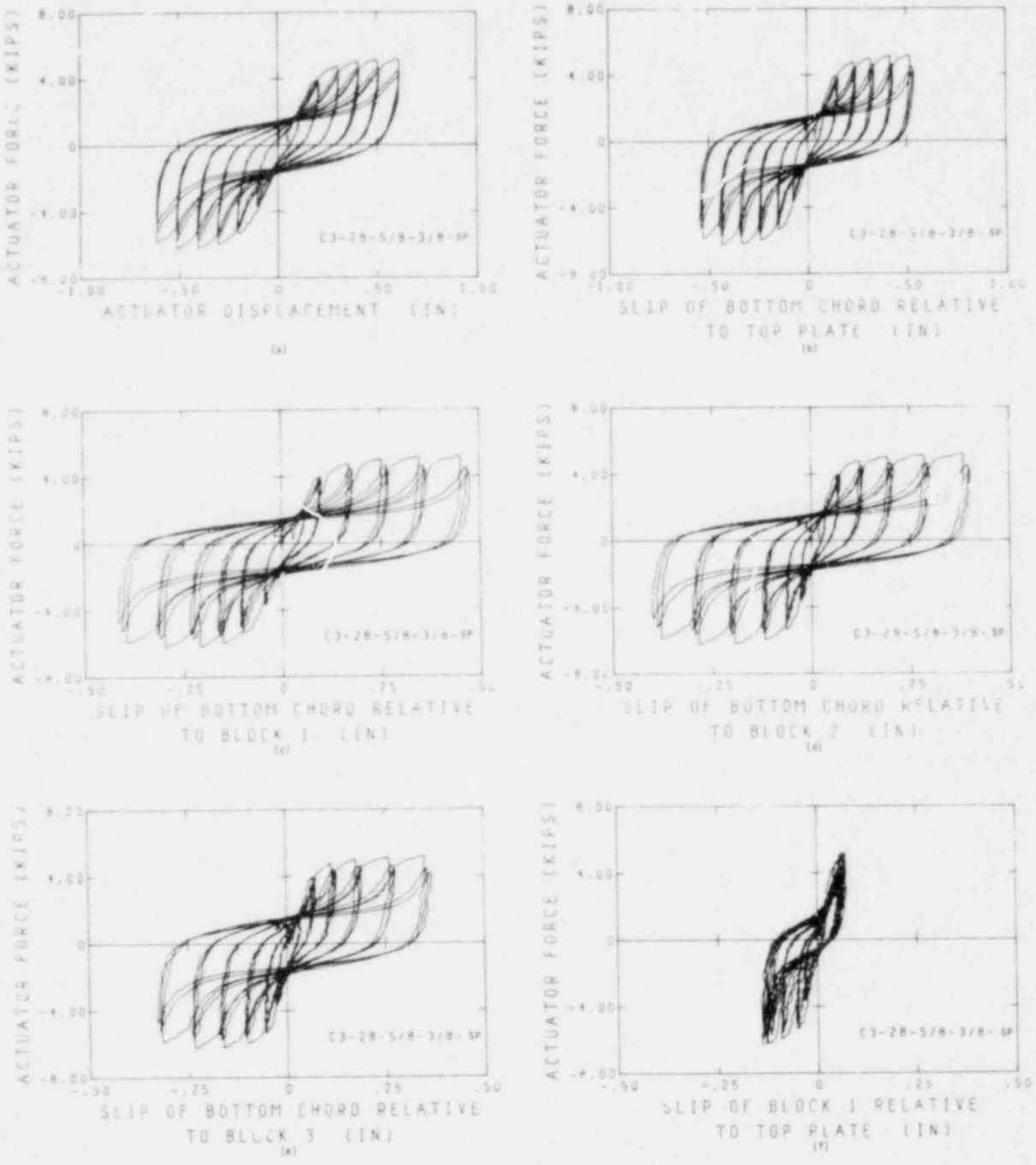

FIGURE 4.13 MEASURED DEFORMATION OF SPECIMEN C3-28-5/8-3/8-SP

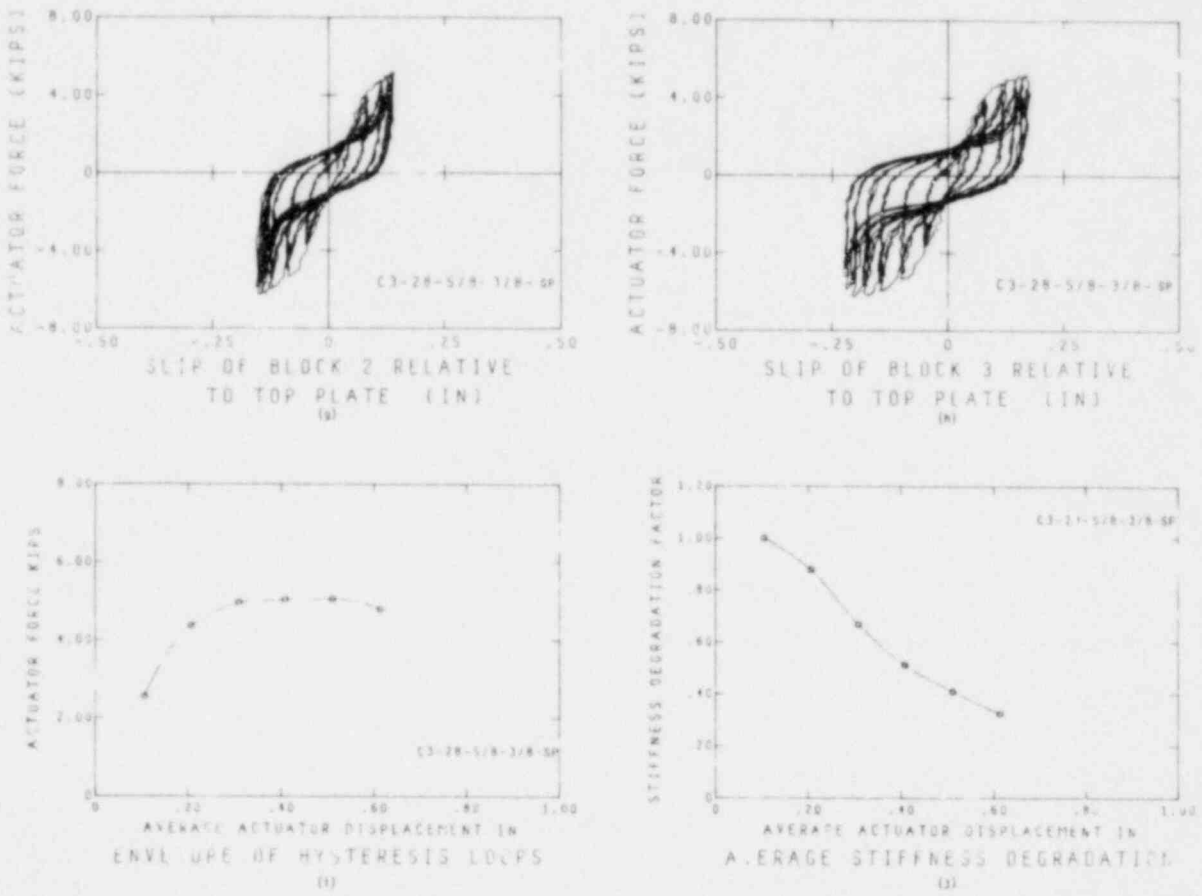

FIGURE 4.13(CONT.) MEASURED DEFORMATION OF SPECIMEN C3-28-5/8-3/8-SP

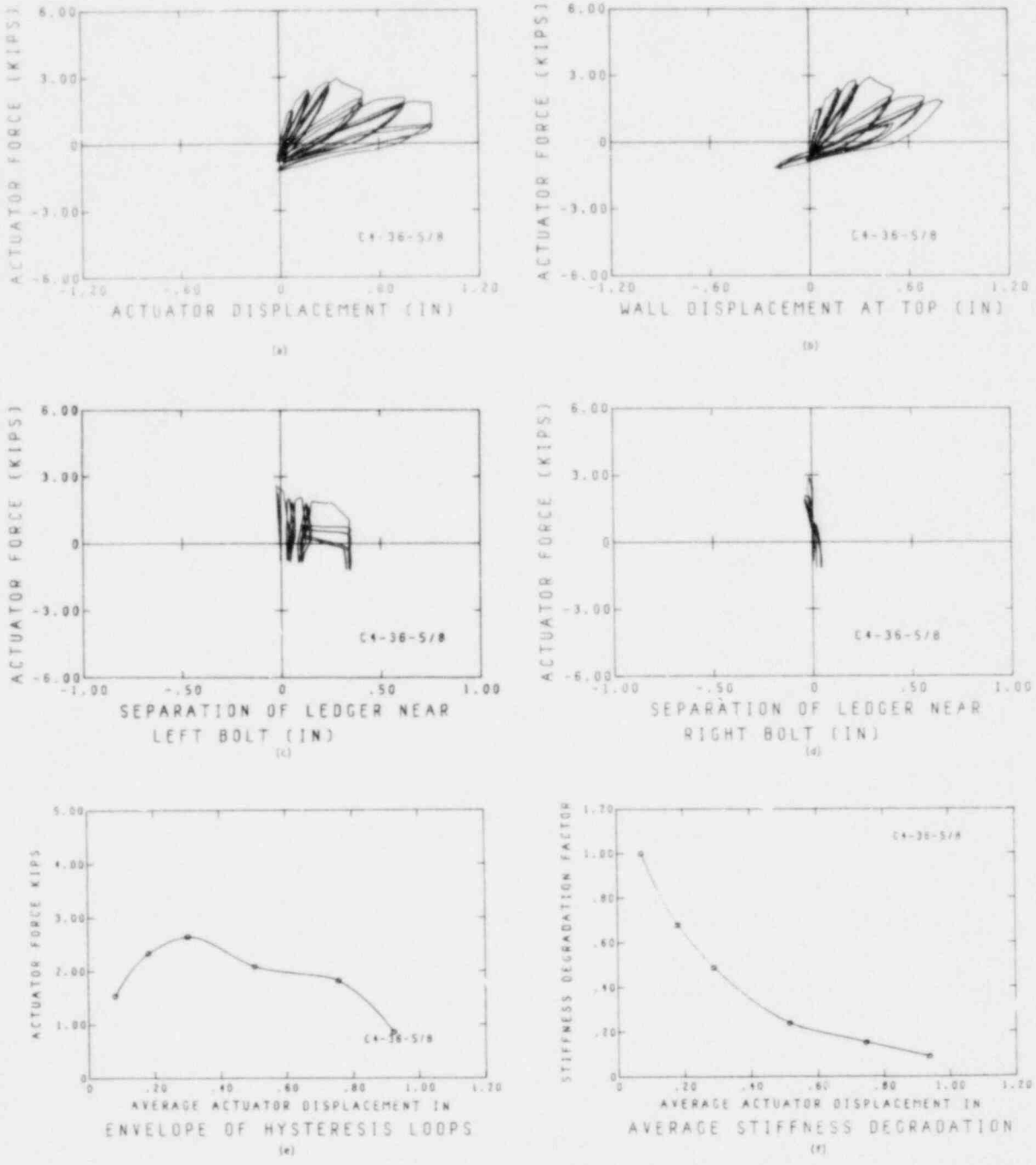

FIGURE 4.14 MEASURED DEFORMATION OF SPECIMEN C4-36-5/8

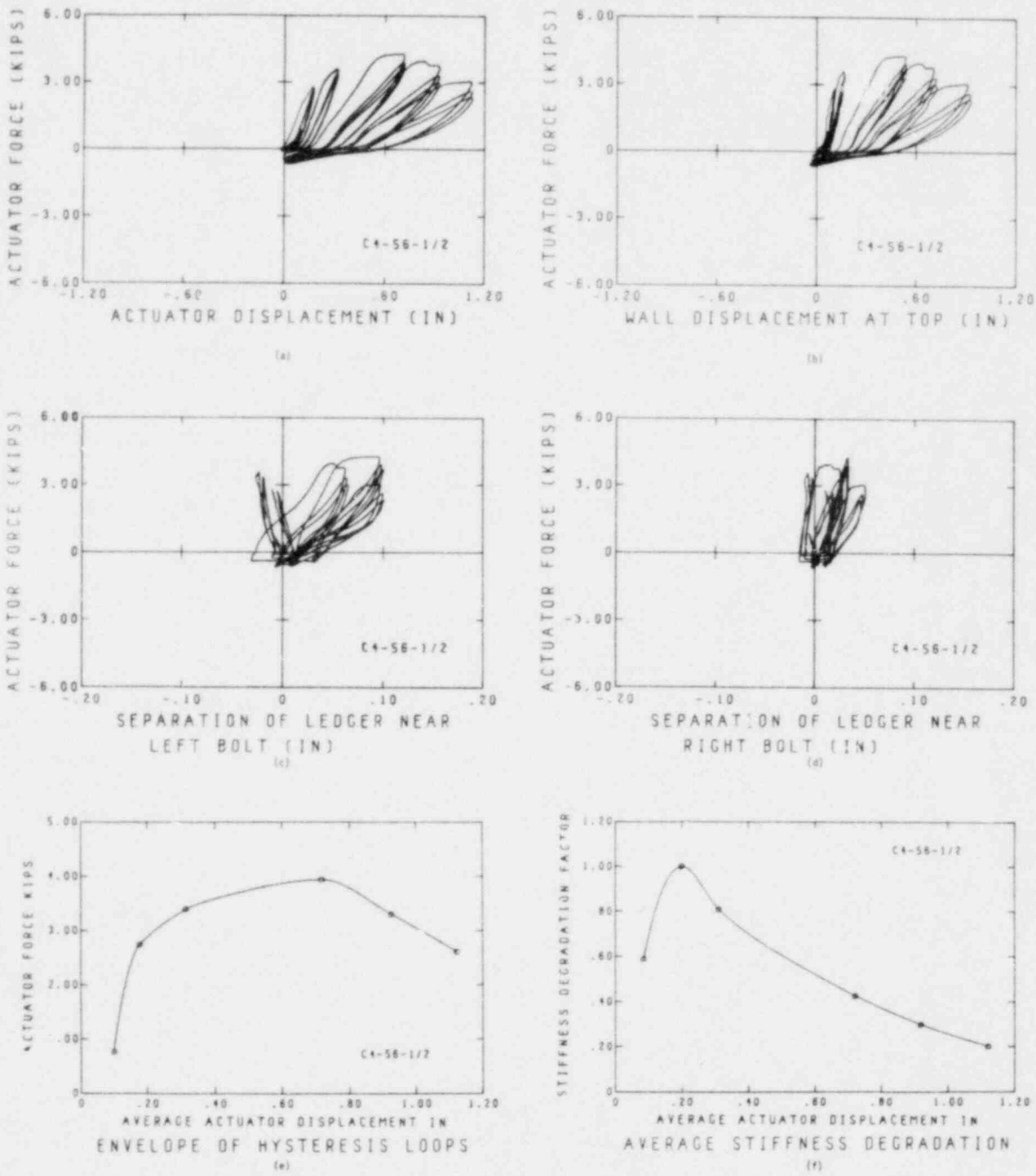

FIGURE 4.15 MEASURED DEFORMATION OF SPECIMEN C4-56-1/2

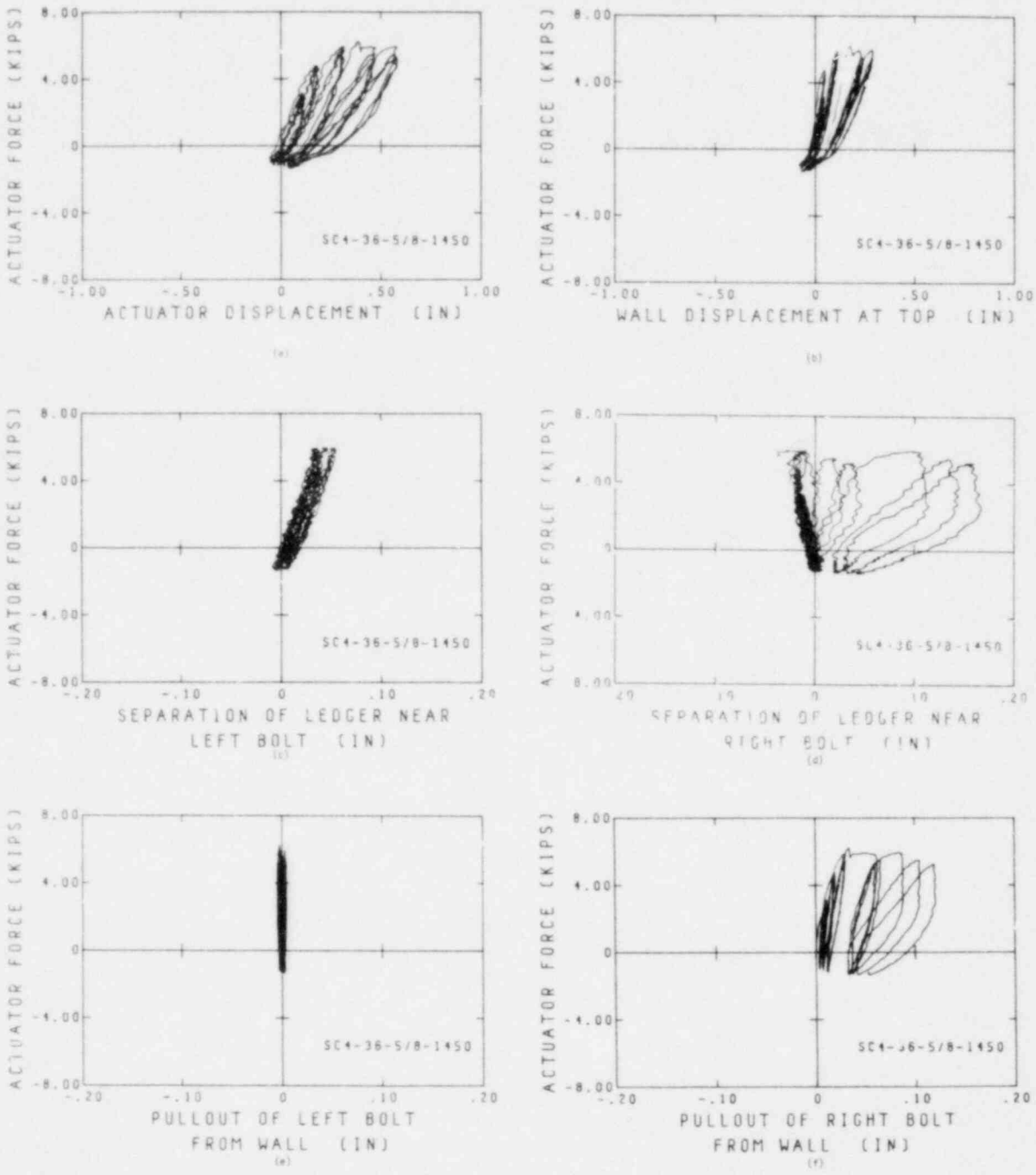

FIGURE 4.16 MEASURED DEFORMATION OF SPECIMEN SC4-36-5/8-1450

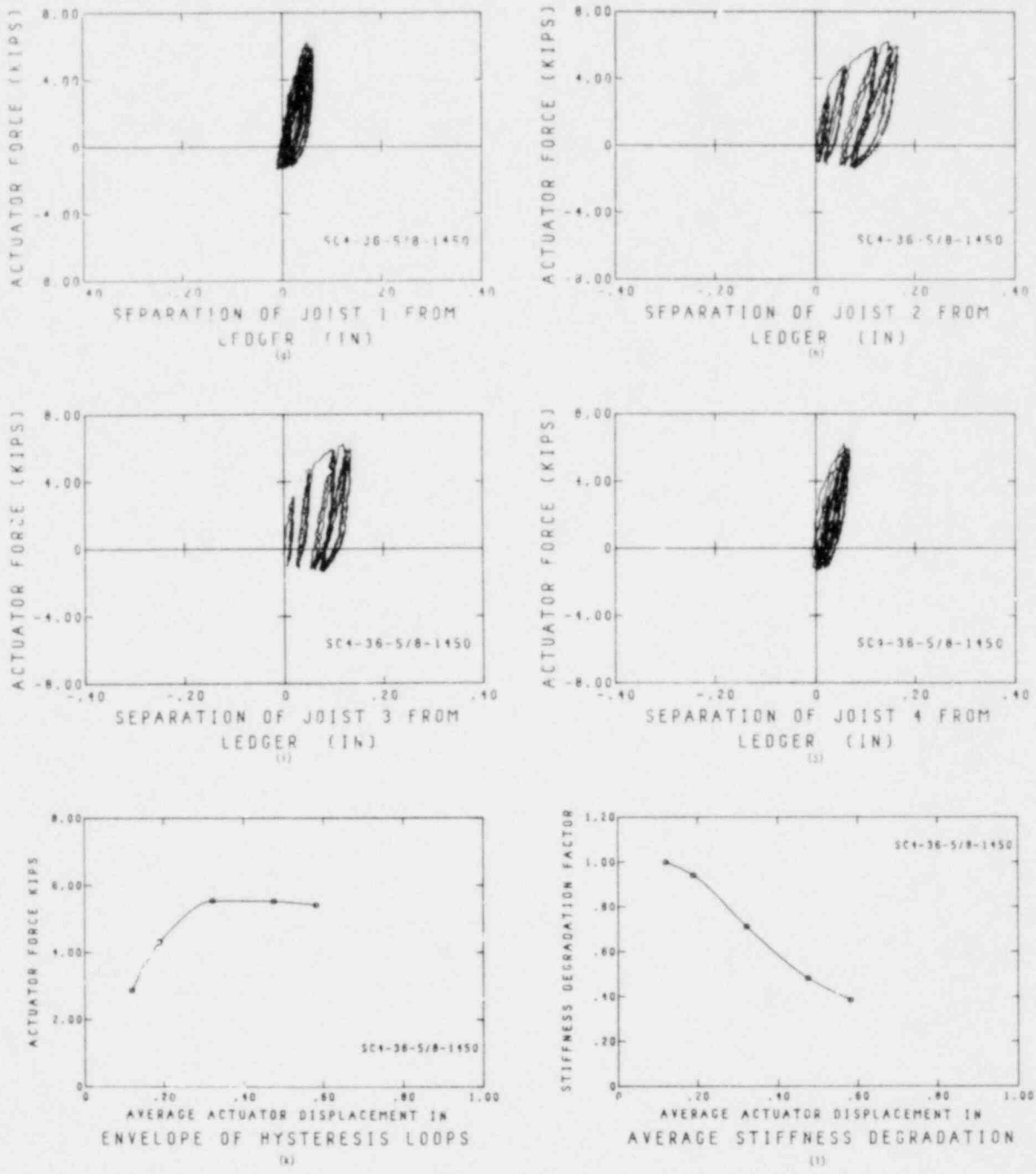

FIGURE 4.16(CONT.) MEASURED DEFORMATION OF SPECIMEN SC4-36-5/8-1450

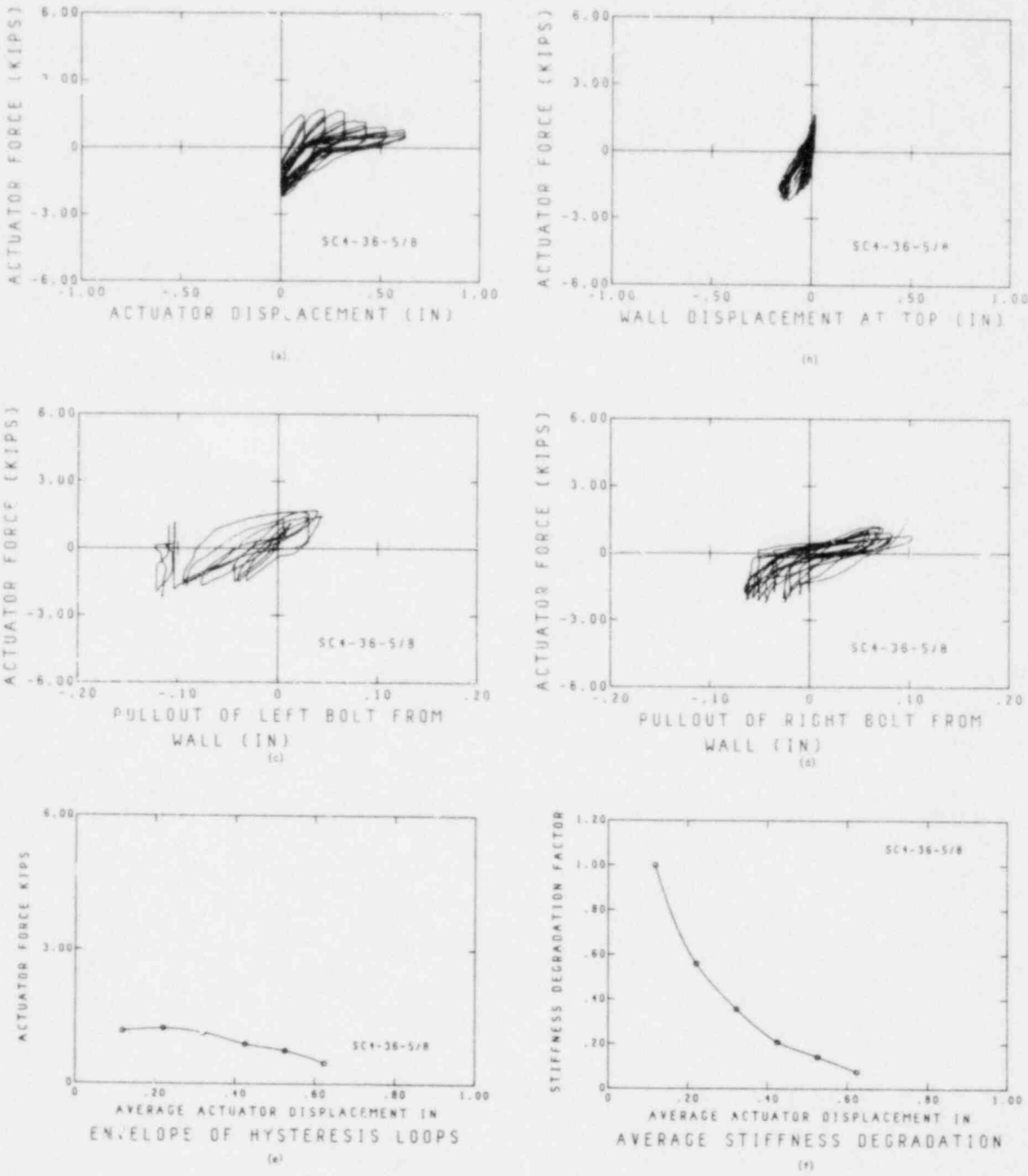

FIGURE 4.17 MEASURED DEFORMATION OF SPECIMEN SC4-36-5/8

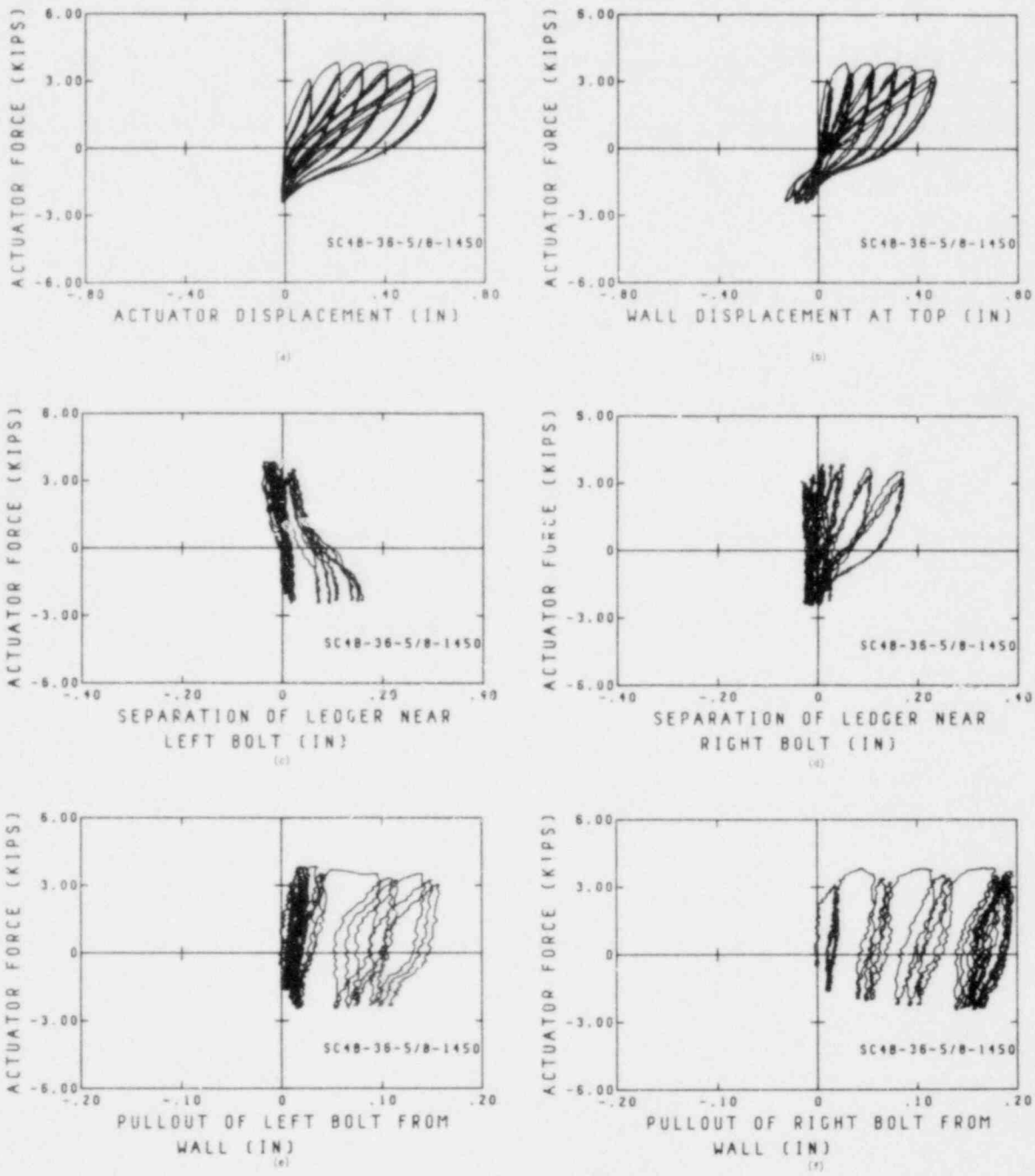

FIGURE 4.18 MEASURED DEFORMATION OF SPECIMEN SC4B-36-5/8-1450

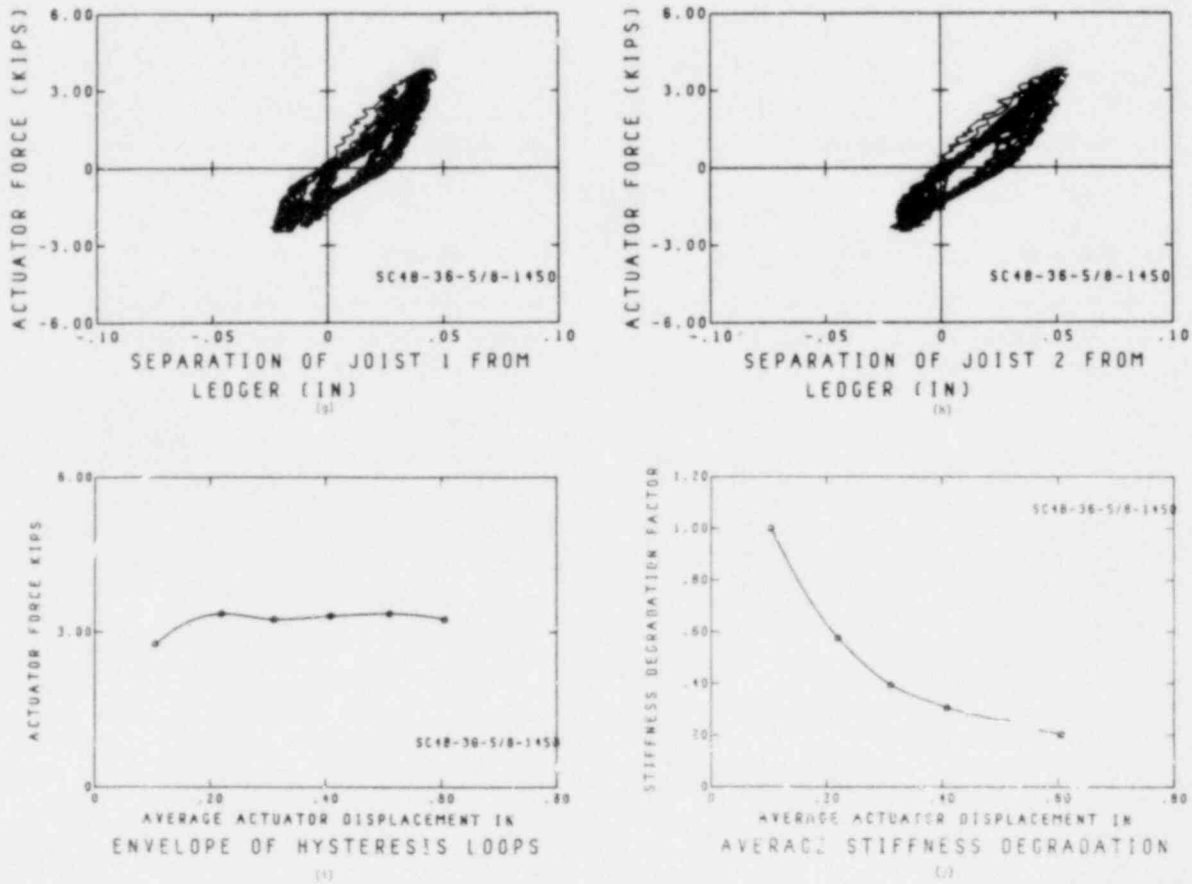

FIGURE 4.18(CONT.) MEASURED DEFORMATION OF SPECIMEN SC4B-36-5/8-1450

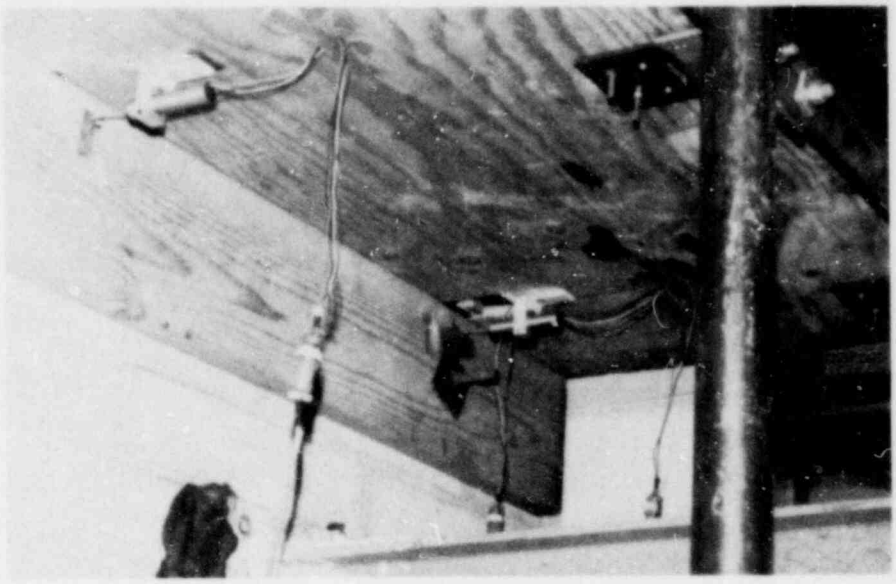

FIGURE 4.19 MEASUREMENT OF PLYWOOD-LEDGER SEPARATION

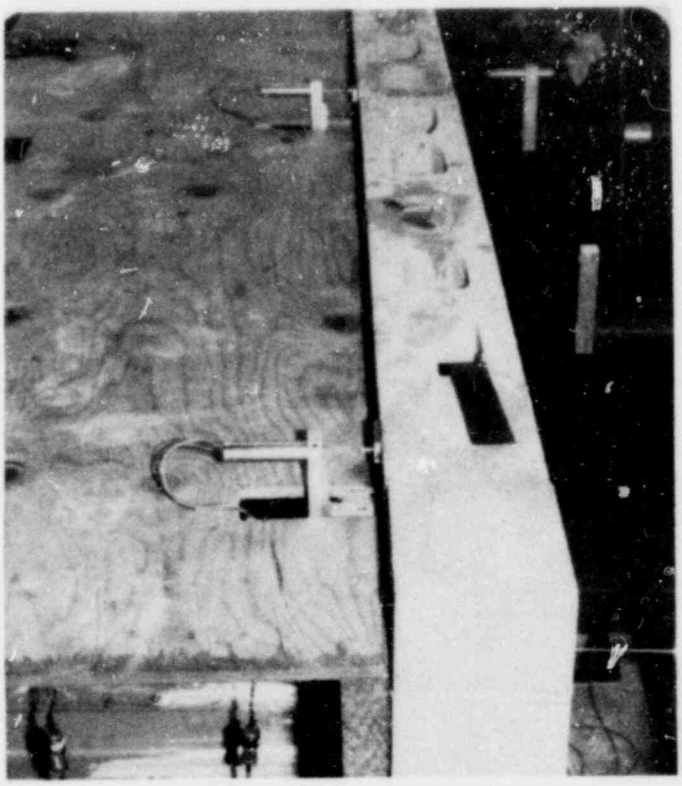

FIGURE 4.20 MEASUREMENT OF LEDGER-WALL SEPARATION

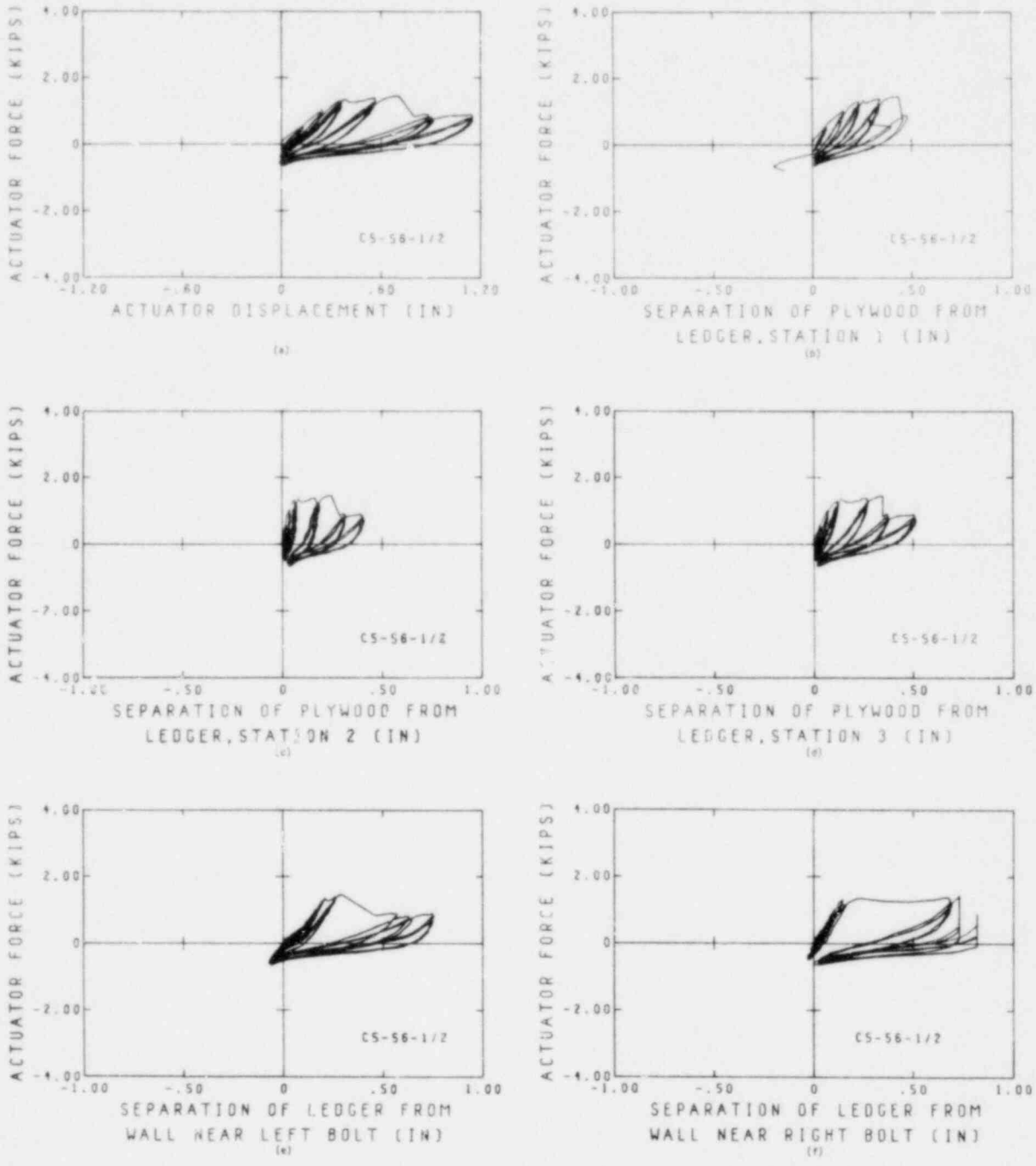

FIGURE 4.21 MEASURED DEFORMATION OF SPECIMEN C5-56-1/2

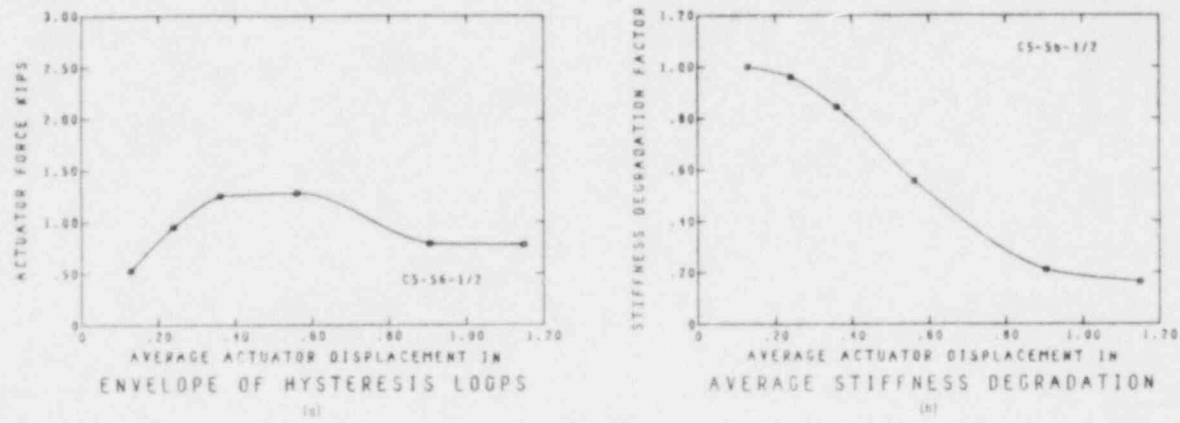

FIGURE 4.21(CONT.) MEASURED DEFORMATION OF SPECIMEN C5-56-1/2

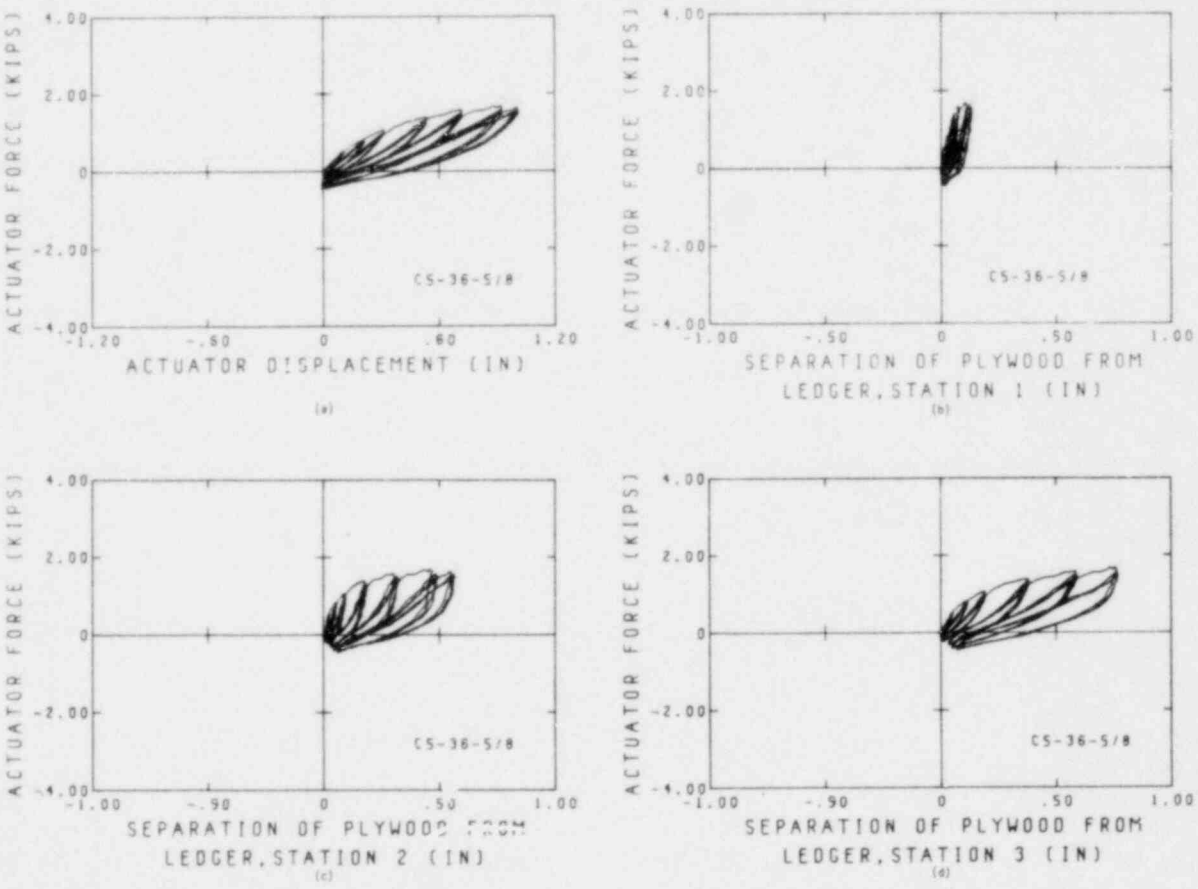

FIGURE 4.22 MEASURED DEFORMATION OF SPECIMEN C5-36-5/8

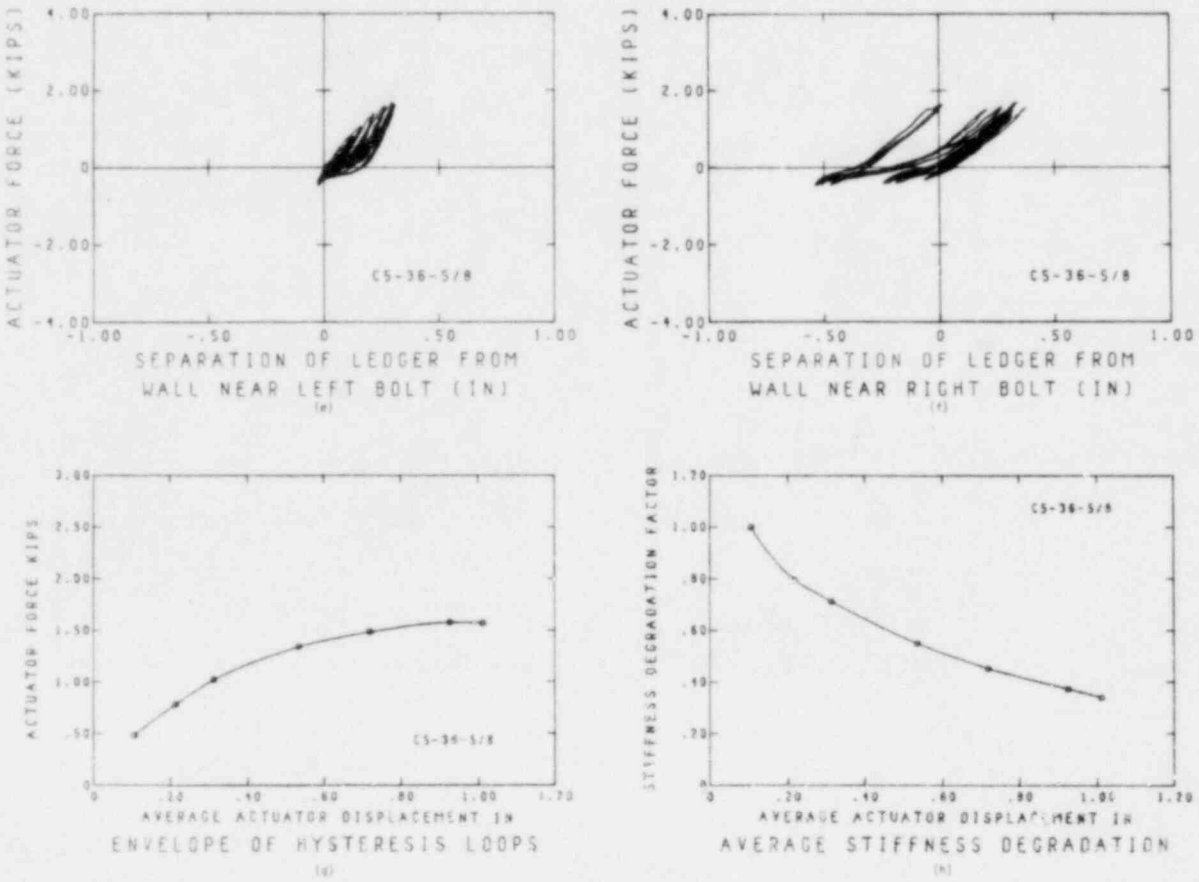

FIGURE 4.22(CONT.) MEASURED DEFORMATION OF SPECIMEN C5-36-5/8

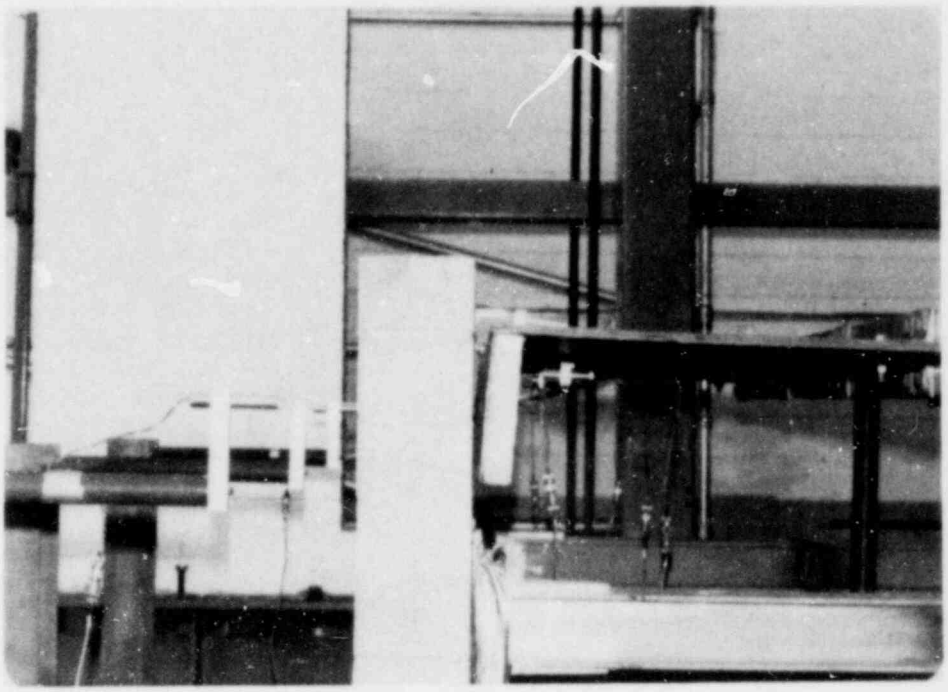

FIGURE 4.23 LEDGER DEFORMATION

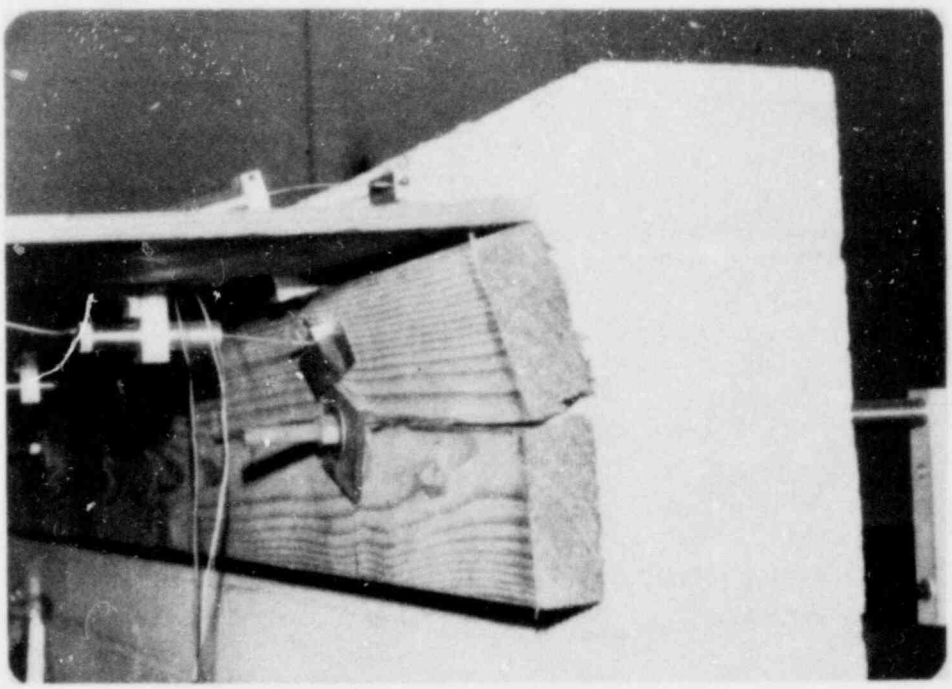

FIGURE 4.24 FAILURE OF LEDGER BOARD IN SPECIMEN C5-56-1/2

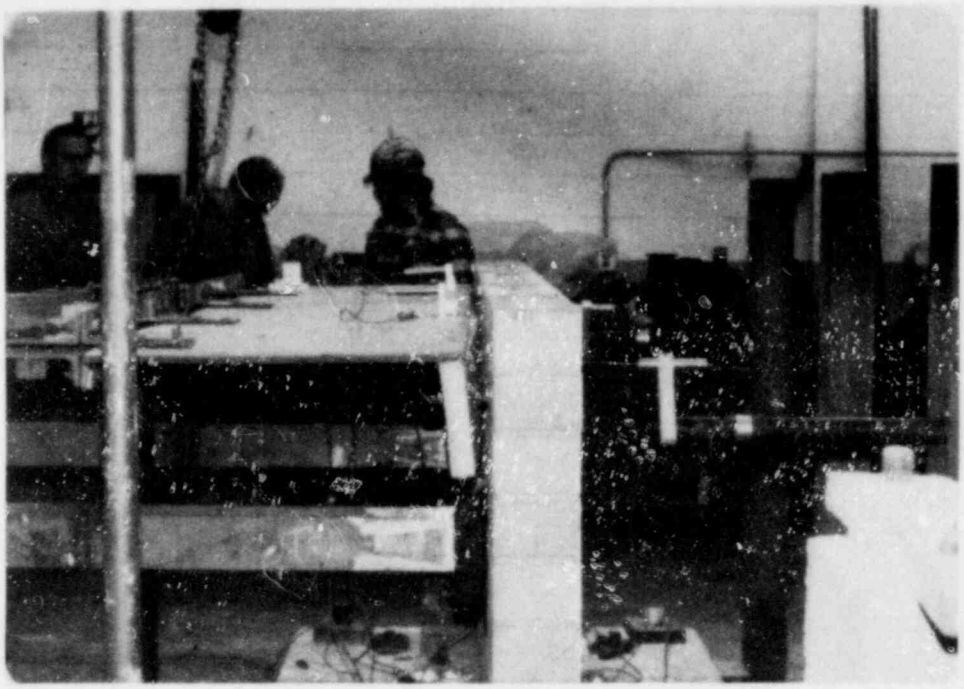

FIGURE 4.25 FAILURE OF LEDGER BOARD IN SPECIMEN C5-36-5/8

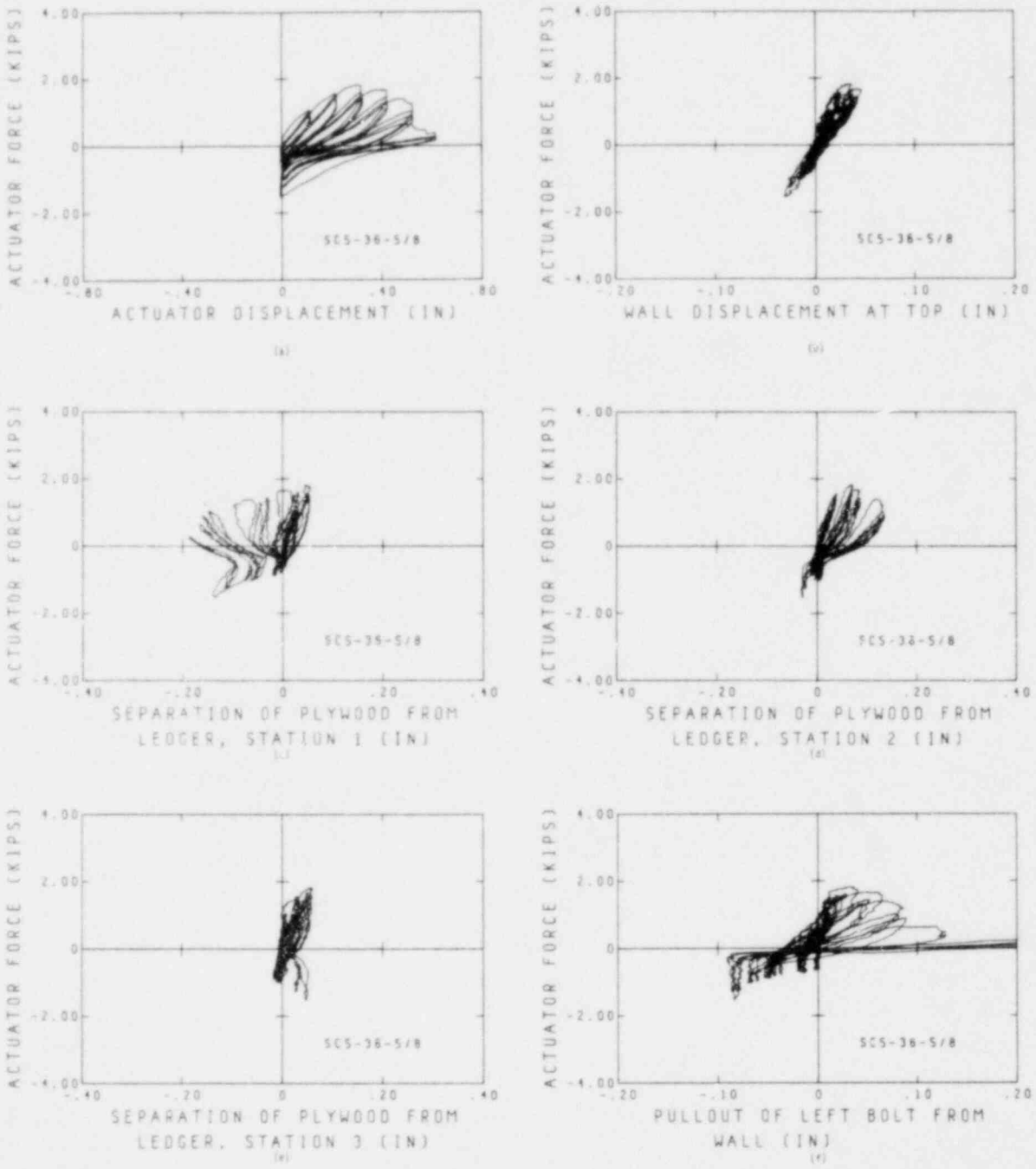

FIGURE 4.26 MEASURED DEFORMATION OF SPECIMEN SC5-36-5/8

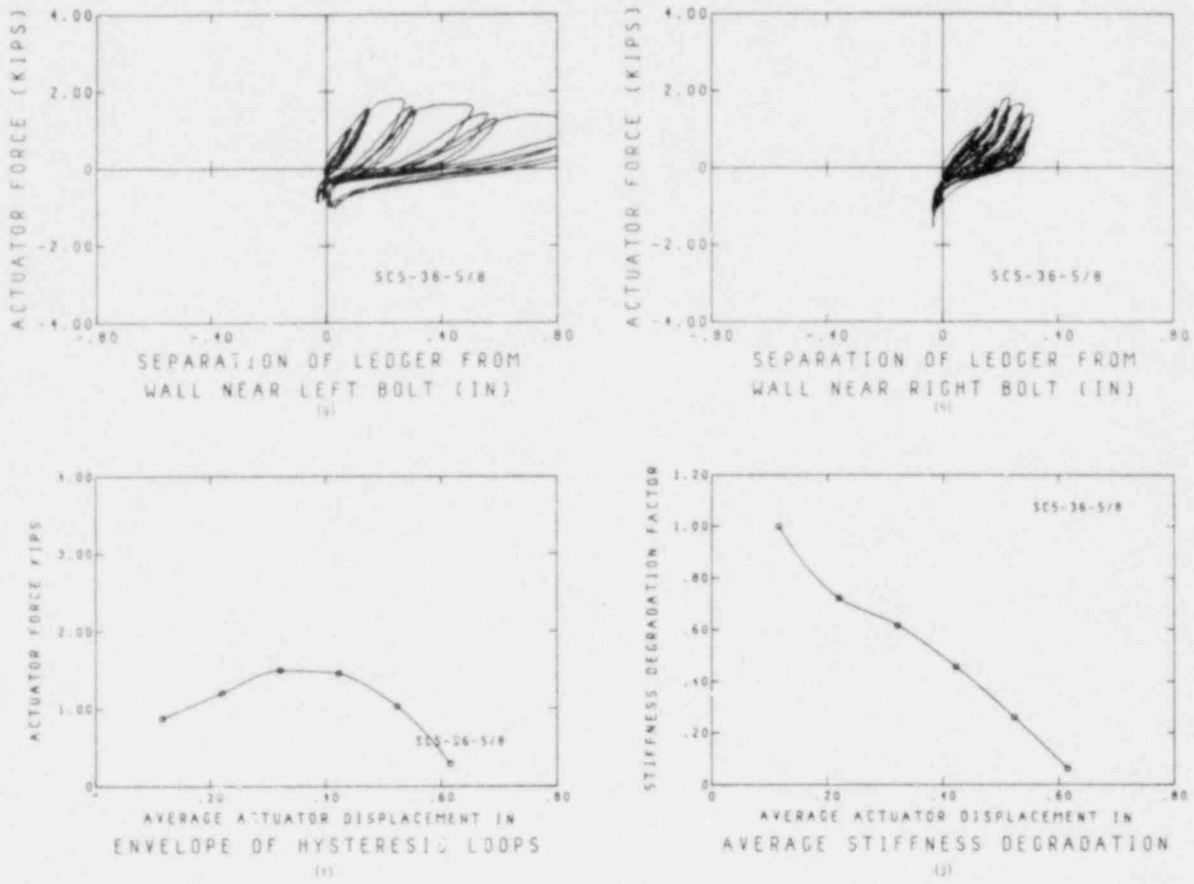

FIGURE 4.26(CONT.) MEASURED DEFORMATION OF SPECIMEN SC5-36-5/8

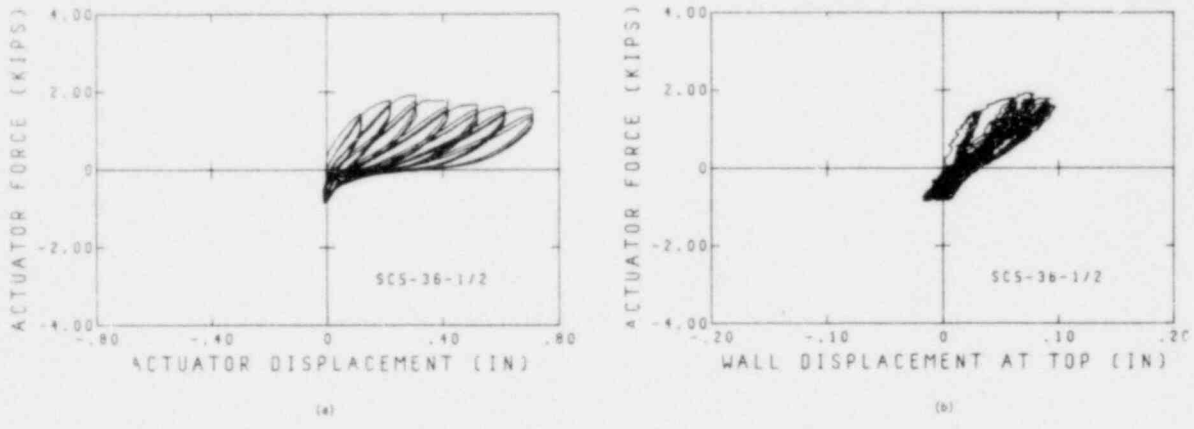

FIGURE 4.27 MEASURED DEFORMATION OF SPECIMEN SC5-36-1/2

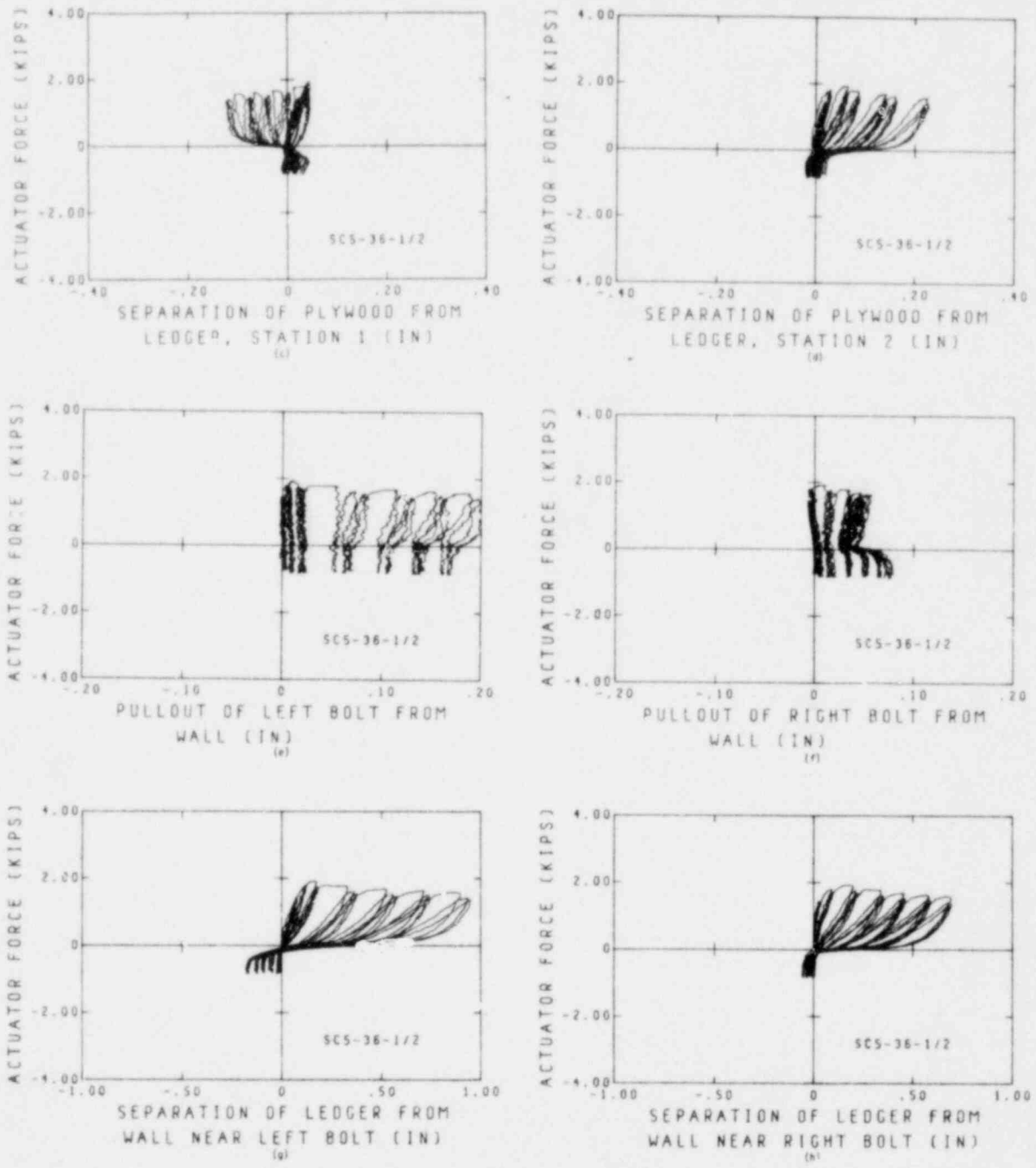

FIGURE 4.27(CONT.) MEASURED DEFORMATION OF SPECIMEN SC5-36-1/2

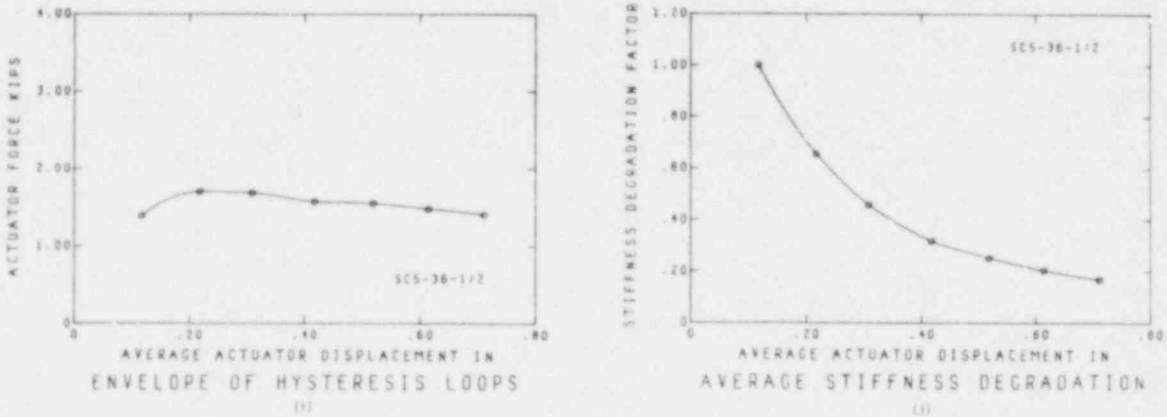

FIGURE 4.27(CONT.) MEASURED DEFORMATION OF SPECIMEN SC5-36-1/2

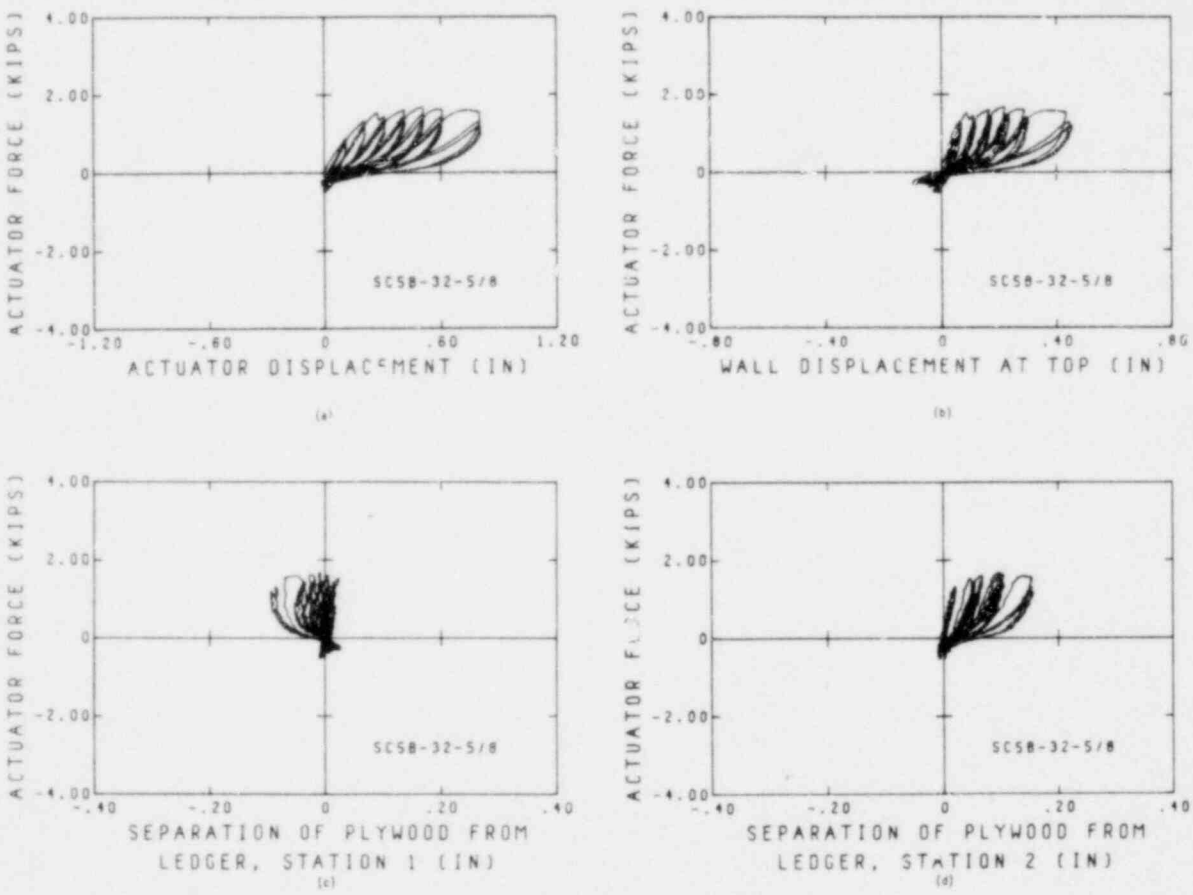

FIGURE 4.28 MEASURED DEFORMATION OF SPECIMEN SC5B-32-5/8

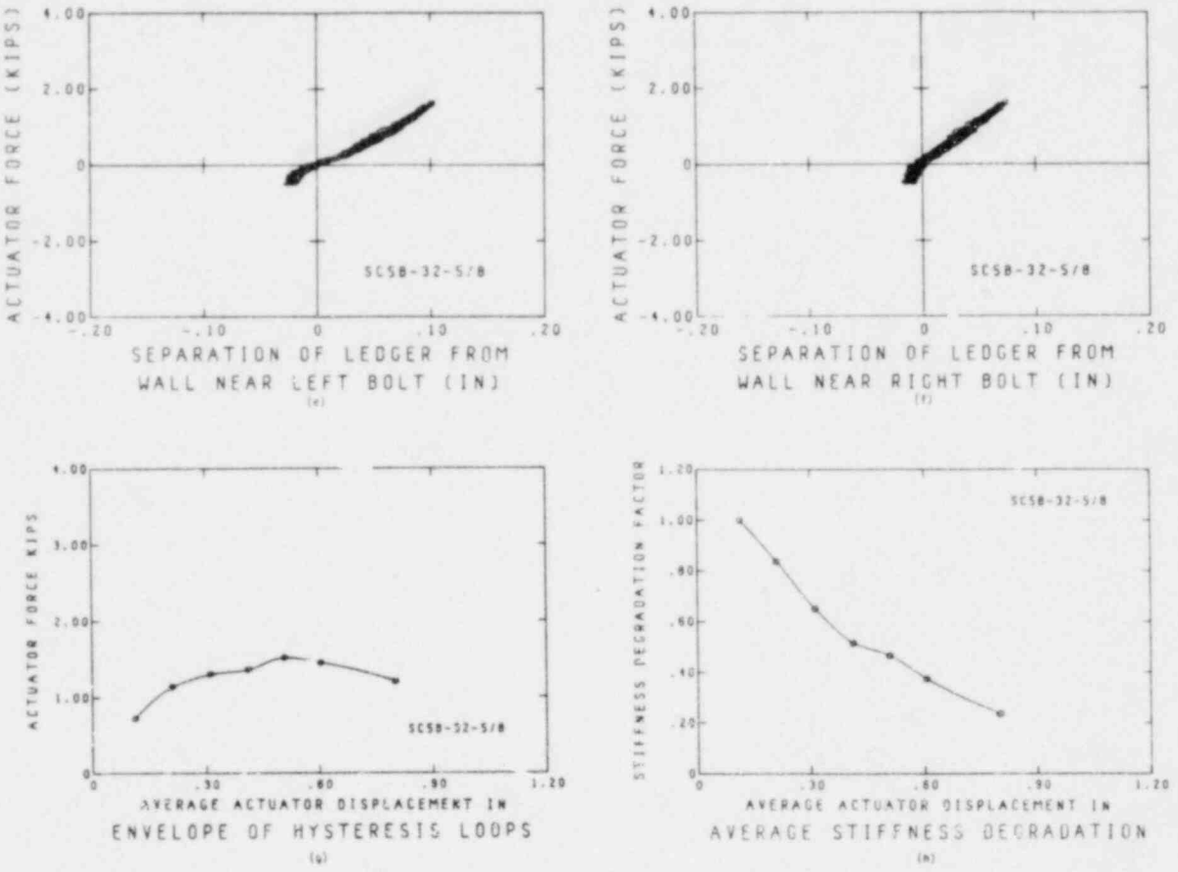

FIGURE 4.28(CONT.) MEASURED DEFORMATION OF SPECIMEN SC5B-32-5/8

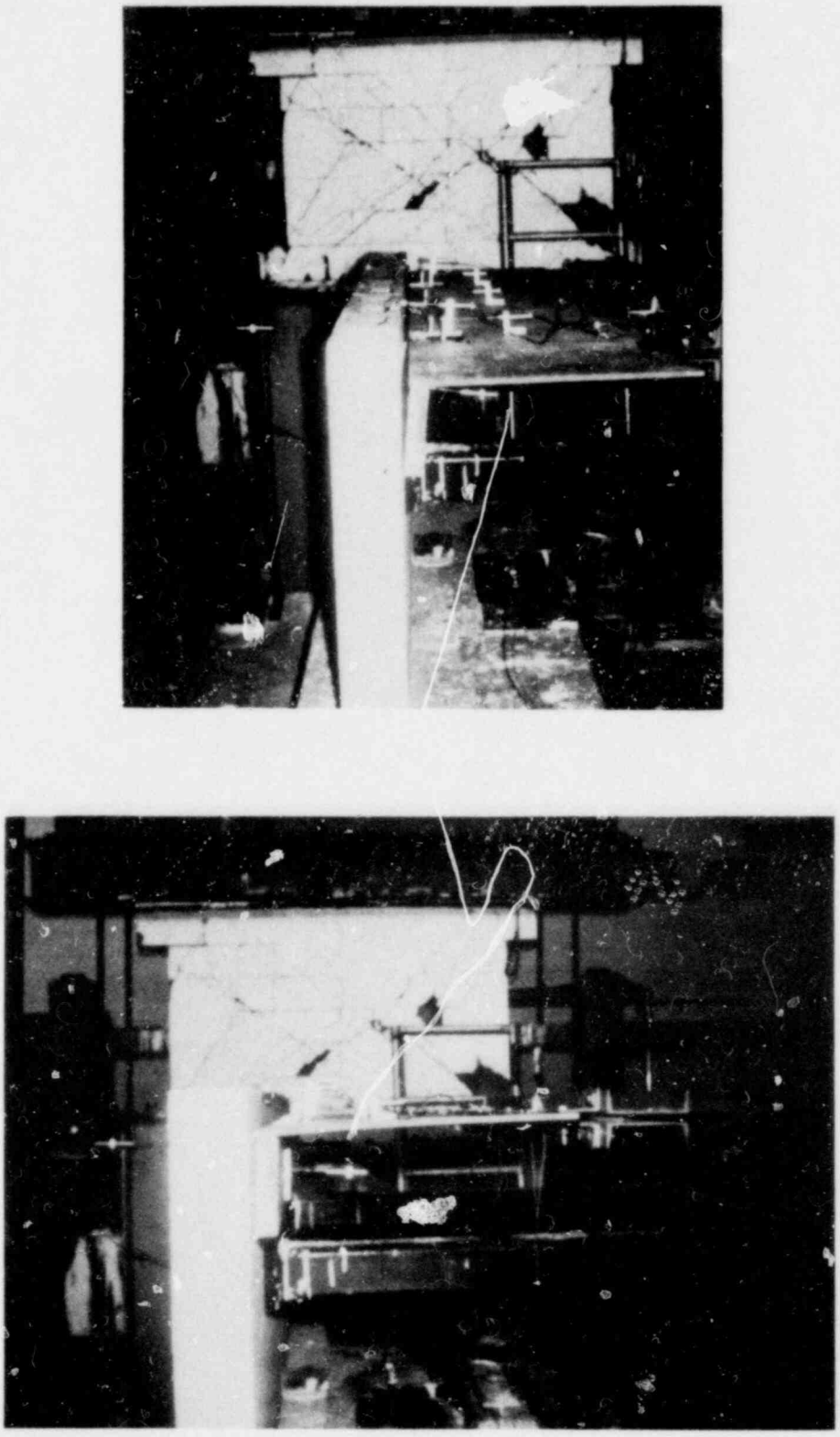

FIGURE 4.29 PLYWOOD AND LEDGER DEFORMATION

5. EVALUATION OF TEST RESULTS

5.1 Introduction

In the preceding chapter, the general behavior of the connection models has been described with the aid of diagrams related to the deformation of the assemblies. All tests were carried to displacement limits at which there was no further increase in the resistance of the connection or until failure had occurred in one part of the assembly. There are several possible modes of failure in a connection. Depending on the loading condition and the relative strength of the components, anchor bolts, nails, or timber parts may be the most critically stressed elements. For the type of connection models included in the test program, an attempt was made to avoid failure of the 8 ft long walls by providing lateral supports for the transversely loaded specimens. For the most part, this measure helped to induce failure in the connection assembly rather than in the wall itself, and wall height was not considered as a parameter. In the following assessment of strength, Uniform Building Code[11] requirements will be taken as the measure for comparison. When appropriate, the discussion will be complemented by observations on the experimental behavior of the connection mock-ups.

5.2 Code Provisions

Table 5.1 lists allowable shear on bolts for masonry. The code provides for an additional 2 in. of embedment for bolts located in the top of columns for buildings in Seismic Zones 2, 3, and 4. Also, masonry strength restrictions apply to 1 and 1-1/8 in. diameter bolt use. The Uniform Building Code does not list any allowable pullout loads for bolts embedded in grouted masonry.

Allowable lateral loads on nails are given in Table 5.2, reproduced

from the Uniform Building Code. Safe pullout loads on common nails are listed in Table 5.3; there are no provisions listed for box nails which have smaller diameters.

Certain general design restrictions apply in the code provisions. First, all allowable stresses and values specified in the UBC for working stress design may be increased one-third when considering lateral forces due to wind or earthquake. Following the poor performance of wood diaphragms during the 1971 San Fernando earthquake, a provision was made that lateral anchorage between roof and masonry walls should be capable of resisting a minimum of 200 lb per foot of wall by means of a positive direct connection[5]. Moreover, in Zones 2, 3, and 4 this anchorage is not to be accomplished by use of toe-nails, or nails subjected to withdrawal. Secondly, wood framing subjected to cross grain bending or tension is not allowed. A reduction factor of 5/6 is specified for the shear resistance of toe-nails. Nails driven parallel to grain of the wood are not allowed for resisting withdrawal forces.

Safe lateral loads for nails have been determined with a view to reducing deflections, and have a minimum strength safety factor of five[10]. In recognition of the great variability in the quality of site workmanship, allowable shear loads for bolts have comparable margins of safety.

5.3 Evaluation of Experimental Results

As stated in Chapter 2, investigation of the behavior of roof connections was undertaken with a view towards complementing a parallel study concerned with the seismic behavior of single-story masonry houses. Selection and design of the connection mock-ups were made in consultation with professional engineers in Arizona and Utah. Local construction

practice (with its idiosyncracies) is therefore reflected in the models tested in the program.

In Table 5.4 a summary is presented of the measured strengths of the connections along with significant features of each test. These include wall material, construction and test phase and type of loading. Two different numbers define the measured resistance. One is the greatest actuator force recorded during any given quarter-cycle excursion, which is usually attained only once. The second definition is synonymous with the greatest ordinate of the hysteresis envelope and corresponds to the largest average resistance of three consecutive cycles of loading. The latter yields a more rational definition for strength because connections would be subjected to a spectrum of loading cycles at different amplitudes during an actual ground motion. All connection mock-ups were subjected initially to three cycles of displacement at an amplitude of 0.1 in. (see Chapter 3), then the imposed displacement amplitude was incremented (usually by 0.1 in.) until no further increase in resistance occurred or until failure took place in the assembly. A stiffness was defined on the basis of average resistance during the initial three cycles, and stiffness values recorded during subsequent cycles were expressed as a fraction of the initial value. Table 5.4 also lists initial stiffness values as well as measured stiffnesses at an imposed displacement of 0.5 in. expressed as a fraction of the initial.

Strength of the connections can be rated on the basis of allowable loads for nails, bolts and framing anchors. In the two cases for which deformation and ultimate failure took place in the walls, allowable loads based on the strength of bolts and nails are also given.

The timber components were assembled in the laboratory after anchoring the walls in place. Construction details described in Chapter 2 were

closely followed so that no major deviations or flaws were built into the specimens. Thus, the allowable loads were determined on the basis of the specified construction. For the comparison contained in Table 5.4, nails and bolts have been taken as the measure of allowable load; strength of walls and timber are excluded from the parameter list. Comparison of measured versus permissable strength is based on the maximum averaged strength. The 1/3 increase in allowable loads has not been considered since loads were applied slowly.

(a) Failure of the connections in group C1 was due to deflection of the nails. Application of the in-plane force to the plywood sheathing resulted in rocking of the bottom chords in which pullout and slip of the nails were combined, as seen in Figs. 4.3 and 4.4. The maximum attained resistance values of 2.42 and 3.55 kips in the 5/8 and 1/2 in. diameter bolt specimens, respectively, reflect this peculiar loading condition, as well as possible effects of load reversals. Application of cyclic loads with gradually increasing displacement amplitudes apparently leads to a significant loss of strength, which was not considered in the experiments upon which code allowable values were based. However, if the rotation of the four bottom chord elements had been reduced through the use of stronger blocking, the shear strength of the assembly would have been greater. Although the 2x6 in. fascia boards imposed some rotational restraint through the action of the two 16d-nails at both ends of the "joists", the effectiveness of this was also red: because of load reversals.

If judgment is based only on the lateral strength of the nails toe-nailed from the joists into the top plate the safe shear force for specimens in group C1 would be 800 lb. (The metal framing anchors

do not contribute to resistance against in-plane shear loads.) Similarly, allowable load only with regard to bolts would be 1,500 lb for C1-28-5/8 and 1,100 lb for C1-28-1/2. Nailing of the plywood to the joists and the fascia boards produces greater allowable resistance, and is not considered for the determination of minimum rated strength. Maximum average resistances of C1-28-5/8 and C1-28-1/2 were 2.30 and 2.99 kips, respectively. The ratio of maximum average resistance to minimum allowable strength thus becomes 2.88 and 3.74 for the two specimens. This ratio is lower than the implicit margin of safety for nails because:

(i) maximum resistance is an average quantity,

(ii) considerable previous working of nails had occurred at the time of maximum resistance, and

(iii) nails were subjected to uplifting coupled with shearing due to the geometry of the assembly.

(b) The allowable lateral strength of the specimens in group C2, based on nails and framing anchors combined, is 1,380 lb since framing anchors have rated resistance to forces applied parallel to the joists. While the actual diameter of anchor bolts would be dictated by the requirements of the design, it appears advisable to distinguish between shear loads on bolts applied parallel or normal to the face shell. The limited number of bolt shear tests carried out as part of the material control program, suggests that bolt failure due to splitting of the face shell and the grout bearing against it, may become a significant parameter. The increased resistance is reflected in the higher values for maximum single peak or average strength values given in Table 5.4.

(c) For specimens in group C3, which were tested by applying transverse forces to the two ties, it is debatable whether the actual behavior of

the connection under field conditions, is similar to the highly idealized mode of the tests. Ignoring any contribution from the dry-wall to transverse strength, six 16d-nails driven into the two 2x4 in. chords would yield an allowable load of 480 lb. Rotation of the "bottom chord" into which the truss ties were nailed produced a pullout effect on nails, as shown in Fig. 4.9(b). This rotation due to the load transmitted from the top edge of the simulated truss chord (see Fig. 2.5), was resisted by four 16d-nails driven horizontally from the chord to each of the two nailing blocks. The most critical loading direction on the assembly is opposite to that shown in Fig. 4.9(b), when the chord subjected the nails to direct pullout. In this mode of response, however, the allowable force would be based on nail pullout strength, and would also depend on the exact location where the nails were driven into the blocking. Experimental observations of this type of connection on a small masonry house subjected to simulated earthquakes[2,3] did not indicate any pullout of nails in the blocks, implying a somewhat different response mechanism. Contrary to this, inspection of the nail holes in the truss bottom chord after the shaking table tests indicated a similar pattern of nail working to that for the in-plane connection tests. Hence, it can be concluded that the three C3 type connections tested in-plane represented a more accurate modeling of actual structural behavior. Ratios of maximum average resistance to allowable loads also reflect this similarity, and are of the same order of magnitude as those corresponding to the C1 and C2 groups. Allowable shear for 3/8 in. diameter bolts was taken to be the same as that for reinforced gypsum concrete.

Initial stiffness values are not totally representative of the connection proper, because they include such parasitic effects as deformation of the walls, especially in the transverse direction. Nevertheless, stiffness quantities for connections of type C3 are in agreement with the manner of loading and measured strength. Also, the stiffness reduction at an imposed displacement of 0.5 in. is similar for similarly loaded specimens.

(d) For models of type C4 and C5 subjected to both eccentric and symmetric transverse forces the anchor bolts were in direct tension for which no provisions are made in the UBC. Largely inspired by the poor performance of roof diaphragm connections during the 1971 San Fernando earthquake[4], a provision was included in the 1976 edition of the UBC requiring appropriate mechanical anchorage of masonry walls to roofs. A special requirement applicable to Zones 2, 3 and 4 further stipulates that such anchorage shall not be accomplished by wood framing members subjected to cross grain tension. As described in Chapter 4, failure of the C4 type connection was primarily a consequence of bolt pullout. For this mode of failure, there is an intimate interrelationship between maximum connection strength and bolt location, masonry unit and grout strength and grout placement. This interaction is reflected in the scatter of the entries in Table 5.4. The following observations may be made from the tabulated values:

(i) Bolt pullout strength appears to be independent of bolt size for the embedment and masonry strength considered.

(ii) Gravity loading does not reduce connection strength.

(iii) Use of grout rather than mortar for embedment of bolts produces superior strength.

In eccentrically loaded connections of type C5, the ledger appeared to be the most vulnerable link in the assembly. The oversized 2-1/2 in. square metal plates failed to prevent splitting in the ledger due to cross-grain tension and warping. When even larger metal plates were employed in the symmetrically loaded connections, there was an immediate increase in initial stiffness and failure was forced into the bolts instead. Still, ledger deformation was significant as evidenced in the ledger-plywood separation diagrams presented in Chapter 4.

Allowable load on the connection assemblies of type C4 was determined on the basis of the shear resistance of nails in the joist hanger and the contribution of the plywood sheathing. For type C5, this was simply the shear resistance of 6d-nails spaced equally on an 8 ft long ledger. Although no failure in either group was attributable to nails, a comparison with measured resistance is included in Table 5.4 for completeness. An overall appraisal of connections in the C4 and C5 types supports the implied philosophy behind code requirements related to the use of bolts in direct tension.

TABLE 5.1

ALLOWABLE SHEAR ON BOLTS

Diameter of Bolt, in.	Embedment in.	Solid Masonry kips	Grouted Masonry kips
1/2	4	0.35	0.55
5/8	4	0.50	0.75
3/4	5	0.75	1.10
7/8	6	1.00	1.50
1	7	1.25	1.85
1-1/8	8	1.50	2.25

from reference (11).

TABLE 5.2

SAFE LATERAL STRENGTH AND REQUIRED PENETRATION OF BOX AND COMMON NAILS DRIVEN PERPENDICULAR TO GRAIN

Size of Nail	Standard Length, in.	Penetration Required in.	Allowable Load, lb
Box Nails			
6d	2	1-1/4	47
8d	2-1/2	1-1/2	59
10d	3	1-5/8	71
12d	3-1/4	1-5/8	71
16d	3-1/2	1-3/4	80
20d	4	2-1/8	104
30d	4-1/2	2-1/4	116
40d	5	2-1/2	132
Common Nails			
6d	2	1-1/4	63
8d	2-1/2	1-1/2	78
10d	3	1-5/8	94
12d	3-1/4	1-5/8	94
16d	3-1/2	1-3/4	107
20d	4	2-1/8	139
30d	4-1/2	2-1/4	154
40d	5	2-1/2	176
50d	5-1/2	2-3/4	202
60d	6	2-7/8	223

Notes: (1) Values listed are for Douglas Fir, Larch or Southern Pine.

(2) For wood diaphragms these values may be increased 30 percent.

from reference (11).

TABLE 5.3

SAFE PULLOUT RESISTANCE OF COMMON WIRE NAILS

Kind of Wood	Size of Nail									
	6d	8d	10d	12d	16d	20d	30d	40d	50d	60d
Douglas Fir, Larch	29	34	38	38	42	49	53	58	63	68
Southern Pine	34	39	44	44	49	57	61	67	73	79
Other Species	Listed in UBC Standard No. 25-17									

Note: These values are for nails inserted perpendicular to grain of wood, in pounds per linear inch of penetration into the main member.

from reference (11).

TABLE 5.4
SUMMARY OF TEST RESULTS

Type	Reference Code	Wall Material	Construction Phase	Test Phase	Type of Loading	Rated Strength Nailing kips	Rated Strength Bolts kips	Max. Resistance kips	Max. Average Resistance kips	Max. Av. Resistance / Min. Rated Strength	Initial Stiffness kip/in.	Ratio of Stiffness at 0.5 in. Disp. to Initial Stiffness	Failure Due to
C1	C1-28-5/8	Concrete Block	1	1	In-plane	0.80	1.50	2.42	2.30	2.88	9.24	0.52	Nails
	C1-28-1/2	Concrete Block	1	1	In-plane	0.80	1.10	3.55	2.99	3.74	12.12	0.46	Nails
C2	SC2-28-5/8	Concrete Block	1	2	Sym. Out-of-plane	1.38	1.50	4.02	3.63	2.63	15.88	0.42	Nails
	SC2-28-5/8(2)	Concrete Block	1	2	Sym. Out-of-plane	1.38	1.50	4.10	3.54	2.57	16.56	0.41	Nails
C3	C3-32-1/2	Concrete Block	1	1	Eccentric Out-of-plane	0.48	1.10	0.90	0.72	1.50	3.15	0.41	Nails
	C3-52-3/8	Concrete Block	1	1	Eccentric Out-of-plane	0.48	0.65	0.84	0.69	1.44	2.15	0.65	Nails
	C3-28-3/8-IP	Concrete Block	1	2	In-plane	0.64	0.65	2.42	1.91	2.98	11.29	0.34	Nails
	C3-28-5/8-IP	Concrete Block	1	2	In-plane	0.64	1.10	2.10	1.75	2.73	12.58	0.25	Nails
	C3-28-5/8-3/8-SP	Concrete Block	1	2	In-plane	1.94	1.75	6.26	5.04	2.88	24.85	0.41	Nails
C4	C4-36-5/8	Concrete Block	1	1	Eccentric Out-of-plane	1.43	—	2.95	2.59	1.81	18.86	0.24	Bolt Pullout
	C4-56-1/2	Concrete Block	1	1	Eccentric Out-of-plane	1.43	—	4.29	3.95	2.76	15.45	0.60	Wall
	SC4-36-5/8-1450	Concrete Block	1	2	Sym. Out-of-plane, Roof Dead Load	1.43	—	6.26	5.51	3.85	24.28	0.48	Bolt Pullout
	SC4-36-5/8	Concrete Block	2	2	Sym. Out-of-plane	1.43	—	1.46	1.24	0.87	10.29	0.14	Bolt Pullout
	SC4B-36-5/8-1450	Brick	2	2	Sym. Out-of-plane, Roof Dead Load	1.43	—	3.85	3.35	2.34	26.54	0.25	Wall & Bolt Pullout
C5	C5-56-1/2	Concrete Block	1	1	Eccentric Out-of-plane	0.61	—	1.40	1.28	2.10	4.11	0.56	Ledger
	C5-36-5/8	Concrete Block	1	1	Eccentric Out-of-plane	0.61	—	1.70	1.57	2.57	4.64	0.55	Ledger
	SC5-36-5/8	Concrete Block	2	2	Sym. Out-of-plane	0.61	—	1.81	1.50	2.46	7.48	0.26	Bolt Pullout
	SC5-36-1/2	Concrete Block	2	2	Sym. Out-of-plane	0.61	—	1.92	1.70	3.79	11.90	0.25	Bolt Pullout
	SC5B-32-5/8	Brick	2	2	Sym. Out-of-plane	0.61	—	1.68	1.56	2.49	6.45	0.47	Wall

6. CONCLUDING REMARKS

6.1 Summary

The strength and behavior under load reversals of the following five basic types of timber roof - masonry wall connections were tested, with emphasis on Seismic Zone 2 conditions:

- C1 load bearing gable roof connections subjected to in-plane loads applied to truss rafters
- C2 load bearing gable roof connections (identical to C1) subjected to out-of-plane loads (actuator force) applied to rafters
- C3 non-load bearing gable roof connections subjected to in-plane and out-of-plane loads
- C4 load bearing flat roof connections subjected to out-of-plane loads
- C5 non-load bearing flat roof connections subjected to out-of-plane loads.

Structural details of these connections are presented in Chapter 2.

A careful distinction was made between the behavior of the connections for in-plane (i.e., parallel to the plane of the wall segment) loads and transverse loads (i.e., normal to the plane of the wall segment). Other parameters tested were the type of unit used in constructing the wall, addition of roof dead load, diameter of the bolts, and eccentric or symmetric application of the simulated earthquake forces to the entire connection assembly.

Connection specimens in the C1 and C2 groups represented a portion of a bearing wall with truss bottom chords at a spacing of 2 ft nailed perpendicular to a single 2x6 in. top plate (Figs. 2.2 and 2.3, respectively). In these specimens, two of the four joist chords were also secured to the

top plate by means of metal framing anchors. In group C1 the in-plane strength of the assembly was determined by applying three displacement controlled cycles of loading at a selected amplitude into the plywood sheathing, and repeating this at successively increasing amplitudes until no further increase in load was detected. The maximum resistances of both C1 specimens were well above the allowable force according to the Uniform Building Code, but the factor of safety intended in the code provisions, without taking into account the permissable 1/3 increase, was not achieved. There are two reasons for this. First, under the application of the lateral force the joists displaced in a mode which combined slipping with rolling, and the toe-nails were pulled up from the top plate. Secondly, the reversal of the applied shear load produced a "softening" action on the nails for which allowable loads have been determined from monotonic load experiments. In group C2, the horizontal load was applied parallel to the joists so that the metal framing anchors also, effectively resisted the imposed displacements. On the whole, observed strengths of the connections in both groups were satisfactory and failure occurred in the nailed parts of the assemblies indicating a potential source of energy dissipation for similar details built into actual structures. Bolt size did not play a role in determining strength. The strength and mode of failure could be determined in a realistic manner, although both C1 and C2 were essentially two-dimensional representations of an actual connection.

Connections in group C3 represented the gabled end of a truss roof system parallel to a transverse wall. The dimension corresponding to the height of the trusses was again not represented in the actual models and the transfer of inertia effects between the roof diaphragm and the wall was simulated, either by applying transverse cyclic forces to the "truss-ties" placed 6 ft apart (Fig. 2.5), or by applying in-plane forces to the

bottom chord nailed to the top plate through 1-ft long blocking. The former arrangement represented a less realistic modelling of the structural behavior (see Section 5.3(c)). However, the connection assembly derives its strength largely from the pullout strength of nails which deteriorated rapidly as the imposed displacements were increased. Because of the low strength of the connection in the transverse direction, the anchor bolts were not stressed to near their capacity, and relative slip of the top plate was not significant. When the same connection was subjected to cyclic in-plane loads deformations were largely concentrated at the bottom chord-block interface, but the overall rigidity and strength of the assembly was significantly increased.

Specimens of type C4 and C5 (shown in Figs. 2.7 and 2.8, respectively) represent typical practice in flat roof connections in areas where seismic considerations are not of primary concern, such as Arizona. The models tested in this group were actual representations of the connections in that no dimension was omitted in the test structures for modeling purposes. The ledgers bolted to the vertical face of the wall segments in two locations 4 ft apart had a nominal thickness of 3 in. for C4 and 2 in. for C5. Both groups of connections were subjected to transverse forces. Because of the greater thickness of the ledger board and the stiffening effect of the four joists connected to it, the deformations of the ledger in C4 were insignificant, and failure occurred primarily in the bolts which pulled out of their embedments in the walls. Strength of the timber parts of the assembly was adequate. In two C4 connections a vertical roof load of 180 lb/ft was simulated by placing weights above the ledger. This did not appear to cause a consistent adverse effect on measured strength. For one specimen having a brick wall, pullout of the bolt was delayed due to the greater flexural strength of the face shell of the

masonry unit, but no consistent differences could be extracted from the results regarding the material.

In connections of type C5, the ledger was subjected to cross-grain tension, both on account of the manner in which the plywood sheathing was nailed to the exposed top edge of the ledger as well as the way by which the ledger was connected to the bolts. Predictably, these specimens exhibited very poor behavior and failure occurred through either excessive deformation and splitting of the ledger, or by inadequate bolt pullout strength. The 2-1/2 in. square metal plate washers did not augment ledger strength noticeably, and the 6x2-1/2 in. washers placed with the long side vertical increased the likelihood of bolt withdrawal although splitting of the ledger was prevented.

6.2 Conclusions and Recommendations for Further Research

On the basis of the measured strength and observed behavior of the connections tested in the experimental program, the following conclusions are drawn:

(1) In cases where cyclic shear forces are applied to nailed timber connections, the apparent factors of safety, based on code provisions, may be substantially reduced (from an inherent value of 5 to about 3) when local deformations result in simultaneous slip and pullout.

(2) The type of truss rafter-to-top plate-to-masonry wall connection considered in types C1 and C2 is adequate for both in- and out-of-plane forces.

(3) Transverse strength of type C3 connections is generally poor but of secondary importance compared with their in-plane strength which was determined to be adequate.

(4) For connections C1, C2, and C3, bolt size appeared not to affect the measured strength. However, it would still be advisable to employ a minimum of 1/2-in. diameter bolts with embedment lengths equal to or greater than code minimum requirements.

(5) The limiting factor in the strength of a ledger type connection without additional mechanical anchorage is either the withdrawal resistance of the anchor bolts or the strength of the ledger board itself. Both of these quantities fluctuate greatly so that present code requirements calling for positive anchorage of wood diaphragms to masonry walls are appropriate.

(6) Strength of ledger connections against horizontal traction forces parallel to the plane of the wall should be investigated. In this type of loading direct anchorage devices would not be effective initially and resistance would be derived solely from bolts.

(7) Use of hollow clay masonry units and simulation of gravity loads in C4 type models did not cause significantly altered response characteristics.

REFERENCES

1. U.S. Department of Housing and Urban Development, HUD Minimum Property Standards: One and Two Family Dwellings, Washington, D.C., 1973.

2. Gülkan, P., R. L. Mayes, and R. W. Clough, "Shaking Table Study of Single-Story Masonry Houses, Volume 1: Test Structures 1 and 2", Report No. UCB/EERC-79/23, Earthquake Engineering Research Center, University of California, Berkeley, 1979.

3. Gülkan, P., R. L. Mayes, and R. W. Clough, "Shaking Table Study of Single-Story Masonry Houses, Volume 2: Test Structures 3 and 4", Report No. UCB/EERC-79/24, Earthquake Engineering Research Center, University of California, Berkeley, 1979.

4. San Fernando, California, Earthquake of February 9, 1971, U.S. Department of Commerce, National Oceanic and Atmospheric Administration, Washington, D.C., 1973.

5. Bower, W.H., "Anchorage of Walls to Wood Diaphragms," Proceedings, 44th Annual Convention of the Structural Engineers Association of California, 1975.

6. Amrhein, J.E., "Some Research Needs of Earthquake-Resistant Masonry," in Earthquake Resistant Masonry Construction: National Workshop, edited by R.A. Crist and L. E. Cattaneo, NBS Building Science Series 106, Washington, D.C., 1977.

7. Meehan, J.F., "Suggested Researchable Items Relating to Masonry Construction," in Earthquake Resistant Masonry Construction: National Workshop, edited by R.A. Crist and L.E. Cattaneo, NBS Building Science Series 106, Washington, D.C., 1977.

8. Ralph W. Goers and Associates, A Methodology for Seismic Design and Construction of Single Family Dwellings, Department of Housing and Urban Development, Division of Energy, Building Technology and Standards, September, 1976.

9. Vanderbilt, M.D., J.R. Goodman, M.E. Criswell, and J. Bodig, "A Rational Analysis and Design Procedure for Wood Joist Floor Systems," report to the National Science Foundation, Colorado State University, Fort Collins, Colorado, November, 1974.

10. Western Woods Use Book, Western Wood Products Association, Portland, Oregon, 1973.

11. Uniform Building Code, International Conference of Building Officials, Whittier, California, 1976 edition.

12. Wilkinson, T.L., "Theoretical Lateral Resistance of Nailed Joists," Journal of the Structural Division, ASCE, Vol. 97, No. ST5, May, 1971, pp. 1381-1398.

13. Wilkinson, T.L., "Analysis of Nailed Joints with Dissimilar Members," Journal of the Structural Division, ASCE, Vol. 98, No. ST9, September, 1972, pp. 2005-2013.

14. Degenkolb, H.J., and L.A. Wyllie, "Design-Lateral Forces," Chapter 7 of Western Woods Use Book, Western Wood Products Association, Portland, Oregon, 1973.

15. Bower, W.H., "Lateral Analysis of Plywood Diaphragms," Journal of the Structural Division, ASCE, Vol. 100, No. ST4, April, 1974, pp. 759-772.

16. Carney, J.M., "Bibliography on Wood and Plywood Diaphragms," Journal of the Structural Division, ASCE, Vol. 101, No. ST11, November, 1975, pp. 2423-2436.

17. Gülkan, P., R. L. Mayes, R.W. Clough, and R. Hendrickson, "An Experimental Investigation on the Seismic Behavior of Single-Story Masonry Houses," Proceedings of the North American Masonry Conference, University of Colorado, Boulder, Colorado, August, 1978.

18. Omote, Y., R.L. Mayes, R.W. Clough, and S.W. Chen, "Effect of Test Technique on Masonry Shear Strength," Proceedings of the Sixth World Conference on Earthquake Engineering, New Delhi, India, 1977.

19. Blume, J.A., and J. Proulx, "Shear in Grouted Brick Masonry Wall Elements," Report to Western States Clay Products Institute from J.A. Blume and Associates, San Francisco, California, August, 1968.

EARTHQUAKE ENGINEERING RESEARCH CENTER REPORTS

NOTE: Numbers in parenthesis are Accession Numbers assigned by the National Technical Information Service; these are followed by a price code. Copies of the reports may be ordered from the National Technical Information Service, 5285 Port Royal Road, Springfield, Virginia, 22161. Accession Numbers should be quoted on orders for reports (PB --- ---) and remittance must accompany each order. Reports without this information were not available at time of printing. Upon request, EERC will mail inquirers this information when it becomes available.

EERC 67-1 "Feasibility Study Large-Scale Earthquake Simulator Facility," by J. Penzien, J.G. Bouwkamp, R.W. Clough and D. Rea - 1967 (PB 187 905)A07

EERC 68-1 Unassigned

EERC 68-2 "Inelastic Behavior of Beam-to-Column Subassemblages Under Repeated Loading," by V.V. Bertero - 1968 (PB 184 888)A05

EERC 68-3 "A Graphical Method for Solving the Wave Reflection-Refraction Problem," by H.D. McNiven and Y. Mengi - 1968 (PB 187 943)A03

EERC 68-4 "Dynamic Properties of McKinley School Buildings," by D. Rea, J.G. Bouwkamp and R.W. Clough - 1968 (PB 187 902)A07

EERC 68-5 "Characteristics of Rock Motions During Earthquakes," by H.B. Seed, I.M. Idriss and F.W. Kiefer - 1968 (PB 188 338)A03

EERC 69-1 "Earthquake Engineering Research at Berkeley," - 1969 (PB 187 906)A11

EERC 69-2 "Nonlinear Seismic Response of Earth Structures," by M. Dibaj and J. Penzien - 1969 (PB 187 904)A08

EERC 69-3 "Probabilistic Study of the Behavior of Structures During Earthquakes," by R. Ruiz and J. Penzien - 1969 (PB 187 886)A06

EERC 69-4 "Numerical Solution of Boundary Value Problems in Structural Mechanics by Reduction to an Initial Value Formulation," by N. Distefano and J. Schujman - 1969 (PB 187 942)A02

EERC 69-5 "Dynamic Programming and the Solution of the Biharmonic Equation," by N. Distefano - 1969 (PB 187 941)A03

EERC 69-6 "Stochastic Analysis of Offshore Tower Structures," by A.K. Malhotra and J. Penzien - 1969 (PB 187 903)A09

EERC 69-7 "Rock Motion Accelerograms for High Magnitude Earthquakes," by H.B. Seed and I.M. Idriss - 1969 (PB 187 940)A02

EERC 69-8 "Structural Dynamics Testing Facilities at the University of California, Berkeley," by R.M. Stephen, J.G. Bouwkamp, R.W. Clough and J. Penzien - 1969 (PB 189 111)A04

EERC 69-9 "Seismic Response of Soil Deposits Underlain by Sloping Rock Boundaries," by H. Dezfulian and H.B. Seed 1969 (PB 189 114)A03

EERC 69-10 "Dynamic Stress Analysis of Axisymmetric Structures Under Arbitrary Loading," by S. Ghosh and E.L. Wilson 1969 (PB 189 026)A10

EERC 69-11 "Seismic Behavior of Multistory Frames Designed by Different Philosophies," by J.C. Anderson and V. V. Bertero - 1969 (PB 190 662)A10

EERC 69-12 "Stiffness Degradation of Reinforcing Concrete Members Subjected to Cyclic Flexural Moments," by V.V. Bertero, B. Bresler and H. Ming Liao - 1969 (PB 202 942)A07

EERC 69-13 "Response of Non-Uniform Soil Deposits to Travelling Seismic Waves," by H. Dezfulian and H.B. Seed - 1969 (PB 191 023)A03

EERC 69-14 "Damping Capacity of a Model Steel Structure," by D. Rea, R.W. Clough and J.G. Bouwkamp - 1969 (PB 190 663)A06

EERC 69-15 "Influence of Local Soil Conditions on Building Damage Potential during Earthquakes," by H.B. Seed and I.M. Idriss - 1969 (PB 191 036)A03

EERC 69-16 "The Behavior of Sands Under Seismic Loading Conditions," by M.L. Silver and H.B. Seed - 1969 (AD 714 982)A07

EERC 70-1 "Earthquake Response of Gravity Dams," by A.K. Chopra - 1970 (AD 709 640)A03

EERC 70-2 "Relationships between Soil Conditions and Building Damage in the Caracas Earthquake of July 29, 1967," by H.B. Seed, I.M. Idriss and H. Dezfulian - 1970 (PB 195 762)A05

EERC 70-3 "Cyclic Loading of Full Size Steel Connections," by E.P. Popov and R.M. Stephen - 1970 (PB 213 545)A04

EERC 70-4 "Seismic Analysis of the Charaima Building, Caraballeda, Venezuela," by Subcommittee of the SEAONC Research Committee: V.V. Bertero, P.F. Fratessa, S.A. Mahin, J.H. Sexton, A.C. Scordelis, E.L. Wilson, L.A. Wyllie, H.B. Seed and J. Penzien, Chairman - 1970 (PB 201 455)A06

EERC 70-5 "A Computer Program for Earthquake Analysis of Dams," by A.K. Chopra and P. Chakrabarti - 1970 (AD 723 994)A05

EERC 70-6 "The Propagation of Love Waves Across Non-Horizontally Layered Structures," by J. Lysmer and L.A. Drake 1970 (PB 197 896)A01

EERC 70-7 "Influence of Base Rock Characteristics on Ground Response," by J. Lysmer, H.B. Seed and P.B. Schnabel 19[illegible] (PB 197 897)A03

EERC 70-8 "Applicability of Laboratory Test Procedures for Measuring Soil Liquefaction Characteristics under Cyclic Loading," by H.B. Seed and W.H. Peacock - 1970 (PB 198 016)A03

EERC 70-9 "A Simplified Procedure for Evaluating Soil Liquefaction Potential," by H.B. Seed and I.M. Idriss - 1970 (PB 198 009)A03

EERC 70-10 "Soil Moduli and Damping Factors for Dynamic Response Analysis," by H.B. Seed and I.M. Idriss - 1970 (PB 197 869)A03

EERC 71-1 "Koyna Earthquake of December 11, 1967 and the Performance of Koyna Dam," by A.K. Chopra and [illegible]. Chakrabarti 1971 (AD 731 496)A06

EERC 71-2 "Preliminary In-Situ Measurements of Anelastic Absorption in Soils Using a Prototype Earthquake Simulator," by R.D. Borcherdt and P.W. Rodgers - 1971 (PB 201 454)A03

EERC 71-3 "Static and Dynamic Analysis of Inelastic Frame Structures," by F.L. Porter and G.H. Powell - 1971 (PB 210 135)A06

EERC 71-4 "Research Needs in Limit Design of Reinforced Concrete Structures," by V.V. Bertero - 1971 (PB 202 943)A04

EERC 71-5 "Dynamic Behavior of a High-Rise Diagonally Braced Steel Building," by D. Rea, A.A. Shah and J.G. Bouwkamp 1971 (PB 203 584)A06

EERC 71-6 "Dynamic Stress Analysis of Porous Elastic Solids Saturated with Compressible Fluids," by J. Ghaboussi and E. L. Wilson - 1971 (PB 211 396)A06

EERC 71-7 "Inelastic Behavior of Steel Beam-to-Column Subassemblages," by H. Krawinkler, V.V. Bertero and E.P. Popov 1971 (PB 211 335)A14

EERC 71-8 "Modification of Seismograph Records for Effects of Local Soil Conditions," by P. Schnabel, H.B. Seed and J. Lysmer - 1971 (PB 214 450)A03

EERC 72-1 "Static and Earthquake Analysis of Three Dimensional Frame and Shear Wall Buildings," by E.L. Wilson and H.H. Dovey - 1972 (PB 212 904)A05

EERC 72-2 "Accelerations in Rock for Earthquakes in the Western United States," by P.B. Schnabel and H.B. Seed - 1972 (PB 213 100)A03

EERC 72-3 "Elastic-Plastic Earthquake Response of Soil-Building Systems," by T. Minami - 1972 (PB 214 868)A08

EERC 72-4 "Stochastic Inelastic Response of Offshore Towers to Strong Motion Earthquakes," by M.K. Kaul - 1972 (PB 215 713)A05

EERC 72-5 "Cyclic Behavior of Three Reinforced Concrete Flexural Members with High Shear," by E.P. Popov, V.V. Bertero and H. Krawinkler - 1972 (PB 214 555)A05

EERC 72-6 "Earthquake Response of Gravity Dams Including Reservoir Interaction Effects," by P. Chakrabarti and A.K. Chopra - 1972 (AD 762 330)A08

EERC 72-7 "Dynamic Properties of Pine Flat Dam," by D. Rea, C.Y. Liaw and A.K. Chopra - 1972 (AD 763 928)A05

EERC 72-8 "Three Dimensional Analysis of Building Systems," by E.L. Wilson and H.H. Dovey - 1972 (PB 222 438)A06

EERC 72-9 "Rate of Loading Effects on Uncracked and Repaired Reinforced Concrete Members," by S. Mahin, V.V. Bertero, D. Rea and M. Atalay - 1972 (PB 224 520)A08

EERC 72-10 "Computer Program for Static and Dynamic Analysis of Linear Structural Systems," by E.L. Wilson, K.J. Bathe, J.E. Peterson and H.H.Dovey - 1972 (PB 220 437)A04

EERC 72-11 "Literature Survey - Seismic Effects on Highway Bridges," by T. Iwasaki, J. Penzien and R.W. Clough - 1972 (PB 215 613)A19

EERC 72-12 "SHAKE-A Computer Program for Earthquake Response Analysis of Horizontally Layered Sites," by P.B. Schnabel and J. Lysmer - 1972 (PB 220 207)A06

EERC 73-1 "Optimal Seismic Design of Multistory Frames," by V.V. Bertero and H. Kamil - 1973

EERC 73-2 "Analysis of the Slides in the San Fernando Dams During the Earthquake of February 9, 1971," by H.B. Seed, K.L. Lee, I.M. Idriss and F. Makdisi - 1973 (PB 223 402)A14

EERC 73-3 "Computer Aided Ultimate Load Design of Unbraced Multistory Steel Frames," by M.B. El-Hafez and G.H. Powell 1973 (PB 248 315)A09

EERC 73-4 "Experimental Investigation into the Seismic Behavior of Critical Regions of Reinforced Concrete Components as Influenced by Moment and Shear," by M. Celebi and J. Penzien - 1973 (PB 215 884)A09

EERC 73-5 "Hysteretic Behavior of Epoxy-Repaired Reinforced Concrete Beams," by M. Celebi and J. Penzien - 1973 (PB 239 568)A03

EERC 73-6 "General Purpose Computer Program for Inelastic Dynamic Response of Plane Structures," by A. Kanaan and G.H. Powell - 1973 (PB 221 260)A08

EERC 73-7 "A Computer Program for Earthquake Analysis of Gravity Dams Including Reservoir Interaction," by P. Chakrabarti and A.K. Chopra - 1973 (AD 766 271)A04

EERC 73-8 "Behavior of Reinforced Concrete Deep Beam-Column Subassemblages Under Cyclic Loads," by O. Küstü and J.G. Bouwkamp - 1973 (PB 246 117)A12

EERC 73-9 "Earthquake Analysis of Structure-Foundation Systems," by A.K. Vaish and A.K. Chopra - 1973 (AD 766 272)A07

EERC 73-10 "Deconvolution of Seismic Response for Linear Systems," by R.B. Reimer - 1973 (PB 227 179)A08

EERC 73-11 "SAP IV: A Structural Analysis Program for Static and Dynamic Response of Linear Systems," by K.-J. Bathe, E.L. Wilson and F.E. Peterson - 1973 (PB 221 967)A09

EERC 73-12 "Analytical Investigations of the Seismic Response of Long, Multiple Span Highway Bridges," by W.S. Tseng and J. Penzien - 1973 (PB 227 816)A10

EERC 73-13 "Earthquake Analysis of Multi-Story Buildings Including Foundation Interaction," by A.K. Chopra and J.A. Gutierrez - 1973 (PB 222 970)A03

EERC 73-14 "ADAP: A Computer Program for Static and Dynamic Analysis of Arch Dams," by R.W. Clough, J.M. Raphael and S. Mojtahedi - 1973 (PB 223 763)A09

EERC 73-15 "Cyclic Plastic Analysis of Structural Steel Joints," by R.B. Pinkney and R.W. Clough - 1973 (PB 226 843)A08

EERC 73-16 "QUAD-4: A Computer Program for Evaluating the Seismic Response of Soil Structures by Variable Damping Finite Element Procedures," by I.M. Idriss, J. Lysmer, R. Hwang and H.B. Seed - 1973 (PB 229 424)A05

EERC 73-17 "Dynamic Behavior of a Multi-Story Pyramid Shaped Building," by R.M. Stephen, J.P. Hollings and J.G. Bouwkamp - 1973 (PB 240 718)A06

EERC 73-18 "Effect of Different Types of Reinforcing on Seismic Behavior of Short Concrete Columns," by V.V. Bertero, J. Hollings, O. Küstü, R.M. Stephen and J.G. Bouwkamp - 1973

EERC 73-19 "Olive View Medical Center Materials Studies, Phase I," by B. Bresler and V.V. Bertero - 1973 (PB 235 986)A06

EERC 73-20 "Linear and Nonlinear Seismic Analysis Computer Programs for Long Multiple-Span Highway Bridges," by W.S. Tseng and J. Penzien - 1973

EERC 73-21 "Constitutive Models for Cyclic Plastic Deformation of Engineering Materials," by J.M. Kelly and P.P. Gillis 1973 (PB 226 024)A03

EERC 73-22 "DRAIN - 2D User's Guide," by G.H. Powell - 1973 (PB 227 016)A05

EERC 73-23 "Earthquake Engineering at Berkeley - 1973," (PB 226 033)A11

EERC 73-24 Unassigned

EERC 73-25 "Earthquake Response of Axisymmetric Tower Structures Surrounded by Water," by C.Y. Liaw and A.K. Chopra 1973 (AD 773 052)A09

EERC 73-26 "Investigation of the Failures of the Olive View Stairtowers During the San Fernando Earthquake and Their Implications on Seismic Design," by V.V. Bertero and R.G. Collins - 1973 (PB 235 106)A13

EERC 73-27 "Further Studies on Seismic Behavior of Steel Beam-Column Subassemblages," by V.V. Bertero, E. Krawinkler and E.P. Popov - 1973 (PB 234 172)A06

EERC 74-1 "Seismic Risk Analysis," by C.S. Oliveira - 1974 (PB 235 920)A06

EERC 74-2 "Settlement and Liquefaction of Sands Under Multi-Directional Shaking," by R. Pyke, C.K. Chan and H.B. Seed 1974

EERC 74-3 "Optimum Design of Earthquake Resistant Shear Buildings," by D. Ray, K.S. Pister and A.K. Chopra - 1974 (PB 231 172)A06

EERC 74-4 "LUSH - A Computer Program for Complex Response Analysis of Soil-Structure Systems," by J. Lysmer, T. Udaka, H.B. Seed and R. Hwang - 1974 (PB 236 796)A05

EERC 74-5 "Sensitivity Analysis for Hysteretic Dynamic Systems: Applications to Earthquake Engineering," by D. Ray 1974 (PB 233 213)A06

EERC 74-6 "Soil Structure Interaction Analyses for Evaluating Seismic Response," by H.B. Seed, J. Lysmer and R. Hwang 1974 (PB 236 519)A04

EERC 74-7 Unassigned

EERC 74-8 "Shaking Table Tests of a Steel Frame - A Progress Report," by R.W Clough and D. Tang - 1974 (PB 240 869)A0

EERC 74-9 "Hysteretic Behavior of Reinforced Concrete Flexural Members with Special Web Reinforcement," by V.V. Bertero, E.P. Popov and T.Y. Wang - 1974 (PB 236 797)A07

EERC 74-10 "Applications of Reliability-Based, Global Cost Optimization to Design of Earthquake Resistant Structures," by E. Vitiello and K.S. Pister - 1974 (PB 237 231)A06

EERC 74-11 "Liquefaction of Gravelly Soils Under Cyclic Loading Conditions," by R.T. Wong, H.B. Seed and C.K. Chan 1974 (PB 242 042)A03

EERC 74-12 "Site-Dependent Spectra for Earthquake-Resistant Design," by H.B. Seed, C. Ugas and J. Lysmer - 1974 (PB 240 953)A03

EERC 74-13 "Earthquake Simulator Study of a Reinforced Concrete Frame," by P. Hidalgo and R.W. Clough - 1974 (PB 241 944)A13

EERC 74-14 "Nonlinear Earthquake Response of Concrete Gravity Dams," by N. Pal - 1974 (AD/A 006 583)A06

EERC 74-15 "Modeling and Identification in Nonlinear Structural Dynamics - I. One Degree of Freedom Models," by N. Distefano and A. Rath - 1974 (PB 241 548)A06

EERC 75-1 "Determination of Seismic Design Criteria for the Dumbarton Bridge Replacement Structure, Vol. I: Description, Theory and Analytical Modeling of Bridge and Parameters," by F. Baron and S.-H. Pang - 1975 (PB 259 407)A15

EERC 75-2 "Determination of Seismic Design Criteria for the Dumbarton Bridge Replacement Structure, Vol. II: Numerical Studies and Establishment of Seismic Design Criteria," by F. Baron and S.-H. Pang - 1975 (PB 259 408)A11 (For set of EERC 75-1 and 75-2 (PB 259 406))

EERC 75-3 "Seismic Risk Analysis for a Site and a Metropolitan Area," by C.S. Oliveira - 1975 (PB 248 134)A09

EERC 75-4 "Analytical Investigations of Seismic Response of Short, Single or Multiple-Span Highway Bridges," by M.-C. Chen and J. Penzien - 1975 (PB 241 454)A09

EERC 75-5 "An Evaluation of Some Methods for Predicting Seismic Behavior of Reinforced Concrete Buildings," by S.A. Mahin and V.V. Bertero - 1975 (PB 246 306)A16

EERC 75-6 "Earthquake Simulator Study of a Steel Frame Structure, Vol. I: Experimental Results," by R.W. Clough and D.T. Tang - 1975 (PB 243 981)A13

EERC 75-7 "Dynamic Properties of San Bernardino Intake Tower," by D. Rea, C.-Y. Liaw and A.K. Chopra - 1975 (AD/A008 406) A05

EERC 75-8 "Seismic Studies of the Articulation for the Dumbarton Bridge Replacement Structure, Vol. I: Description, Theory and Analytical Modeling of Bridge Components," by F. Baron and R.E. Hamati - 1975 (PB 251 539)A07

EERC 75-9 "Seismic Studies of the Articulation for the Dumbarton Bridge Replacement Structure, Vol. 2: Numerical Studies of Steel and Concrete Girder Alternates," by F. Baron and R.E. Hamati - 1975 (PB 251 540)A10

EERC 75-10 "Static and Dynamic Analysis of Nonlinear Structures," by D.P. Mondkar and G.H. Powell - 1975 (PB 242 434)A08

EERC 75-11 "Hysteretic Behavior of Steel Columns," by E.P. Popov, V.V. Bertero and S. Chandramouli - 1975 (PB 252 365)A11

EERC 75-12 "Earthquake Engineering Research Center Library Printed Catalog," - 1975 (PB 243 711)A26

EERC 75-13 "Three Dimensional Analysis of Building Systems (Extended Version)," by E.L. Wilson, J.P. Hollings and H.H. Dovey - 1975 (PB 243 989)A07

EERC 75-14 "Determination of Soil Liquefaction Characteristics by Large-Scale Laboratory Tests," by P. De Alba, C.K. Chan and H.B. Seed - 1975 (NUREG 0027)A08

EERC 75-15 "A Literature Survey - Compressive, Tensile, Bond and Shear Strength of Masonry," by R.L. Mayes and R.W. Clough - 1975 (PB 246 292)A10

EERC 75-16 "Hysteretic Behavior of Ductile Moment Resisting Reinforced Concrete Frame Components," by V.V. Bertero and E.P. Popov - 1975 (PB 246 388)A05

EERC 75-17 "Relationships Between Maximum Acceleration, Maximum Velocity, Distance from Source, Local Site Conditions for Moderately Strong Earthquakes," by H.B. Seed, R. Murarka, J. Lysmer and I.M. Idriss - 1975 (PB 248 172)A03

EERC 75-18 "The Effects of Method of Sample Preparation on the Cyclic Stress-Strain Behavior of Sands," by J. Mulilis, C.K. Chan and H.B. Seed - 1975 (Summarized in EERC 75-28)

EERC 75-19 "The Seismic Behavior of Critical Regions of Reinforced Concrete Components as Influenced by Moment, Shear and Axial Force," by M.B. Atalay and J. Penzien - 1975 (PB 258 842)A11

EERC 75-20 "Dynamic Properties of an Eleven Story Masonry Building," by R.M. Stephen, J.P. Hollings, J.G. Bouwkamp and D. Jurukovski - 1975 (PB 246 945)A04

EERC 75-21 "State-of-the-Art in Seismic Strength of Masonry - An Evaluation and Review," by R.L. Mayes and R.W. Clough 1975 (PB 249 040)A07

EERC 75-22 "Frequency Dependent Stiffness Matrices for Viscoelastic Half-Plane Foundations," by A.K. Chopra, P. Chakrabarti and G. Dasgupta - 1975 (PB 248 121)A07

EERC 75-23 "Hysteretic Behavior of Reinforced Concrete Framed Walls," by T.Y. Wong, V.V. Bertero and E.P. Popov - 1975

EERC 75-24 "Testing Facility for Subassemblages of Frame-Wall Structural Systems," by V.V. Bertero, E.P. Popov and T. Endo - 1975

EERC 75-25 "Influence of Seismic History on the Liquefaction Characteristics of Sands," by H.B. Seed, K. Mori and C.K. Chan - 1975 (Summarized in EERC 75-28)

EERC 75-26 "The Generation and Dissipation of Pore Water Pressures during Soil Liquefaction," by H.B. Seed, P.P. Martin and J. Lysmer - 1975 (PB 252 648)A03

EERC 75-27 "Identification of Research Needs for Improving Aseismic Design of Building Structures," by V.V. Bertero 1975 (PB 248 136)A05

EERC 75-28 "Evaluation of Soil Liquefaction Potential during Earthquakes," by H.B. Seed, I. Arango and C.K. Chan - 1975 (NUREG 0026)A13

EERC 75-29 "Representation of Irregular Stress Time Histories by Equivalent Uniform Stress Series in Liquefaction Analyses," by H.B. Seed, I.M. Idriss, F. Makdisi and N. Banerjee - 1975 (PB 252 635)A03

EERC 75-30 "FLUSH - A Computer Program for Approximate 3-D Analysis of Soil-Structure Interaction Problems," by J. Lysmer, T. Udaka, C.-F. Tsai and H.B. Seed - 1975 (PB 259 332)A07

EERC 75-31 "ALUSH - A Computer Program for Seismic Response Analysis of Axisymmetric Soil-Structure Systems," by E. Berger, J. Lysmer and H.B. Seed - 1975

EERC 75-32 "TRIP and TRAVEL - Computer Programs for Soil-Structure Interaction Analysis with Horizontally Travelling Waves," by T. Udaka, J. Lysmer and H.B. Seed - 1975

EERC 75-33 "Predicting the Performance of Structures in Regions of High Seismicity," by J. Penzien - 1975 (PB 248 130)A03

EERC 75-34 "Efficient Finite Element Analysis of Seismic Structure - Soil - Direction," by J. Lysmer, H.B. Seed, T. Udaka, R.N. Hwang and C.-F. Tsai - 1975 (PB 253 570)A03

EERC 75-35 "The Dynamic Behavior of a First Story Girder of a Three-Story Steel Frame Subjected to Earthquake Loading," by R.W. Clough and L.-Y. Li - 1975 (PB 248 841)A05

EERC 75-36 "Earthquake Simulator Study of a Steel Frame Structure, Volume II - Analytical Results," by D.T. Tang - 1975 (PB 252 926)A10

EERC 75-37 "ANSR-I General Purpose Computer Program for Analysis of Non-Linear Structural Response," by D.P. Mondkar and G.H. Powell - 1975 (PB 252 386)A08

EERC 75-38 "Nonlinear Response Spectra for Probabilistic Seismic Design and Damage Assessment of Reinforced Concrete Structures," by M. Murakami and J. Penzien - 1975 (PB 259 530)A05

EERC 75-39 "Study of a Method of Feasible Directions for Optimal Elastic Design of Frame Structures Subjected to Earthquake Loading," by N.D. Walker and K.S. Pister - 1975 (PB 257 781)A06

EERC 75-40 "An Alternative Representation of the Elastic-Viscoelastic Analogy," by G. Dasgupta and J.L. Sackman - 1975 (PB 252 173)A03

EERC 75-41 "Effect of Multi-Directional Shaking on Liquefaction of Sands," by H.B. Seed, R. Pyke and G.R. Martin - 1975 (PB 258 781)A03

EERC 76-1 "Strength and Ductility Evaluation of Existing Low-Rise Reinforced Concrete Buildings - Screening Method," by T. Okada and B. Bresler - 1976 (PB 257 906)A11

EERC 76-2 "Experimental and Analytical Studies on the Hysteretic Behavior of Reinforced Concrete Rectangular and T-Beams," by S.-Y.M. Ma, E.P. Popov and V.V. Bertero - 1976 (PB 260 843)A12

EERC 76-3 "Dynamic Behavior of a Multistory Triangular-Shaped Building," by J. Petrovski, R.M. Stephen, E. Gartenbaum and J.G. Bouwkamp - 1976 (PB 273 279)A07

EERC 76-4 "Earthquake Induced Deformations of Earth Dams," by N. Serff, H.B. Seed, F.I. Makdisi & C.-Y. Chang - 1976 (PB 292 065)A08

EERC 76-5 "Analysis and Design of Tube-Type Tall Building Structures," by H. de Clercq and G.H. Powell - 1976 (PB 252 220) A10

EERC 76-6 "Time and Frequency Domain Analysis of Three-Dimensional Ground Motions, San Fernando Earthquake," by T. Kubo and J. Penzien (PB 260 556)A11

EERC 76-7 "Expected Performance of Uniform Building Code Design Masonry Structures," by R.L. Mayes, Y. Omote, S.W. Chen and R.W. Clough - 1976 (PB 270 098)A05

EERC 76-8 "Cyclic Shear Tests of Masonry Piers, Volume 1 - Test Results," by R.L. Mayes, Y. Omote, R.W. Clough - 1976 (PB 264 424)A06

EERC 76-9 "A Substructure Method for Earthquake Analysis of Structure - Soil Interaction," by J.A. Gutierrez and A.K. Chopra - 1976 (PB 257 783)A08

EERC 76-10 "Stabilization of Potentially Liquefiable Sand Deposits using Gravel Drain Systems," by H.B. Seed and J.R. Booker - 1976 (PB 258 820)A04

EERC 76-11 "Influence of Design and Analysis Assumptions on Computed Inelastic Response of Moderately Tall Frames," by G.H. Powell and D.G. Row - 1976 (PB 271 409)A06

EERC 76-12 "Sensitivity Analysis for Hysteretic Dynamic Systems: Theory and Applications," by D. Ray, K.S. Pister and E. Polak - 1976 (PB 262 859)A04

EERC 76-13 "Coupled Lateral Torsional Response of Buildings to Ground Shaking," by C.L. Kan and A.K. Chopra - 1976 (PB 257 907)A09

EERC 76-14 "Seismic Analyses of the Banco de America," by V.V. Bertero, S.A. Mahin and J.A. Hollings - 1976

EERC 76-15 "Reinforced Concrete Frame 2: Seismic Testing and Analytical Correlation," by R.W. Clough and J. Gidwani - 1976 (PB 261 323)A08

EERC 76-16 "Cyclic Shear Tests of Masonry Piers, Volume 2 - Analysis of Test Results," by R.L. Mayes, Y. Omote and R.W. Clough - 1976

EERC 76-17 "Structural Steel Bracing Systems: Behavior Under Cyclic Loading," by E.P. Popov, K. Takanashi and C.W. Roeder - 1976 (PB 260 715)A05

EERC 76-18 "Experimental Model Studies on Seismic Response of High Curved Overcrossings," by D. Williams and W.G. Godden - 1976 (PB 269 548)A08

EERC 76-19 "Effects of Non-Uniform Seismic Disturbances on the Dumbarton Bridge Replacement Structure," by F. Baron and R.E. Hamati - 1976 (PB 282 981)A16

EERC 76-20 "Investigation of the Inelastic Characteristics of a Single Story Steel Structure Using System Identification and Shaking Table Experiments," by V.C. Matzen and H.D. McNiven - 1976 (PB 258 453)A07

EERC 76-21 "Capacity of Columns with Splice Imperfections," by E.P. Popov, R.M. Stephen and R. Philbrick - 1976 (PB 260 378)A04

EERC 76-22 "Response of the Olive View Hospital Main Building during the San Fernando Earthquake," by S. A. Mahin, V.V. Bertero, A.K. Chopra and R. Collins - 1976 (PB 271 425)A14

EERC 76-23 "A Study on the Major Factors Influencing the Strength of Masonry Prisms," by N.M. Mostaghel, R.L. Mayes, R. W. Clough and S.W. Chen - 1976 (Not published)

EERC 76-24 "GADFLEA - A Computer Program for the Analysis of Pore Pressure Generation and Dissipation during Cyclic or Earthquake Loading," by J.R. Booker, M.S. Rahman and H.B. Seed - 1976 (PB 263 947)A04

EERC 76-25 "Seismic Safety Evaluation of a R/C School Building," by B. Bresler and J. Axley - 1976

EERC 76-26 "Correlative Investigations on Theoretical and Experimental Dynamic Behavior of a Model Bridge Structure," by K. Kawashima and J. Penzien - 1976 (PB 263 388)A11

EERC 76-27 "Earthquake Response of Coupled Shear Wall Buildings," by T. Srichatrapimuk - 1976 (PB 265 157)A07

EERC 76-28 "Tensile Capacity of Partial Penetration Welds," by E.P. Popov and R.M. Stephen - 1976 (PB 262 899)A03

EERC 76-29 "Analysis and Design of Numerical Integration Methods in Structural Dynamics," by H.M. Hilber - 1976 (PB 264 410)A06

EERC 76-30 "Contribution of a Floor System to the Dynamic Characteristics of Reinforced Concrete Buildings," by L.E. Malik and V.V. Bertero - 1976 (PB 272 247)A13

EERC 76-31 "The Effects of Seismic Disturbances on the Golden Gate Bridge," by F. Baron, M. Arikan and R.E. Hamati - 1976 (PB 272 279)A09

EERC 76-32 "Infilled Frames in Earthquake Resistant Construction," by R.E. Klingner and V.V. Bertero - 1976 (PB 265 892)A13

UCB/EERC-77/01 "PLUSH - A Computer Program for Probabilistic Finite Element Analysis of Seismic Soil-Structure Interaction," by M.P. Romo Organista, J. Lysmer and H.B. Seed - 1977

UCB/EERC-77/02 "Soil-Structure Interaction Effects at the Humboldt Bay Power Plant in the Ferndale Earthquake of June 7, 1975," by J.E. Valera, H.B. Seed, C.F. Tsai and J. Lysmer - 1977 (PB 265 795)A04

UCB/EERC-77/03 "Influence of Sample Disturbance on Sand Response to Cyclic Loading," by K. Mori, H.B. Seed and C.K. Chan - 1977 (PB 267 352)A04

UCB/EERC-77/04 "Seismological Studies of Strong Motion Records," by J. Shoja-Taheri - 1977 (PB 269 655)A10

UCB/EERC-77/05 "Testing Facility for Coupled-Shear Walls," by L. Li-Hyung, V.V. Bertero and E.P. Popov - 1977

UCB/EERC-77/06 "Developing Methodologies for Evaluating the Earthquake Safety of Existing Buildings," by No. 1 - B. Bresler; No. 2 - B. Bresler, T. Okada and D. Zisling; No. 3 - T. Okada and B. Bresler; No. 4 - V.V. Bertero and B. Bresler - 1977 (PB 267 354)A08

UCB/EERC-77/07 "A Literature Survey - Transverse Strength of Masonry Walls," by Y. Omote, R.L. Mayes, S.W. Chen and R.W. Clough - 1977 (PB 277 933)A07

UCB/EERC-77/08 "DRAIN-TABS: A Computer Program for Inelastic Earthquake Response of Three Dimensional Buildings," by R. Guendelman-Israel and G.H. Powell - 1977 (PB 270 693)A07

UCB/EERC-77/09 "SUBWALL: A Special Purpose Finite Element Computer Program for Practical Elastic Analysis and Design of Structural Walls with Substructure Option," by D.Q. Le, H. Peterson and E.P. Popov - 1977 (PB 270 567)A05

UCB/EERC-77/10 "Experimental Evaluation of Seismic Design Methods for Broad Cylindrical Tanks," by D.P. Clough (PB 272 280)A13

UCB/EERC-77/11 "Earthquake Engineering Research at Berkeley - 1976," - 1977 (PB 273 507)A09

UCB/EERC-77/12 "Automated Design of Earthquake Resistant Multistory Steel Building Frames," by N.D. Walker, Jr. - 1977 (PB 276 526)A09

UCB/EERC-77/13 "Concrete Confined by Rectangular Hoops Subjected to Axial Loads," by J. Vallenas, V.V. Bertero and E.P. Popov - 1977 (PB 275 165)A06

UCB/EERC-77/14 "Seismic Strain Induced in the Ground During Earthquakes," by Y. Sugimura - 1977 (PB 284 201)A04

UCB/EERC-77/15 "Bond Deterioration under Generalized Loading," by V.V. Bertero, E.P. Popov and S. Viwathanatepa - 1977

UCB/EERC-77/16 "Computer Aided Optimum Design of Ductile Reinforced Concrete Moment Resisting Frames," by S.W. Zagajeski and V.V. Bertero - 1977 (PB 280 137)A07

UCB/EERC-77/17 "Earthquake Simulation Testing of a Stepping Frame with Energy-Absorbing Devices," by J.M. Kelly and D.F. Tsztoo - 1977 (PB 273 506)A04

UCB/EERC-77/18 "Inelastic Behavior of Eccentrically Braced Steel Frames under Cyclic Loadings," by C.W. Roeder and E.P. Popov - 1977 (PB 275 526)A15

UCB/EERC-77/19 "A Simplified Procedure for Estimating Earthquake-Induced Deformations in Dams and Embankments," by F.I. Makdisi and H.B. Seed - 1977 (PB 276 820)A04

UCB/EERC-77/20 "The Performance of Earth Dams during Earthquakes," by H.B. Seed, F.I. Makdisi and P. de Alba - 1977 (PB 276 821)A04

UCB/EERC-77/21 "Dynamic Plastic Analysis Using Stress Resultant Finite Element Formulation," by P. Lukkunapvasit and J.M. Kelly - 1977 (PB 275 453)A04

UCB/EERC-77/22 "Preliminary Experimental Study of Seismic Uplift of a Steel Frame," by R.W. Clough and A.A. Huckelbridge 1977 (PB 278 769)A08

UCB/EERC-77/23 "Earthquake Simulator Tests of a Nine-Story Steel Frame with Columns Allowed to Uplift," by A.A. Huckelbridge - 1977 (PB 277 944)A09

UCB/EERC-77/24 "Nonlinear Soil-Structure Interaction of Skew Highway Bridges," by M.-C. Chen and J. Penzien - 1977 (PB 276 176)A07

UCB/EERC-77/25 "Seismic Analysis of an Offshore Structure Supported on Pile Foundations," by D.D.-N. Liou and J. Penzien 1977 (PB 283 180)A06

UCB/EERC-77/26 "Dynamic Stiffness Matrices for Homogeneous Viscoelastic Half-Planes," by G. Dasgupta and A.K. Chopra - 1977 (PB 279 654)A06

UCB/EERC-77/27 "A Practical Soft Story Earthquake Isolation System," by J.M. Kelly, J.M. Eidinger and C.J. Derham - 1977 (PB 276 814)A07

UCB/EERC-77/28 "Seismic Safety of Existing Buildings and Incentives for Hazard Mitigation in San Francisco: An Exploratory Study," by A.J. Meltsner - 1977 (PB 281 970)A05

UCB/EERC-77/29 "Dynamic Analysis of Electrohydraulic Shaking Tables," by D. Rea, S. Abedi-Hayati and Y. Takahashi 1977 (PB 282 569)A04

UCB/EERC-77/30 "An Approach for Improving Seismic - Resistant Behavior of Reinforced Concrete Interior Joints," by B. Galunic, V.V. Bertero and E.P. Popov - 1977 (PB 290 870)A06

UCB/EERC-78/01 "The Development of Energy-Absorbing Devices for Aseismic Base Isolation Systems," by J.M. Kelly and D.F. Tsztoo - 1978 (PB 284 978)A04

UCB/EERC-78/02 "Effect of Tensile Prestrain on the Cyclic Response of Structural Steel Connec ns, by J.G. Bouwkamp and A. Mukhopadhyay - 1978

UCB/EERC-78/03 "Experimental Results of an Earthquake Isolation System using Natural Rubber Bearings," by J.M. Eidinger and J.M. Kelly - 1978 (PB 281 686)A04

UCB/EERC-78/04 "Seismic Behavior of Tall Liquid Storage Tanks," by A. Niwa - 1978 (PB 284 017)A14

UCB/EERC-78/05 "Hysteretic Behavior of Reinforced Concrete Columns Subjected to High Axial and Cyclic Shear Forces," by S.W. Zagajeski, V.V. Bertero and J.G. Bouwkamp - 1978 (PB 283 858)A13

UCB/EERC-78/06 "Inelastic Beam-Column Elements for the ANSR-I Program," by A. Riahi, D.G. Row and G.H. Powell - 1978

UCB/EERC-78/07 "Studies of Structural Response to Earthquake Ground Motion," by O.A. Lopez and A.K. Chopra - 1978 (PB 282 790)A05

UCB/EERC-78/08 "A Laboratory Study of the Fluid-Structure Interaction of Submerged Tanks and Caissons in Earthquakes," by R.C. Byrd - 1978 (PB 284 957)A08

UCB/EERC-78/09 "Model for Evaluating Damageability of Structures," by I. Sakamoto and B. Bresler - 1978

UCB/EERC-78/10 "Seismic Performance of Nonstructural and Secondary Structural Elements," by I. Sakamoto - 1978

UCB/EERC-78/11 "Mathematical Modelling of Hysteresis Loops for Reinforced Concrete Columns," by S. Nakata, T. Sproul and J. Penzien - 1978

UCB/EERC-78/12 "Damageability in Existing Buildings," by T. Blejwas and B. Bresler - 1978

UCB/EERC-78/13 "Dynamic Behavior of a Pedestal Base Multistory Building," by R.M. Stephen, E.L. Wilson, J.G. Bouwkamp and M. Button - 1978 (PB 286 650)A08

UCB/EERC-78/14 "Seismic Response of Bridges - Case Studies," by R.A. Imbsen, V. Nutt and J. Penzien - 1978 (PB 286 503)A10

UCB/EERC-78/15 "A Substructure Technique for Nonlinear Static and Dynamic Analysis," by D.G. Row and G.H. Powell - 1978 (PB 288 077)A10

UCB/EERC-78/16 "Seismic Risk Studies for San Francisco and for the Greater San Francisco Bay Area," by C.S. Oliveira - 1978

UCB/EERC-78/17 "Strength of Timber Roof Connections Subjected to Cyclic Loads," by P. Gülkan, R.L. Mayes and R.W. Clough - 1978

For sale by the National Technical Information Service, U. S. Department of Commerce, Springfield, Virginia 22161.

See back of report for up to date listing of EERC reports.